NASA-CR-198881

JPL Publication 95-5

The JPL Mars Gravity Field, Mars50c, Based Upon Viking and Mariner 9 Doppler Tracking Data

Alexander S. Konopliv
William L. Sjogren

(NASA-CR-198881) THE JPL MARS GRAVITY FIELD, Mars50c, BASED UPON VIKING AND MARINER 9 DOPPLER TRACKING DATA (JPL) 83 p

N95-30344

Unclas

G3/91 0056665

February 1995

National Aeronautics and
Space Administration

Jet Propulsion Laboratory
California Institute of Technology
Pasadena, California

JPL Publication 95-5

The JPL Mars Gravity Field, Mars50c, Based Upon Viking and Mariner 9 Doppler Tracking Data

Alexander S. Konopliv
William L. Sjogren

February 1995

National Aeronautics and
Space Administration

Jet Propulsion Laboratory
California Institute of Technology
Pasadena, California

The research described in this publication was carried out by the Jet Propulsion Laboratory, California Institute of Technology, under a contract with the National Aeronautics and Space Administration.

Acknowledgments

The authors thank Dave Smith of Goddard Space Flight Center for providing us with the Doppler tracking data used for this gravity field. We would also like to thank Ray Wimberly for his continuing efforts at trying to locate some of the Viking data. Chuck Yoder, Jim Williams, Myles Standish, Bob Jacobson, and Frank Nicholson discussed different aspects of this work. Gene Hanover graciously provided his handwritten notes on the attitude of the Viking orbiters. Nicole Rappaport provided the spherical harmonic representation of Olympus Mons. Edward Christensen and Bruce Banerdt reviewed this manuscript. Finally, this work was funded by the Multimission Operations Systems Office at the Jet Propulsion Laboratory.

Abstract

This report summaries the current JPL efforts of generating a Mars gravity field from Viking 1 and 2 and Mariner 9 Doppler tracking data. The Mars50c solution is a complete gravity field to degree and order 50, with solutions as well for the gravitational mass of Mars, Phobos, and Deimos. The constants and models used to obtain the solution are given, and the method for determining the gravity field is presented. The gravity field is compared to the best current gravity field Goddard Mars Model 1 (GMM1) of Goddard Space Flight Center.

Table of Contents

List of Figures

List of Tables

1. Introduction

This report describes the JPL Mars gravity field, Mars50c, that is being provided to the Mars Global Surveyor project. Mars50c is a complete gravity field to degree and order 50 with solutions for the gravitational masses of Mars, Phobos, and Deimos and the ephemerides of Phobos and Deimos. This new field shows significantly better fitting to the Doppler data than previous models. This improvement is probably due to a combination of attitude maneuver modeling not in previous studies and the application of a different a priori technique on the gravity field. This gravity field is considered as an intermediate product with fine-tune adjustments to come as funding permits.

The first spacecraft measures of the gravity of Mars were extracted from Mariner 4 radio tracking data (Null, 1969) with the determination of total mass and oblateness. That mass value is in very close agreement to the results of this article and Smith et al. (1993). The next refinement came from Mariner 9 data. The Doppler radio tracking data were analyzed by many investigators, but they produced only low degree harmonic models. Generally these models were expanded to degree and order six, which did, however, reveal the large Tharsis anomaly (Lorell et al., 1972; 1973; Born 1974; Jordan and Lorell 1975; Reasenberg et al., 1975; and Sjogren et al., 1975). In 1976, the Viking 1 and 2 orbiters produced a new unique set of data where periapsis altitudes were near 300 km, as compared to 1400 for Mariner 9. However, again gravity modeling with harmonics was at relatively low degree and order (6-12) (Reasenberg, 1977; Gapcynski et al., 1977; Christensen and Williams, 1979; Christensen and Balmino, 1979). Balmino et al, (1982) using the CDC 750 CYBER computer in France pushed the expansion to degree and order 18 (360 parameters) which was a large effort at that time.

The 1990s ushered in a new era for high-resolution gravity field models using classical spherical harmonics. Prior to this, line-of-sight Doppler residual analysis revealed high-frequency structure and its correlation with topography (Sjogren, 1979). The revolution in computer capacity, speed, and cost reduction have allowed harmonic models to expand to 60th degree and order (3720 parameters) for the Moon (Konopliv et al., 1993b), 60th and 75th degree and order (5775 parameters) for Venus (Konopliv et al., 1995a, 1995b), and 30th degree and order (960 parameters, Lemoine, 1992) and 50th degree and order (2600 parameters, Smith et al, 1993) for Mars. These models show detailed structure and allow analysis of individual features. As a result, much of the old data acquired on Mariner 9 in 1971 and Viking 1 and 2 in 1976 to 1978 are being reanalyzed using new techniques and new computing power.

The results of this report were generated on an HP755 workstation that produced an iteration on all Mariner 9 and Viking data in 96 hours of continuous run time for the complete model and ancillary parameters. We show how a newly developed a priori technique has refined the resolution and has allowed the model parameters to maximize their amplitude. Even with this ability, small systematic signatures still remain in the data that suggest higher degree and order harmonics may need to be estimated.

The data set for this solution is identical to the data set used to determine the Goddard Mars Model-1 (GMM1) of Smith et al. (1993) and includes Viking 1, Viking 2, and Mariner 9 Doppler tracking data. Smith et. al. (1993) provides a complete description of the data set, i.e., groundtrack coverage, data time spans, number of Doppler points, orbit information, etc.. Much background information on Mars gravity determination (modeling of forces on the spacecraft, media calibrations, range data, etc.) is also documented by Lemoine (1992).

2. Doppler Tracking

The Viking 1 and 2 orbiters and Mariner 9 spacecraft were tracked with two-way coherent Doppler acquired at the Deep Space Network complexes at Goldstone, California; Madrid, Spain; and Canberra, Australia. The Doppler data set used in this effort was originally collected by Edward Christensen at JPL and carried to France for cooperative Mars gravity work with George Balmino at Centre National des Etudes Spatiales (CNES). George then passed the data on to Dave Smith at Goddard for their Mars gravity effort and now the data has come full circle as Goddard returned the data to JPL for our gravity efforts. The data set is mostly complete, but there are some passes missing (for example, the Viking 2 pass over Isidis on January 5, 1978) and the sample time of the data is 60 seconds, whereas the original gravity data were 10-second samples. In addition, we only have S-band uplink with S-band downlink data and do not have any of the the S-band uplink with X-band downlink data. We have an ongoing low-level effort to try and locate some of the Viking data (we have at least found the original data set that Edward Christensen took to France). Many of the magnetic tapes have been lost in storage and some have been damaged and are unreadable on the Univac computer.

The Doppler data are processed in many time spans or arcs of about 3 or 4 days in length. Appendices 1, 2, and 3 list the data arcs created for the Mars50c gravity field effort for each orbiter along with the number of points for the arc, the periapse altitude, and the periapse latitude. All the Mariner 9 data were highly eccentric with an orbital period of 12 hours, an inclination of 64 degrees, and a high periapse altitude (>1300 km). The Viking orbiters were highly eccentric orbiters with about a 24-hour orbital period. The Viking 1 orbit maintained about a 39-degree inclination throughout its lifetime with the first part of the mission (to March 11, 1977) in a high periapse altitude (≈1500 km) orbit and the second part of the mission in a low periapse altitude (≈300 km) orbit. Viking 2 changed inclinations several times with 50- and 75-degree inclinations for the high periapse altitude (≈1500 km) orbits and 80-degree inclination for the lower periapse altitude orbits of 700 km and 300 km. Figure 1 shows the combined Viking 1 and 2 coverage below 500 km altitude. There are no low-altitude observations in the higher latitude regions of both the north and south pole.

3. Modeling

The Doppler tracking data were processed using JPL's Orbit Determination Program (ODP, see Moyer, 1971) in the coordinate system defined by the Earth's mean equator at J2000. The ODP estimates the spacecraft state and other parameters using a weighted least-squares filter based upon the square root of the information matrix (see Bierman, 1977). The parameters that are estimated consist of arc-dependent or local variables (spacecraft state, etc.) that are determined separately for each data arc (i.e., the arcs listed in Appendices 1, 2, and 3) and global variables (harmonic coefficients, etc.) that are common to all the data arcs.

Initially, we converge the data arcs only with the local variables using the nominal values for the global variables. The observations of each arc are weighted according to data root mean square (rms) of that arc with a separate rms for each tracking station pass and the rms including corrections for the count times of the observations. The actual data weight used is the rms multiplied by a factor of two with an additional correction factor for the observation elevation. The GMM1 gravity field (Smith et al., 1993) was used as the nominal field for the generation of the Mars50c gravity model and the generation of the satellite ephemeris of Phobos and Deimos. The

Figure 1: Viking 1 and 2 Observation Coverage Below 500 km

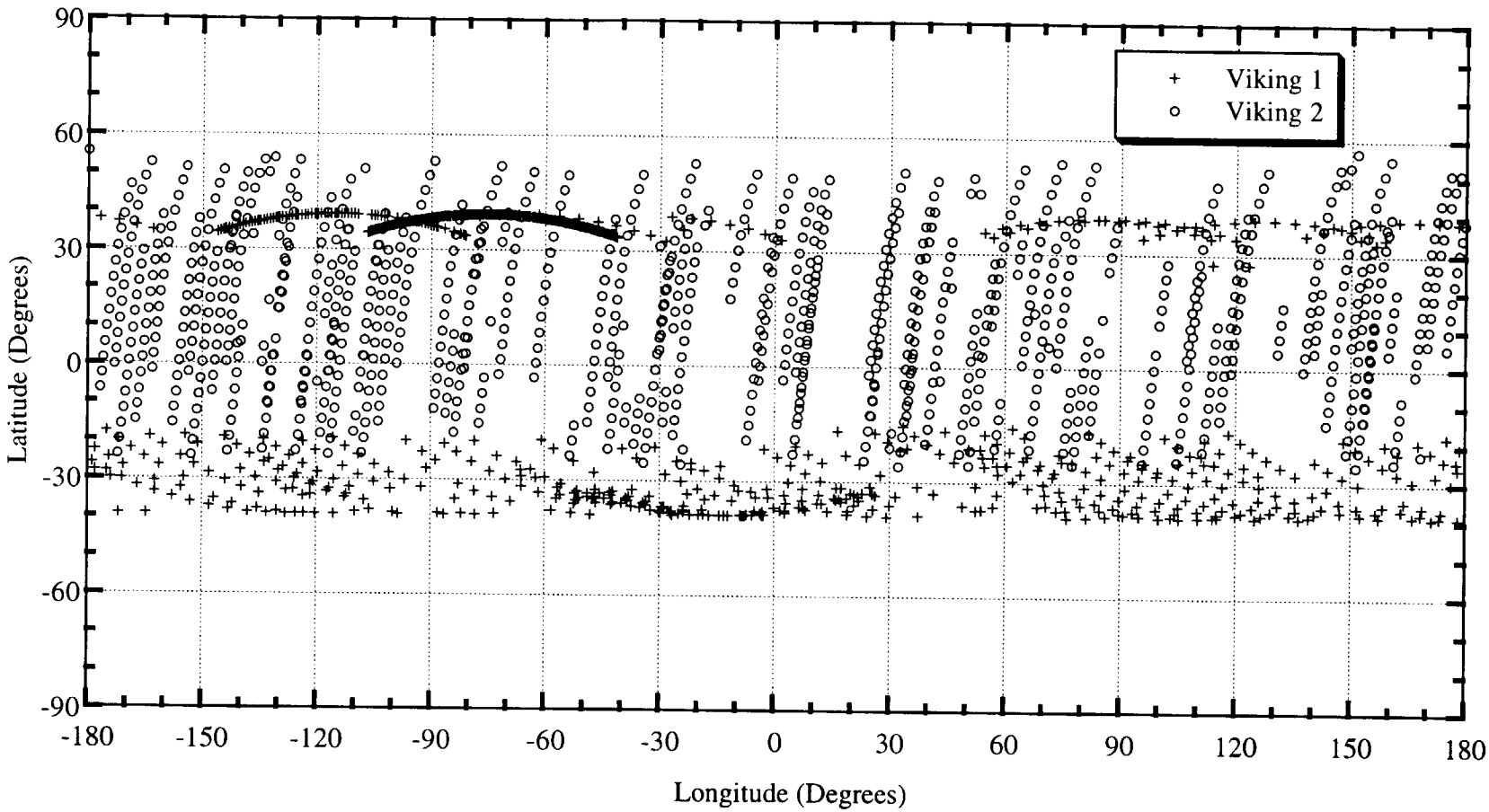

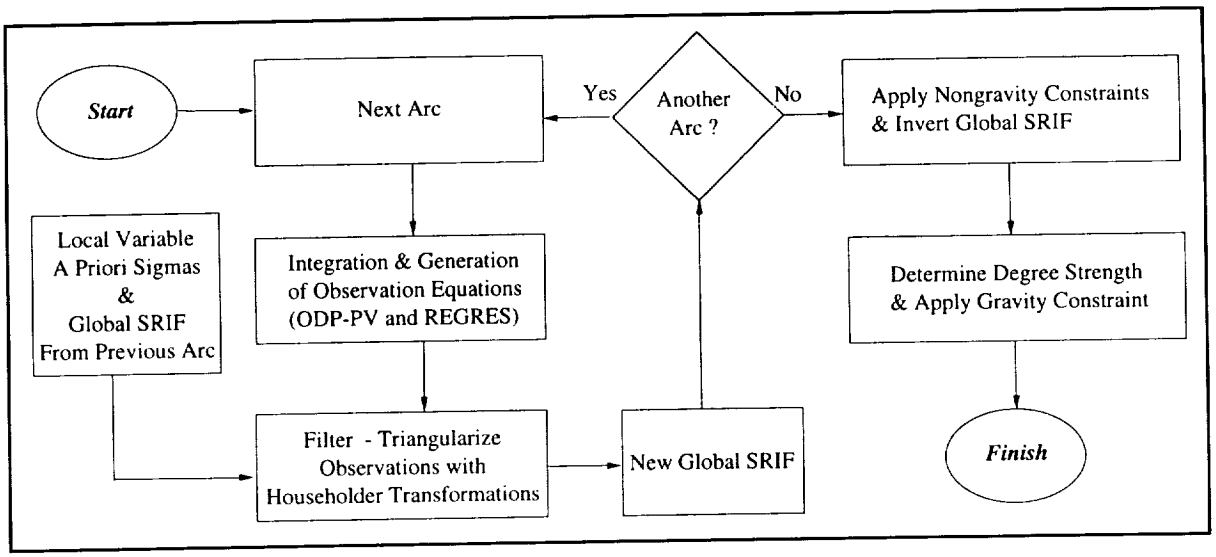

Figure 2: Flowchart of Gravity Field Determination

use of an accurate gravity model (GMM1) made the determination of Mars50c much easier, especially concerning data editing.

Once the local variables are converged, the global parameters are determined with a technique described by Ellis (1980) that merges only the global parameter portion of the square root information (or SRIF) arrays from all the arcs, but is equivalent to solving for the global parameters plus local parameters of all arcs. This method is outlined in Figure 2. For the first arc, the a priori SRIF matrix for the global variables is the zero matrix (i.e., no a priori) whereas for each successive arc, the a priori SRIF for the global parameters is the resulting global SRIF from the previous arc. The global SRIF is easily determined from the SRIF of all parameters (local plus global) if the parameters are ordered such that all the local parameters are before the global parameters. In this case, the SRIF for the global parameters is just the lower triangular subsection of the entire SRIF (i.e., the rows for the global variables). The process can be divided into subsets of data. In actuality, separate global SRIF arrays are determined for the Viking 1, Viking 2, and Mariner 9 data sets, and the global SRIF arrays are merged allowing for fine-tune adjustments of the data set weights. Once the global SRIF array is determined, the global variables are constrained with a priori constraints. The a priori constraint on the gravity field will be discussed in the next section.

The following global parameters are estimated: the normalized spherical harmonic coefficients ($\bar{C}_{nm}$, $\bar{S}_{nm}$) of the gravity field complete to degree and order 50 (2597 parameters), the gravitational constant times the mass of Mars (GM), the GM of Phobos, the GM of Deimos, and the ephemerides of Phobos and Deimos (18 parameters). The spherical harmonic expansion of the gravitational potential U is given by

$$U = \frac{GM}{r} + \frac{GM}{r} \sum_{n=2}^{\infty} \sum_{m=0}^{n} \left(\frac{a_e}{r}\right)^n P_{nm}(\sin \phi) \left[C_{nm}\cos m\lambda + S_{nm}\sin m\lambda\right] \tag{1}$$

where r is the distance from the center of the body, a_e is the mean radius of the body and is equal to 3394.2 km for our Mars models, P_{nm} is the associated Legendre polynomial, ϕ is the latitude, λ is the longitude, and C_{nm} and S_{nm} are the spherical harmonic coefficients for degree n and order m. The normalized coefficients $\bar{C}_{nm}$ and $\bar{S}_{nm}$ are solved for and are related to the unnormalized coefficients by (see Kaula, 1966)

$$(\bar{C}_{nm} \text{ or } \bar{S}_{nm}) = \left[\frac{(n+m)!}{(2-\delta_{0m})(2n+1)(n-m)!}\right]^{1/2} (C_{nm} \text{ or } S_{nm}) \tag{2}$$

where δ_{0m} is the Kronecker delta function and $\bar{C}_{n0} = -\bar{J}_n$. The harmonic coefficients of degree one are fixed to zero since the origin of the coordinate system is chosen to be the center of mass of the body.

For each data arc, the local variables estimated are the spacecraft state, three solar pressure coefficients, a base density for the lower altitude Viking orbits (about 300-km periapse altitude), known gas leaks and attitude maneuvers as spacecraft velocity increments, and one ionosphere dayside and one nightside parameter. The solar pressure coefficients also dilute the adverse effects of any unmodeled nonconservative spacecraft forces such as gas leaks. The ionosphere model is a simple model that assumes a fixed Earth ionospheric bulge tied to the local mean solar time for the duration of the arc (see Moyer, 1984).

The Viking orbiters had a three-axis stabilized attitude control system with a cold gas attitude jet assembly on the end of the two solar panels. The control system was coupled and resulted in minimal perturbations to the spacecraft orbit (except for long arcs where these errors could accumulate and become significant). The jets were used to change the orientation of the spacecraft and also to maintain attitude to within a several degree window. The latter required firing the jets several times every hour. Hanover (1977) notes the failure of a Viking 1 roll jet on July 1, 1977 and a Viking 2 yaw jet on Nov. 2, 1977. Hence, all attitude maneuvers after these times are uncoupled and can cause significant perturbations on the orbit. However, the pulses to maintain attitude within the several degree window still mostly canceled because the second pulse is in an equal and opposite direction to within a few degrees (Nicholson, 1995). From the handwritten notes of Gene Hanover (1993), the uncoupled maneuver times (time at the spacecraft) are tabulated in Appendix 4 for Viking 1 and Appendix 5 for Viking 2. These maneuvers are estimated as a velocity increment in three directions. Also included in Appendices 4 and 5 are known gas leak times at the midpoint of the gas leak. The gas leak may last for several hours but we only estimate a velocity increment at the midpoint. After March 17, 1978 for Viking 2, there are so many gas leaks that we estimate a velocity increment every 12 hours in all the data arcs to alleviate the errors in the solution from the gas leak.

The International Astronomical Union (IAU) 1991 (Davies et al., 1992) rotational constants specified the orientation of Mars and, hence, the gravity field. The JPL DE200 planetary ephemeris (Standish, 1980) was used for calculation of the planetary point mass perturbations. The MAR027 Phobos and Deimos satellite ephemeris covered the Viking data time span for the calculation of the point mass accelerations of Phobos and Deimos on the spacecraft, but no forces on Mariner 9 were included due to Phobos and Deimos. MAR027 is a fit of the observations of Phobos and Deimos to the Sinclair/Morley theory.

For the Doppler observables, averaged seasonal troposphere calibrations as given by Chao (1972) were applied. Any observations below 10-degrees elevation were deleted because of

unmodeled troposphere effects. Daily UT1 and polar motion values from the JPL Space91 solution (Gross, 1992) were included and DSN station locations are in the International Earth Rotation Service (IERS) reference frame as given by Folkner (1991) with the AM0-2 plate motion model and solid-Earth tides corrections added. Ideally, future solutions will include the frame tie rotational offset between the IERS and planetary ephemeris frames, solve for the Mars ephemeris, or use an ephemeris such as DE400 in the radio frame.

4. Gravity A Priori

Once all the global information is packed from all the data arcs, the gravity field is constrained with an a priori. The common method to apply an a priori constraint on the gravity field is to constrain each harmonic coefficient toward zero with an uncertainty given by the Kaula rule (1966) for that particular planet (used, for example, in Konopliv et al. 1993a, Konopliv et al. 1993b, Nerem et al. 1993, McNamee et al. 1993, Smith et al., 1993, Lemoine, 1992). The Kaula rule used for Mars is $13 \times 10^{-5} / n^2$ where n is the degree of the coefficient.

The a priori constraint applied for this gravity field evaluates the radial acceleration and its uncertainty on the reference sphere (i.e., $r = a_e$). At that surface, the radial acceleration (a_n) from all coefficients of degree n is given by

$$a_n = \frac{GM}{a_e^2}(n+1)\sum_{m=0}^{n} \bar{P}_{nm}(\sin\phi)\,(\bar{C}_{nm}\cos m\lambda + \bar{S}_{nm}\sin m\lambda) \tag{3}$$

where $\bar{P}_{nm}$ are the normalized associated Legendre polynomials (see Kaula,1966). To create a profile of acceleration contributions versus degree, the rms of the acceleration a_n is obtained over the sphere. The mean of the square of the acceleration $(a_n)_{ms}$ of equation (3) is given by

$$(a_n)_{ms} = \left[\frac{GM}{a_e^2}(n+1)\right]^2 \frac{1}{4\pi}\int_0^{2\pi}\int_{-\pi/2}^{\pi/2}\left[\sum_{m=0}^{n} \bar{P}_{nm}(\sin\phi)\,(\bar{C}_{nm}\cos m\lambda + \bar{S}_{nm}\sin m\lambda)\right]^2 d\phi\, d\lambda$$

Since the spherical harmonics are orthogonal, we obtain

$$(a_n)_{ms} = \left[\frac{GM}{a_e^2}(n+1)\right]^2 \sum_{m=0}^{n} (\bar{C}_{nm}^2 + \bar{S}_{nm}^2)$$

As a good approximation, the rms magnitude spectrum of the gravity coefficients follows the Kaula rule and is given by

$$\left[\frac{\sum_{m=0}^{n} (\bar{C}_{nm}^2 + \bar{S}_{nm}^2)}{2n+1}\right]^{1/2} = K/n^2 \tag{4}$$

where K is the constant for the particular planet (13×10^{-5} for Mars). The expected acceleration profile is then given by (for $n >> 1$)

$$(a_n)_{rms} = \frac{GM}{a_e^2} K\sqrt{2/n} \tag{5}$$

which for Mars is

$$(a_n)_{rms} = 68.35 / \sqrt{n} \text{ milligals} \tag{6}$$

This is the expected "signal" for the acceleration at each point on the surface of the reference sphere. The signal could also be determined empirically by taking the rms of a given gravity field over different regions. However, for this work, only one signal profile is used for all latitudes and longitudes.

The next task is to map the acceleration uncertainty at the surface into an uncertainty profile showing the error in acceleration versus harmonic degree. The acceleration uncertainty from the summed contributions of all coefficients from degree 2 to n, $\sigma(a_{2,n})$ is given by

$$\sigma(a_{2,n}) = \frac{\partial a_{2,n}^T}{\partial \mathbf{G}_{2,n}} \operatorname{cov}(\mathbf{G}_{2,n}) \frac{\partial a_{2,n}}{\partial \mathbf{G}_{2,n}} \tag{7}$$

where $\mathbf{G}_{2,n}$ is the vector of all normalized gravity coefficients from degree 2 to n and $\operatorname{cov}(\mathbf{G}_{2,n})$ is the corresponding covariance. The covariance of the coefficients from degree 2 to n is the covariance as if the higher degree coefficients are not estimated. Hence, it is a truncation, or sub matrix, of the full 50th degree and order covariance without any constraint applied to the gravity field. The partial of the acceleration with respect to the coefficients of degree n and order m are functions of latitude and longitude and are given by

$$\begin{aligned} \frac{\partial a_{2,n}}{\partial \overline{C}_{nm}} &= \frac{GM}{a_e^2} (n+1) \overline{P}_{nm}(\sin\phi) \cos m\lambda \\ \frac{\partial a_{2,n}}{\partial \overline{S}_{nm}} &= \frac{GM}{a_e^2} (n+1) \overline{P}_{nm}(\sin\phi) \sin m\lambda \end{aligned} \tag{8}$$

The uncertainty for the coefficients of degree n, $\sigma(a_n)$ is then given by the difference of the sum total error to degree n and the sum total error to degree n-1 as

$$\sigma(a_n) = \sigma(a_{2,n}) - \sigma(a_{2,n-1}) \tag{9}$$

Figure 3 shows the expected acceleration profile from the Kaula rule of equation (6) and the unconstrained acceleration uncertainty profile as given by equation (9) for Olympus Mons, the north pole, and the south pole. Also displayed are the actual contributions per degree to the peak value of Olympus Mons for the Mars50c gravity field. In this case, the actual signal is substantially stronger than the Kaula rule. The crossing point of the Kaula signal with the acceleration uncertainty is called the degree strength of the gravity field for that particular latitude and longitude. For degrees greater than the degree strength, the "noise" in the data exceeds the "signal." Based

upon the Kaula rule, the degree strengths for Olympus Mons, the north pole, and the south pole are 26, 19, and 14, respectively. Figure 4 displays the degree strength on a global scale with the maximum degree strength about harmonic degree 30 near the low-altitude periapse locations.

The basic idea of our gravity constraint method is to constrain the "noise" of the gravity field to zero with some uncertainty when the "noise" exceeds the "signal." The acceleration at the surface from all harmonic coefficients greater than or equal to the degree strength is constrained to zero with an uncertainty approximately equal to the expected signal at the degree strength. This amounts to generating observations over the entire surface of the sphere based upon the degree strength at each latitude and longitude. An observation ($a_{D,50}$) for degree strength D is

$$a_{D,50} = \frac{GM}{a_e^2} \sum_{n=D}^{50} \sum_{m=0}^{n} (n+1)\, \overline{P}_{nm}(\sin\phi)\, (\overline{C}_{nm}\cos m\lambda + \overline{S}_{nm}\sin m\lambda) \tag{10}$$

and the linearized observation equation is given by (Bierman,1977)

$$z_i = \mathbf{A}_i\, \mathbf{x} + v_i$$

where z_i is the difference between the observed value (zero in this case) and the nominal value of the observation (the accumulated acceleration at the surface for degrees D to 50 from the GMM1 gravity model as given by equation (10)), $\mathbf{A}_i$ is the row vector of observation partials, $\mathbf{x}$ is the vector of estimated parameters (differences in the gravity coefficients from the nominal GMM1 model), and v_i is the observation error. The partials $\mathbf{A}_i$ to construct the observation equation are

$$\mathbf{A}_i = \frac{\partial a_{D,50}}{\partial \mathbf{G}}$$

where $\mathbf{G}$ is the vector of all gravity coefficients. The elements of $\mathbf{A}_i$ for coefficients with degrees less than the degree strength D are zero and, otherwise, are again given by the partials of equation (8).

The observations are then merged with the unconstrained gravity SRIF array using Householder transformations. In normal form, the constrained gravity estimate $\mathbf{x}$ is written as

$$\mathbf{x} = \left[\mathrm{cov}(\mathbf{G})^{-1} + \mathbf{A}^T\mathbf{W}\mathbf{A}\right]^{-1} \left[\mathrm{cov}(\mathbf{G})^{-1}\mathbf{x}_{noap} + \mathbf{A}^T\mathbf{W}\mathbf{z}\right] \tag{11}$$

where cov($\mathbf{G}$) is the unconstrained covariance of the gravity coefficients, $\mathbf{A}$ is the matrix of observation partials with each row an observation, $\mathbf{W}$ is the diagonal weight matrix, $\mathbf{x}_{noap}$ is the unconstrained gravity estimate, and $\mathbf{z}$ is the vector of linearized observations. The new constrained covariance $\mathbf{P}$ is then

$$\mathbf{P} = \left[\mathrm{cov}(\mathbf{G})^{-1} + \mathbf{A}^T\mathbf{W}\mathbf{A}\right]^{-1} \tag{12}$$

The observations should be spaced such that at least three observations are generated over the shortest harmonic wavelength. The weight used for an observation is then proportional to the area between observations and is approximately equal to the signal at the degree strength (i.e., 10 to 20

milligals). For Mars50c, the observations are globally spaced on a rectangular grid of latitude and longitude with a spacing of two degrees. However, since the actual signals of Olympus Mons and the other Tharsis volcanos are substantially stronger than the Kaula rule, the a priori observations over these regions are relaxed. The a priori over Olympus Mons is removed completely and the a priori over the other three volcanos is reduced by over an order of magnitude to several hundred milligals. Instead of relaxing the a priori, one could use the observed signal profile over the volcanos in place of the Kaula rule, and the degree strength would increase to about degree 40 for Olympus. The a priori is also relaxed because the data are weighted according to the rms fit from the GMM1 model. Future iterations on the gravity field will have a lower rms fit and hence tighter data weight.

The result on the acceleration uncertainty profiles from applying the a priori observations on the gravity field is displayed in Figure 5 for the Mars50c gravity field. The result for the polar regions is a damped sinusoidal behavior for the uncertainty but very smooth behavior for the better determined equatorial regions. The uncertainty for Olympus shows a large growth for the degrees greater than about 40, but the signal in Figure 3 shows that there is limited strength for degrees greater than 40 in the resulting gravity field. The observation data weights could be fine-tuned to suppress the poles slightly further, but most likely will not change the result significantly.

The main advantage of using this spatial constraint instead of a straight Kaula rule on the spectrum appears to be better determination of peak amplitudes. Since the well determined degrees are not constrained directly (only somewhat through correlations), the amplitudes (and coefficients) for those degrees are not biased toward zero. It is also flexible in allowing relaxation of selected regions for any reason, such as incorrect data weighting. We originally published a similar but different surface a priori technique in Konopliv et al (1995a), and this method evolved from that work. We expect this method to be further refined as our efforts continue.

5. Mass and Other Determinations

The solutions and formal uncertainties for the gravitational masses (km^3/s^2) of Mars, Phobos, and Deimos are given in Table 1. The solutions are given for Viking data only (Mars50b) and for Viking and Mariner 9 data (Mars50c). The addition of the Mariner 9 data doesn't change the mass solutions much. Since there is no estimate of Phobos and Deimos masses with the Mariner 9 data, these solutions only change through the correlation with the gravity field. Our GM solution agrees well with the solution from Smith et al. (1993) of 42828.36 ± 0.05 and is within a formal one-sigma.

The solution for the Phobos and Deimos ephemerides (a total of 9 parameters for each satellite) only improves the parameters 401BET and 401GAM and does so by a factor of 20 based upon the formal statistics (i.e., improves Phobos only and not Deimos). The a priori uncertainty on the ephemeris is given by the formal covariance of the Phobos and Deimos observations fit to the

Table 1: Mars Gravitational Mass Solutions

Body	Viking Data Only (Mars50b)	Viking + Mariner 9 (Mars50c)
Mars:	42828.368 ± 0.0087	42828.370 ± 0.0086
Phobos:	(7.106 ± 0.013) x 10^{-4}	(7.090 ± 0.012) x 10^{-4}
Deimos:	(1.586 ± 0.081) x 10^{-4}	(1.589 ± 0.081) x 10^{-4}

Sinclair/Morley theory. These parameters are related to the precession of periapse and the orbit plane, respectively. The resulting solution delta probably absorbs the effect of J_3 on the orbital plane which is not included in this satellite theory (Jacobson, 1995). With future solutions, we hope to use an updated version of the Sinclair/Morley theory being developed by Jacobson that will include the J_3 effect, and the ephemeris will be extended to include the Mariner 9 time frame. With this new ephemeris, we will be able to test how well our ephemeris corrections fit the Phobos and Deimos observations that were used to generate the ephemeris. Also solved for are the J_2 of Phobos and Deimos. However the solution for J_2 is about twice the formal statistic and the formal statistic is about twice the Phobos J_2 value as determined by Jim Miller (1990).

As a test, the Mars pole and rotation rate were estimated but the resulting solution change from the IAU 1991 values was about the same size as the formal statistics. The formal errors from the Mars50c solution are 0.0016 and 0.0007 degrees for the pole right ascension and declination and 5.3×10^{-6} degrees/day for the rotation rate. The pole orientation error is slightly greater than the orientation error as determined from the Viking lander data, which has errors in the Mars' equator inclination and node of 0.0004 and 0.0009 degrees, respectively (Standish, 1995). The Viking lander data, however, determines the rotation rate to a much higher accuracy of 0.11×10^{-6} degrees/day. Hence, there is no new rotational information in the gravity data.

6. Gravity Field Results

Appendix 6 lists all the 50 x 50 normalized coefficients and their formal uncertainties of the Mars50c gravity field where the zonal coefficients are $J_n = -C_{n0}$. A file containing the complete field can be requested from the authors at ask@krait.jpl.nasa.gov. The normalized C_{21} and S_{21} coefficients and sigmas for the Viking-only solution (Mars50b) are $(129 \pm 92) \times 10^{-10}$ and $(-223 \pm 91) \times 10^{-10}$, respectively. The rms of the range residuals of the Viking landers (Standish, 1995) is 7 meters where the solution is for the Mars orientation without any offset between the principal axis from the rotational pole (i.e., no wobble is included). A 10^{-8} value of C_{21} and S_{21} results in a principal axes offset of about 24 meters from the rotational pole, and since the Viking landers detected no offset on the order of 7 meters, the C_{21} and S_{21} values should be no greater than 30×10^{-10}. The Mars50b solutions are within about two sigma of this value but the Mars50c solution is within about four sigma of this value. The Mariner 9 data substantially reduce the formal error for these coefficients. We interpret this to mean that the Mariner 9 data need to be deweighted slightly (in the next solution) probably due to being plagued with gas leaks (O'Neil, 1973). The principal axes solutions are determined from the second degree coefficients and are given in Table 2.

The surface acceleration for Mars50c is displayed in Figure 6, with the GMM1 model displayed in the same format in Figure 7 for comparison. The acceleration is the radial acceleration

Table 2: Mars Principal Axes

	Viking Only (Mars50b)		Viking + Mariner 9 (Mars50c)		GMM1	
Axis	Latitude	Longitude	Latitude	Longitude	Latitude	Longitude
1	7.37579e-4	-15.2553	5.07064e-4	-15.2537	7.54161e-5	-15.2560
2	-6.41498e-4	74.7447	1.46352e-4	74.7463	2.58292e-4	74.7440
3	89.9990	123.730	89.9995	-179.154	89.9997	-121.533

at the reference sphere of 3394.2 km in milligals from all the gravity coefficients except the J_2 term. The models are very similar and differ the most in the Tharsis region. The geoid from Mars50c is displayed in Figure 8 (again without J_2) with the Tharsis rise clearly evident.

One method to test the degree strength is to plot the unconstrained gravity solutions for truncations of the global SRIF array at various degrees. The degree strength of Figure 4 matches fairly well with plots of the unconstrained solutions of degree 20, 30 and 40 as displayed in Figures 9, 10, and 11. The higher and lower latitude regions in Figure 9 have gravity amplitudes that oscillate wildly outside the bounds of the contour line values. The equatorial band is determined to about degree 30, the north polar region is determined to about degree 20, and the south polar region is determined to about degree 15.

The uncertainty in the surface acceleration and geoid are displayed in Figures 12 and 13. The uncertainties mostly represent the errors up to the degree strength. The high uncertainties in the Tharsis region are due to the relaxing of the a priori over those regions and include errors for the degrees greater than the degree strength (i.e., 30 to 50). The rms magnitude spectrum is displayed in Figure 14 along with the spectrum from GMM1 and the expected Kaula rule for Mars ($13 \times 10^{-5}/n^2$). The power in the Mars50c gravity field is substantially greater than the power of the GMM1 model and is closer to the expected spectrum as given by the Kaula rule.

The residuals for all the data arcs are displayed in Figures 15 and 16 for Viking 1, in Figures 17 and 18 for Viking 2, and in Figure 19 for Mariner 9 with the Viking arcs divided into the high- and low-altitude arcs. The rms fit for both gravity fields uses the identical modeling assumptions and is converged for that particular gravity field. The Mars50c model has an advantage in that it is determined from these arcs, whereas the GMM1 solution uses different time spans. There is slight improvement versus the GMM1 model for many of the arcs but with especially good improvement for the December 9,1977 arc of Viking 1, which has low multiple periapse passes over Tharsis (the spike in Figure 16). The groundtrack for this arc is displayed in Figure 20 with a symbol plotted every 60 seconds (the actual observations do not completely cover Tharsis). Also during this time, there are several uncoupled attitude maneuvers that are estimated and no doubt absorb some of the gravity signature for both GMM1 and Mars50c. The residuals of this arc for Mars50c and GMM1 are displayed in Figures 21 and 22. Also, there is fairly good improvement for the low-altitude Viking 2 data (300 km periapse) as shown by Figure 18. The increase in rms for the November 1976 time frame is due to solar conjunction.

The surface acceleration for the Tharsis region for Mars50c and GMM1 is displayed in Figures 23 and 24. The scale of these plots is such that they can be overlaid on top of the U.S. Geological Survey (USGS) topographic map of Mars. The Mars50c peaks for the Tharsis volcanos line up very well with the topographic highs and the circular region just to the northwest of Olympus appears in the gravity field. Table 3 is a comparison of selected peak values in milligals at the reference surface and their percent increase of Mars50c over GMM1. By comparing the no a priori solution for degree 30 (Figure 10) with the Mars50c model, it appears that the peak for Isidis should be increased by about 100 milligals by relaxing the surface constraint over Isidis. This is one of the fine-tune adjustments that we plan to incorporate in the next solution. The geoid peaks for Mars50c (see Figure 8) are 1560, 1460, 1500, and 1560 meters for Olympus, Arsia, Pavonis, and Ascraeus, respectively.

Figure 25 shows the groundtrack of a low periapse pass of Viking 2 over Olympus Mons and Arsia Mons where the points on the plot are the actual Doppler observation locations. Figures 26 and 27 show the residual fit for both Mars50c and GMM1 for Olympus Mons and Figures 28 and 29 show the residual fit for the pass over Arsia. The increased peak values of the volcanos reduce the residual amplitude to near the data noise for Arsia and from 20 mm/s to 3 mm/s for

Table 3: Comparison of Peak Values for Surface Features

Peak	Mars50c	GMM1	Percent Increase
Olympus	2387	1438	66
Arsia	1646	844	95
Pavonis	1221	716	71
Ascraeus	1547	861	96
Alba	574	537	7
Isidis	331	246	35
Elysium	378	252	50
North Pole	95	-4	
South Pole	232	127	83

Olympus. Unfortunately, we have not been able to obtain the 10-second data to better examine the remaining signature in the residuals (which are 60-second Doppler points). However, a signature still remains for Olympus Mons suggesting that a gravity field greater than degree and order 50 is needed to model Olympus or that the a priori on the surrounding Tharsis region must be relaxed further. Also, when we apply a straight Kaula a priori on the gravity spectrum and not the spatial a priori, the residual amplitude of Olympus is 9.0 mm/s and the peak gravity value of Olympus is 1733 milligals. So for the Kaula rule solution, there is a substantial reduction in the gravity peak amplitude, and we believe it is further from the true peak value because of the increase in residual amplitude. Figure 30 shows the groundtrack of the Viking 2 low-altitude pass over Pavonis and Ascraeus with the plot symbols again showing the actual Doppler observation locations. The residual plots for Mars50c and GMM1 over these two volcanos are shown in Figures 31, 32, 33, and 34. The residual amplitude for Pavonis is reduced but some gravity signature remains. The residual peak for Ascraeus does better and is reduced to near the data noise. Again, it would be helpful to have the 10-second data. By adjusting the a priori further, obtaining the 10-second Doppler data, and possibly solving to a higher harmonic degree, we should be able to eliminate all the gravity signature in the residuals over the Tharsis volcanos.

Figures 35 and 36 show the Tharsis volcano peak values and their uncertainties versus the harmonic degree at the reference sphere. The peak values are the sum of the contributions for all the degrees up to the indicated degree and not the individual degree contributions as in Figures 3 and 5. We trust the peak values and uncertainties up to degree 30. However, beyond degree 30, the amplitudes may still be suppressed somewhat because the a priori constraint on the surrounding region constrains the coefficients of degree 30 and higher. The uncertainty of the peaks up to degree 40 (60-80 milligals) matches the surrounding uncertainty as given by Figure 12 (i.e., the Olympus peak is 2300 ± 80 for degree 40). The uncertainty for degrees greater than 40 may be realistic in that the true amplitude may be several sigma greater than the Mars50c amplitude, but we do not expect that the true amplitudes are less than the Mars50c amplitudes.

The observed gravity peak values for Olympus Mons, Arsia, Pavonis, and Ascraeus listed in Table 3 are not beyond bounds for the theoretical gravity based on best volume calculations (Wu et al., 1984, 1988). Assuming an average density of 2.7 gm/cm^3 and an uncompensated load, the theoretical gravity of Olympus Mons based upon three flat disks is 2498 milligals with respect to a 2-km high base plain. Assuming a 9-km high base plain, the theoretical gravity peaks for Arsia,

Pavonis, and Ascraeus are 1859, 1309, and 1564 milligals, respectively. For comparison, the observed gravity values must be corrected for the gravity of the surrounding plains. From Figure 23, the correction is small for Olympus and several hundred milligals for Arsia, Pavonis, and Ascraeus. It appears that the volcanos are mostly uncompensated.

We also calculated the theoretical gravity from topography for Olympus using spherical harmonics. The elevations of Olympus were read off the USGS map (see USGS 1982 reference) for Olympus at an interval of one degree for the bounds of -140 to -128 degrees E longitude and 13 to 25 degrees N latitude. A 75th degree and order spherical harmonic model was then fit to this data. Figure 37 shows again the observed gravity peak value versus harmonic degree, but with the gravity from topography shown as well for no compensation and Airy isostatic compensation at depths of 200 and 250 km. For the compensated gravity profiles, we added a bias of 250 milligals to make the gravity from topography match the observed gravity at degree 10 since the surrounding plain around Olympus is not included in the topography, and we used 3.95 gm/cm^3 as the mean density for Mars. Assuming full Airy isostatic compensation, the compensation depth for Olympus is 250 km. Figure 38 shows the gravity from topography for partial Airy compensation. For compensation at a Moho depth of 50 km, the root is only 25 percent of the size needed for full isostasy, and at 100 km depth, Olympus is 35 percent compensated. Again, a bias was added to the theoretical gravity to match observed and theoretical gravity at degree 10 (a 100 mgal bias this time). From the theoretical gravity from topography profiles in Figures 37 and 38, we expect the true gravity to increase for the harmonic degrees 40 to 50, as mentioned before. These curves indicate that the true amplitude of Olympus is near 2500 to 2600 milligals, and this is consistent with the remaining signature in the residuals.

7. Conclusions

The Mars50c gravity field is very similar to the previously determined gravity field of Smith et al. (1993), and the only substantial difference is in the peak values of the volcanos in the Tharsis region. These differences are due in part to the inclusion of attitude maneuver information in the solution that was not available for the GMM1 solution, and the method used to constrain the gravity field in the estimation process. The constraint on the gravity field is no longer spectral but spatial and allows the gravity constraint over Olympus and the other volcanos to be relaxed in order to obtain truer peak amplitudes. As a result, the peak amplitude for Olympus almost doubled and indicates much less isostatic adjustment and probably a stronger lithosphere. These results seem warranted from reduction in the resulting residuals of the Doppler observations. We do not expect the peak ampitudes to be any lower, but they may increase several hundred milligals.

We have also outlined changes for further improvement in our work, and these include a better ephemeris for Phobos and Deimos, a new planetary ephemeris, parameters to absorb the ill effects of the gas leaks of the Mariner 9 spacecraft, searching for additional tracking data -- both new passes of data as well as the 10-second Doppler data, and fine-tune adjustment of the spatial a priori constraint on the gravity field (such as the area surrounding Olympus). The 10-second data would surely be of help in testing these results.

Figure 3: Unconstrained Acceleration Uncertainty Profiles

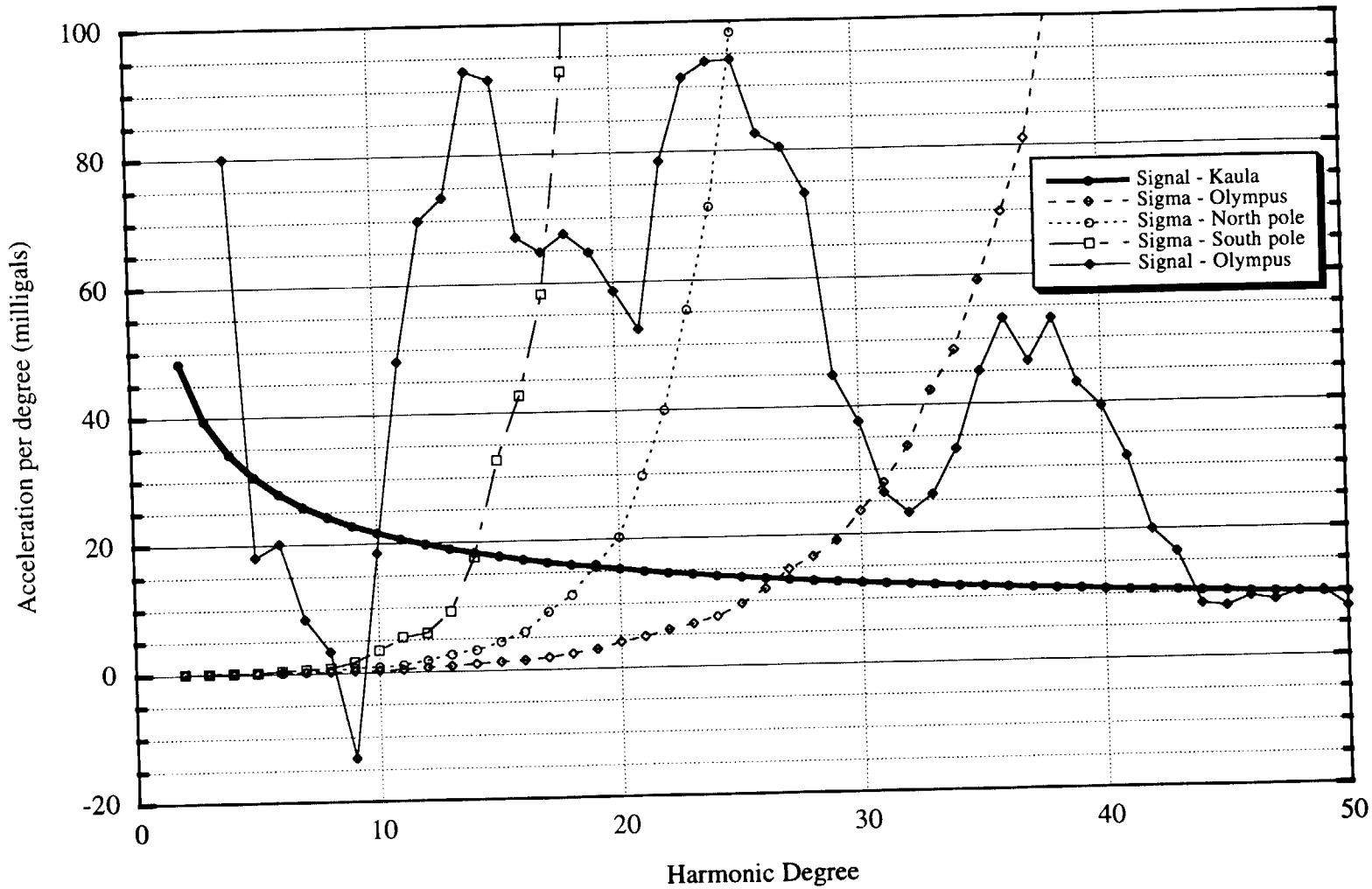

Figure 4: Mars50c Harmonic Degree Strength

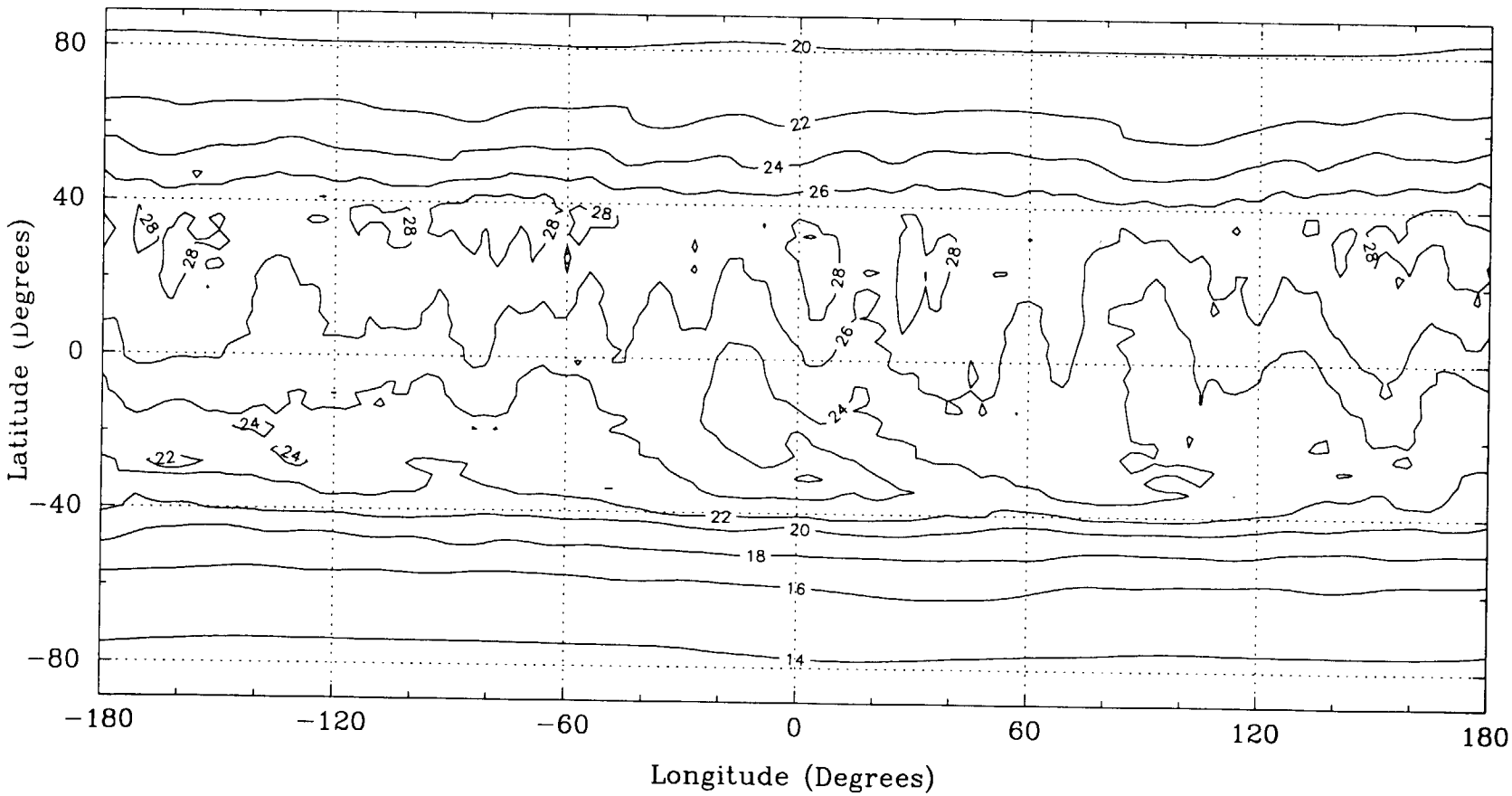

Figure 5: Constrained (Mars50c) Acceleration Uncertainty Profiles

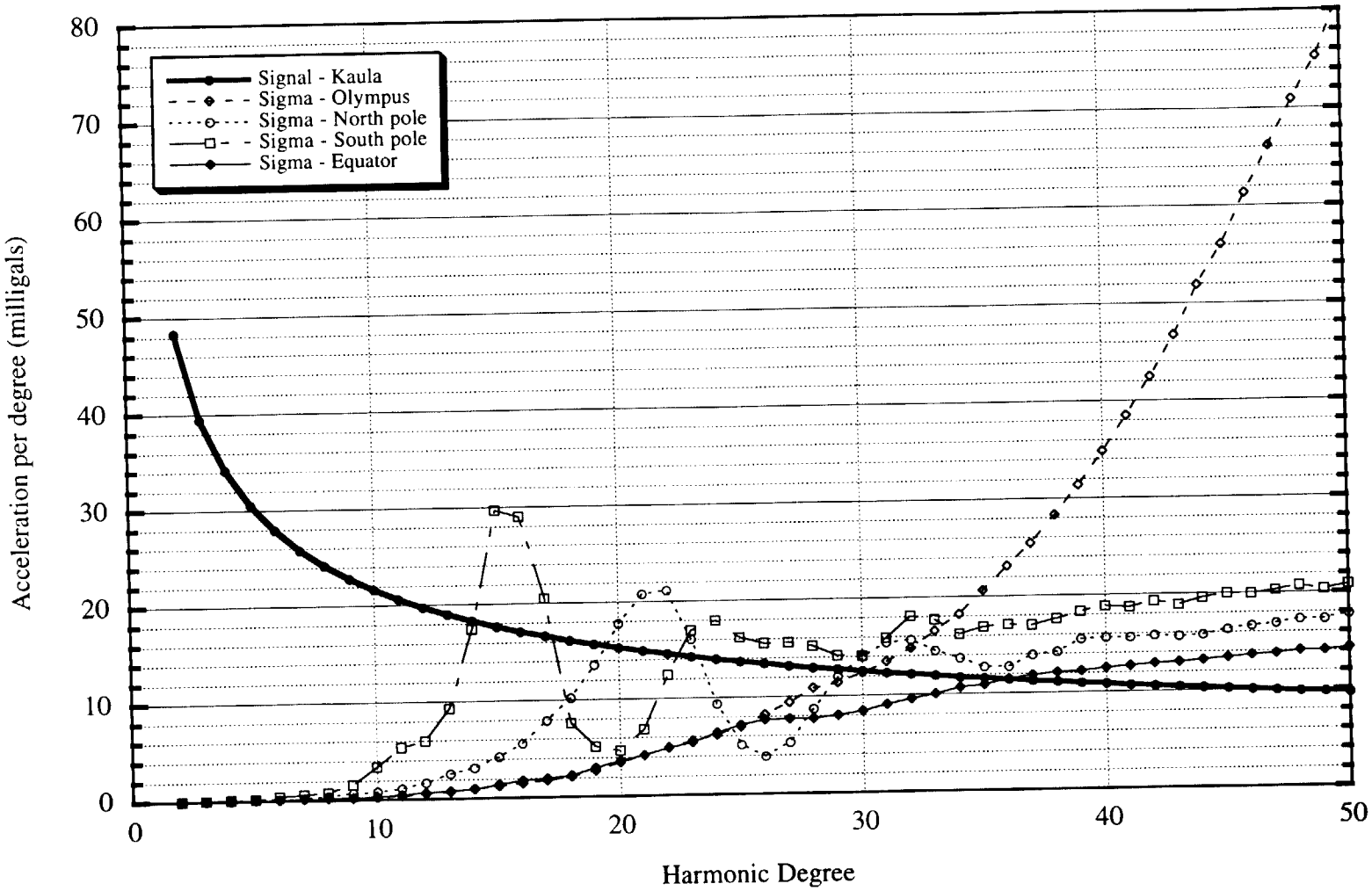

Figure 6: Mars50c Surface Acceleration (mgals, without J2)

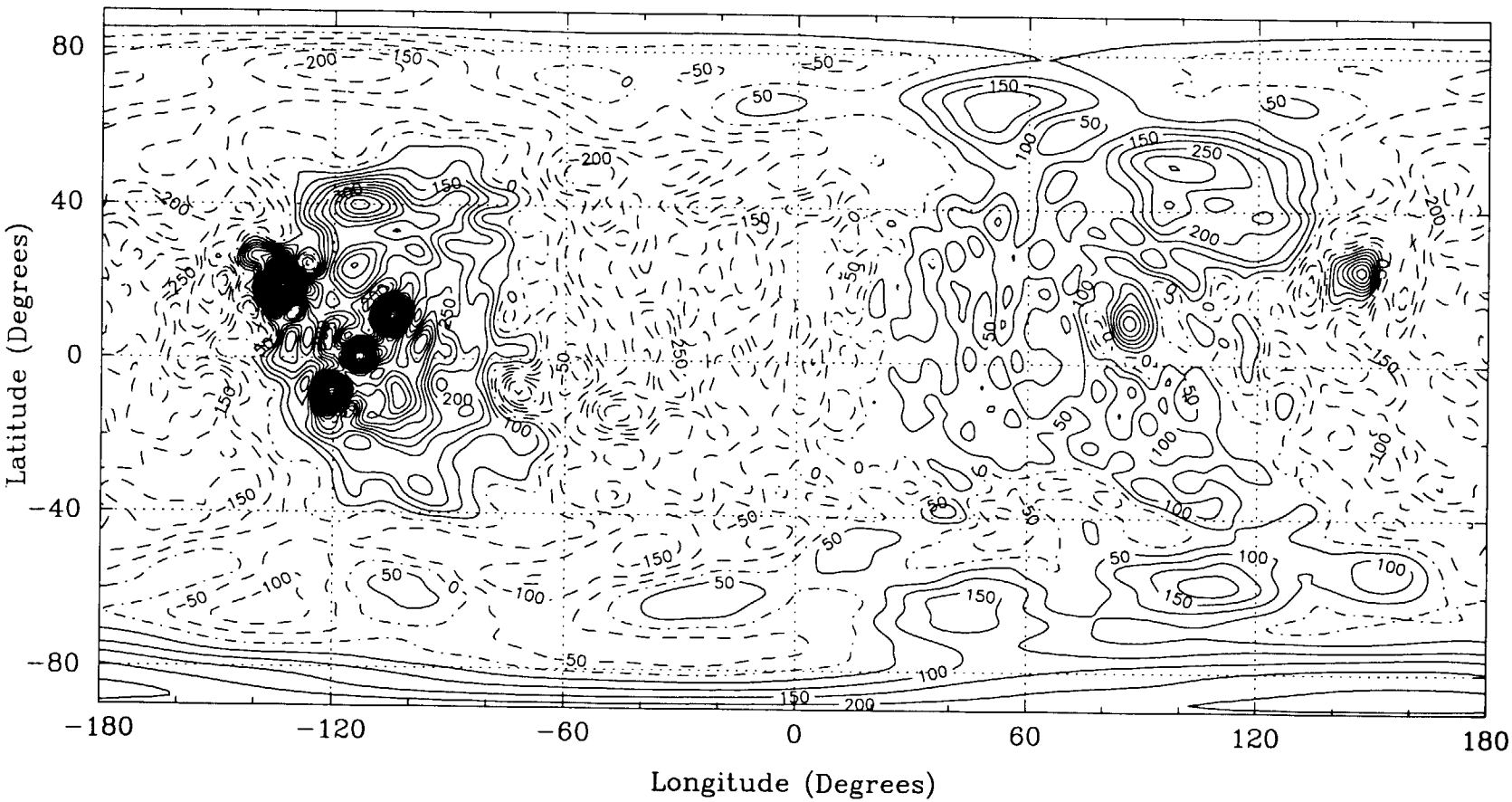

Figure 7: GMM1 Surface Acceleration (mgals, without J2)

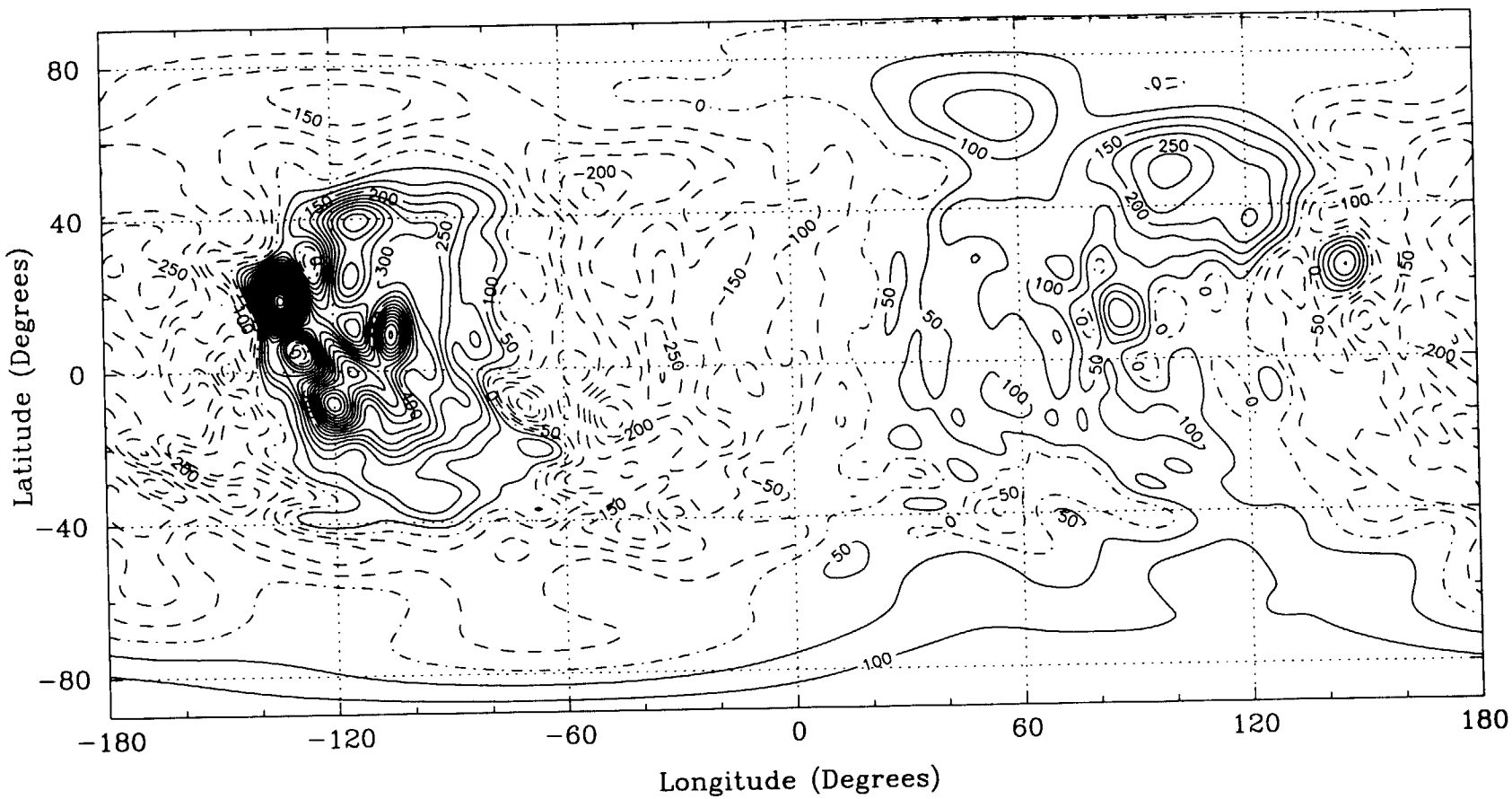

Figure 8: Mars50c Geoid (meters, without J2)

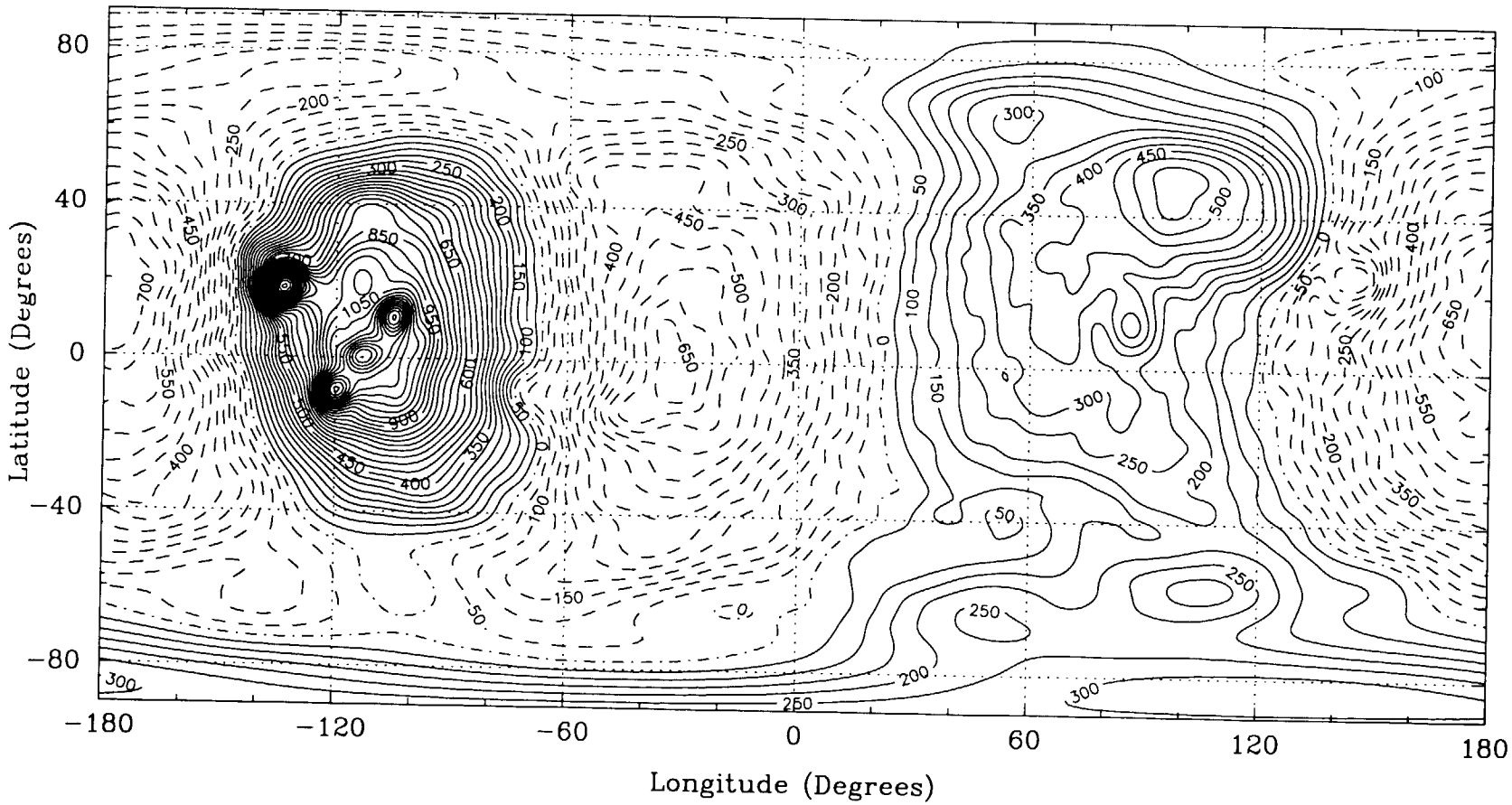

Figure 9: Mars50c No A Priori Constraint, Degree = 40

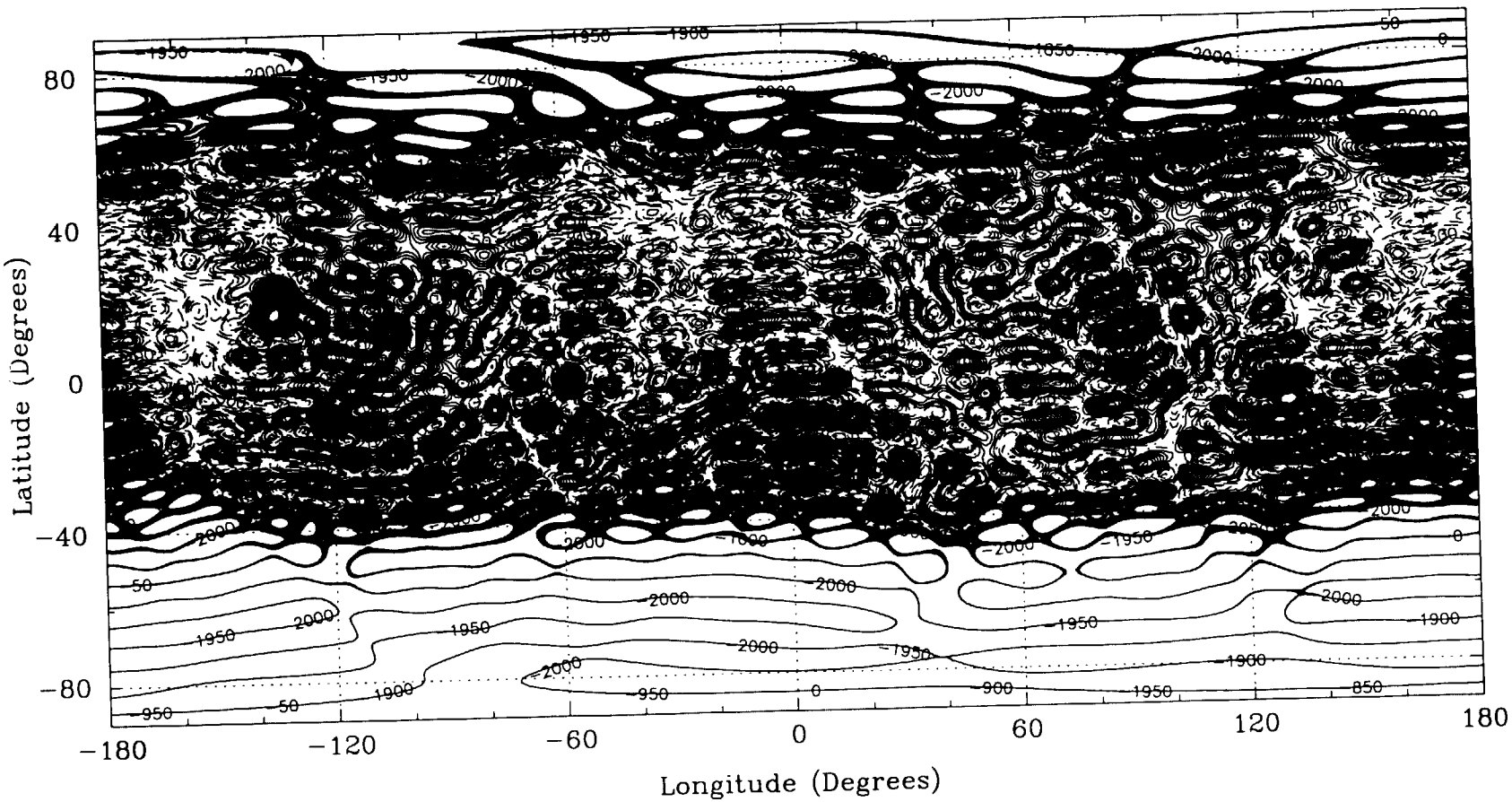

Figure 10: Mars50c No A Priori Constraint, Degree = 30

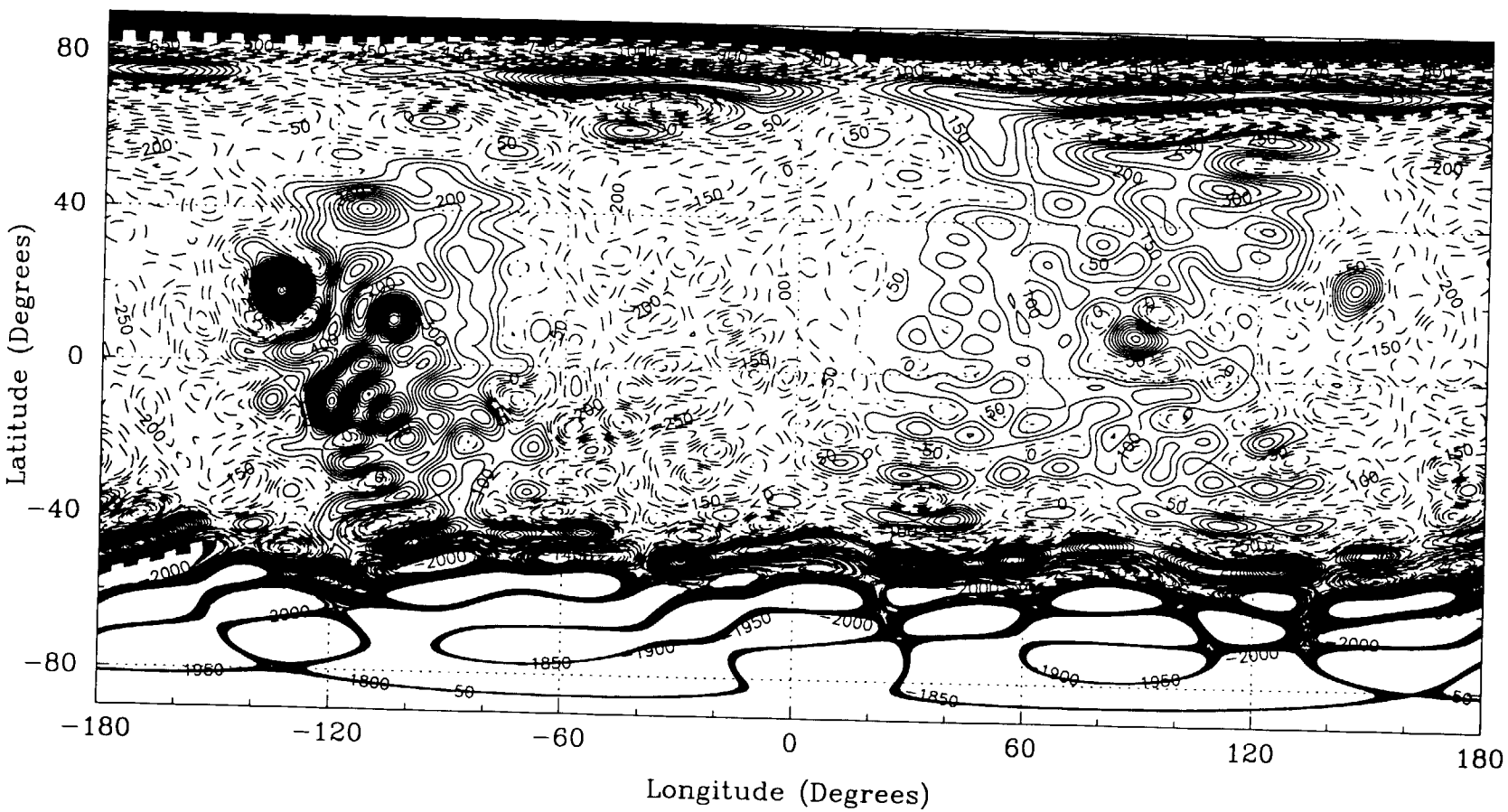

Figure 11: Mars50c No A Priori Constraint, Degree = 20

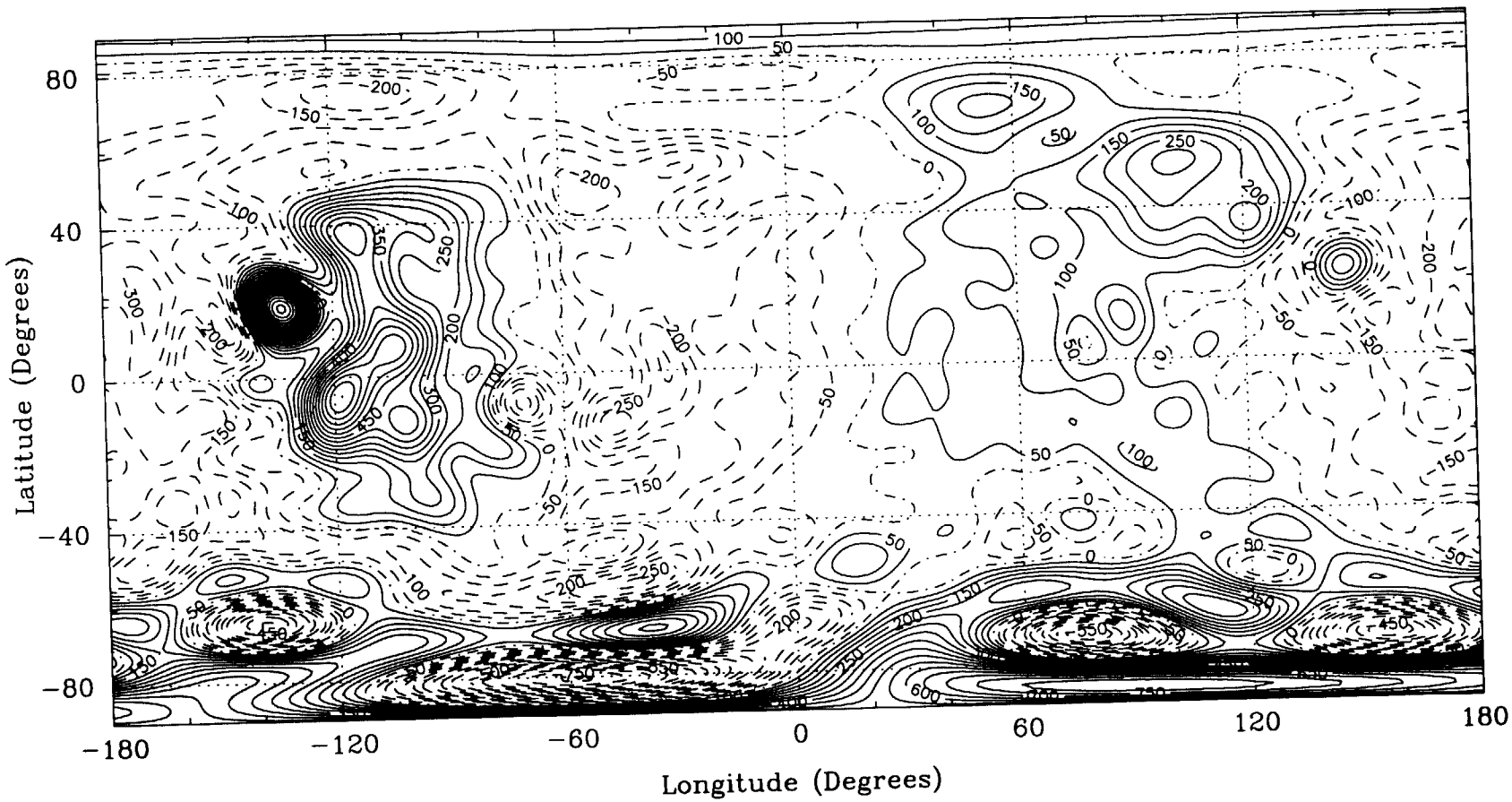

Figure 12: Mars50c Surface Acceleration Uncertainty (mgal)

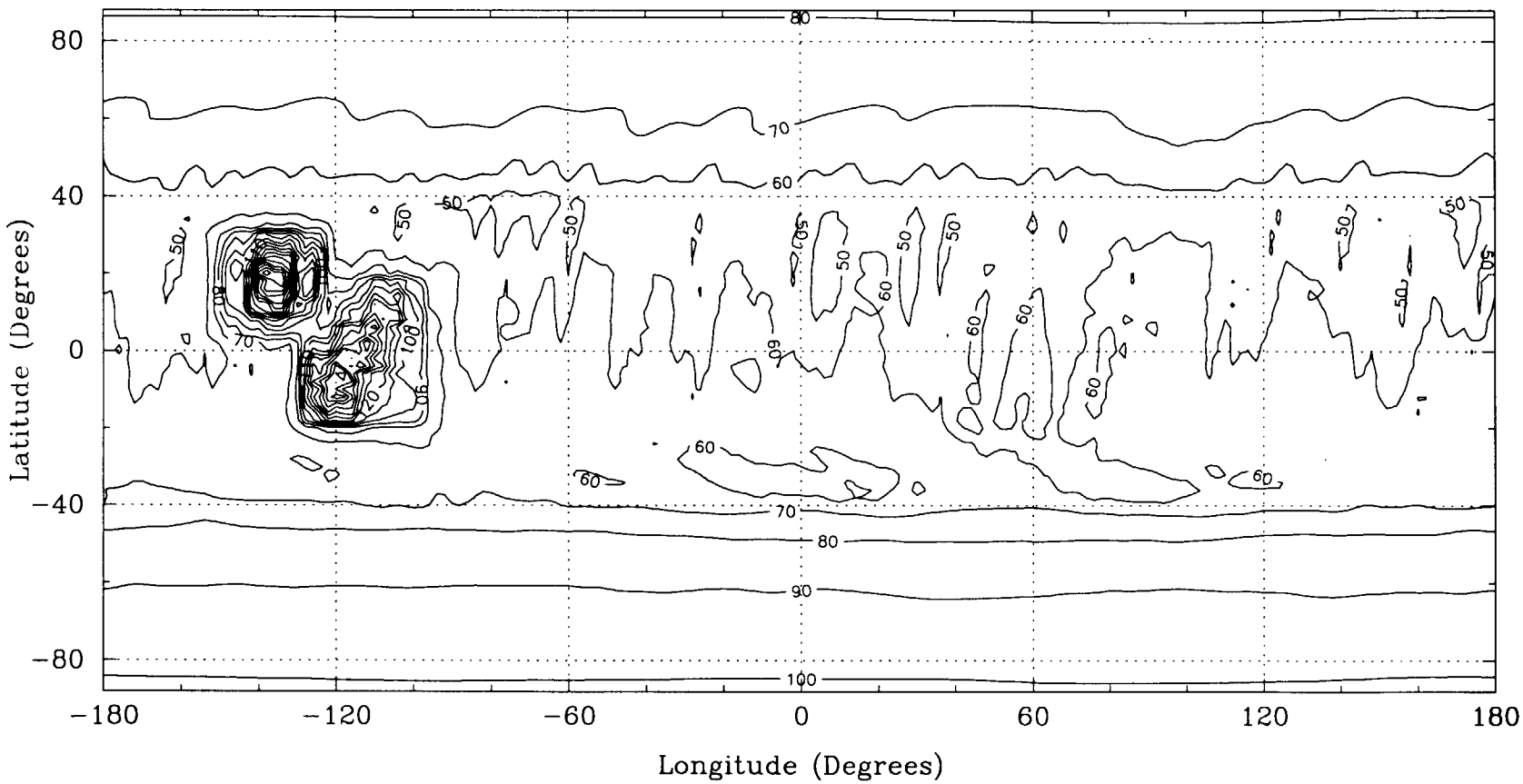

Figure 13: Mars50c Geoid Uncertainty (meters)

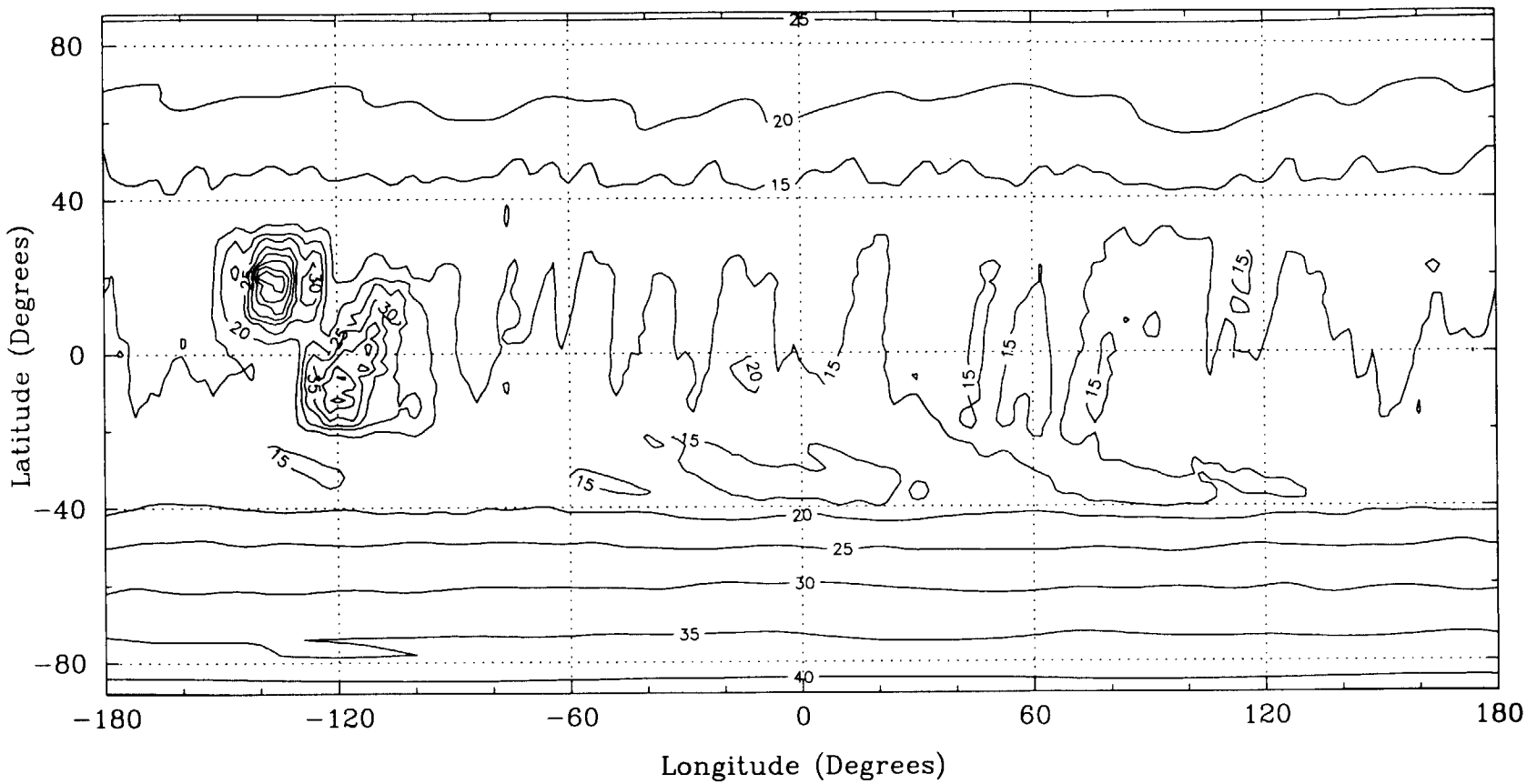

Figure 14: RMS Magnitude Spectrums

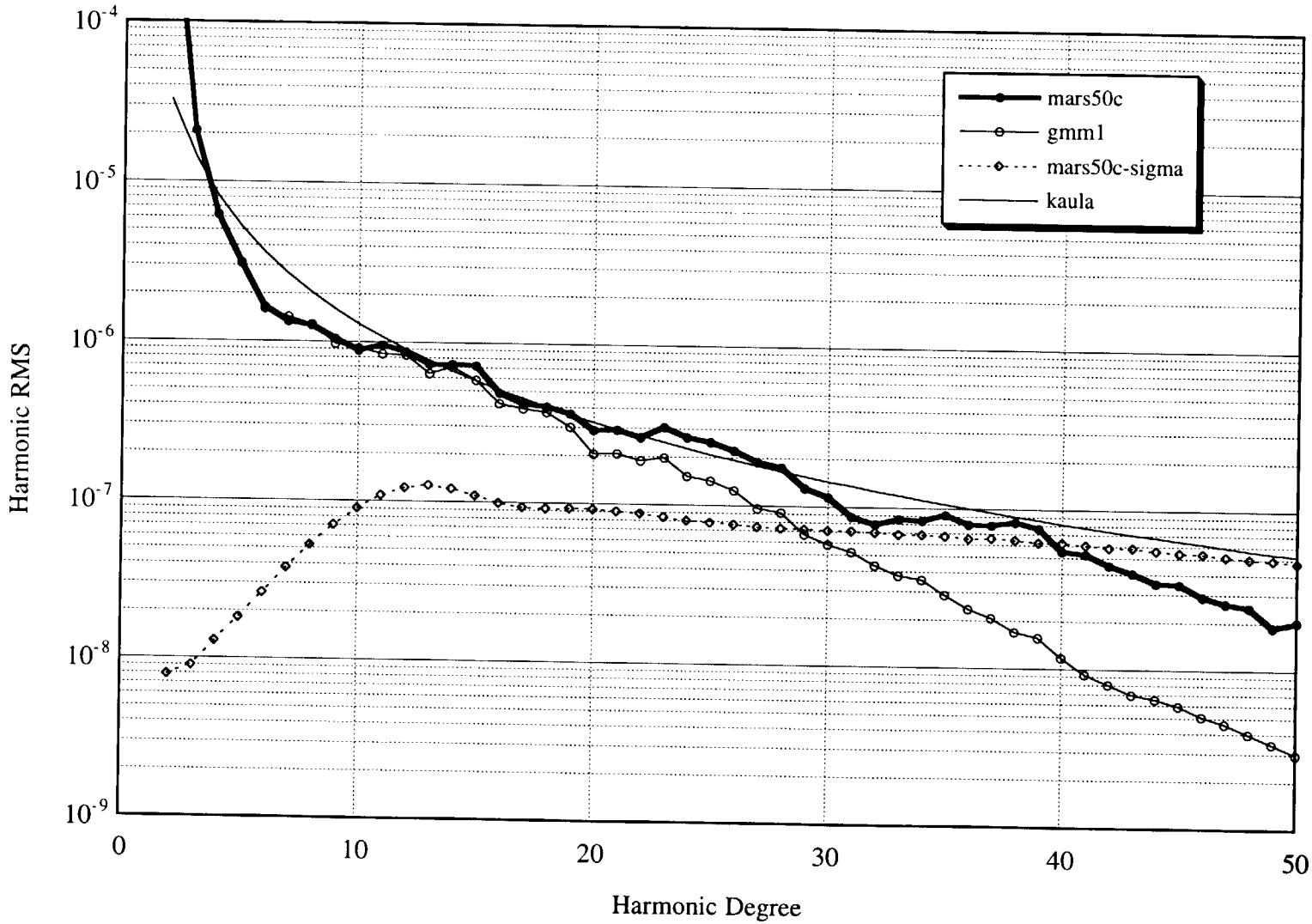

Figure 15: Viking 1 Residual RMS for High Altitude Arcs

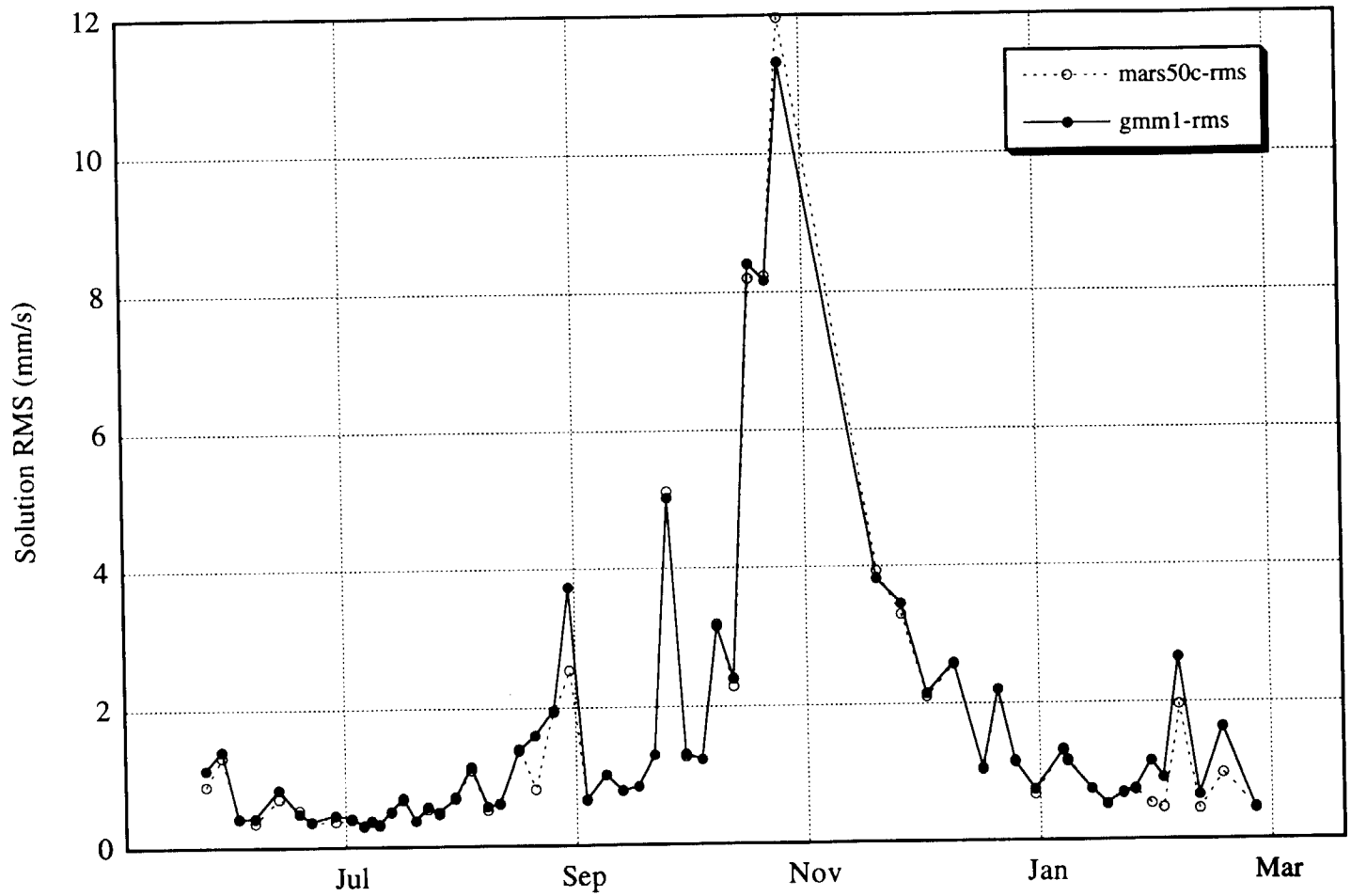

Arcs from Jun 21, 1976 to Mar 10, 1977

Figure 16: Viking 1 Residual RMS for Low Altitude Arcs

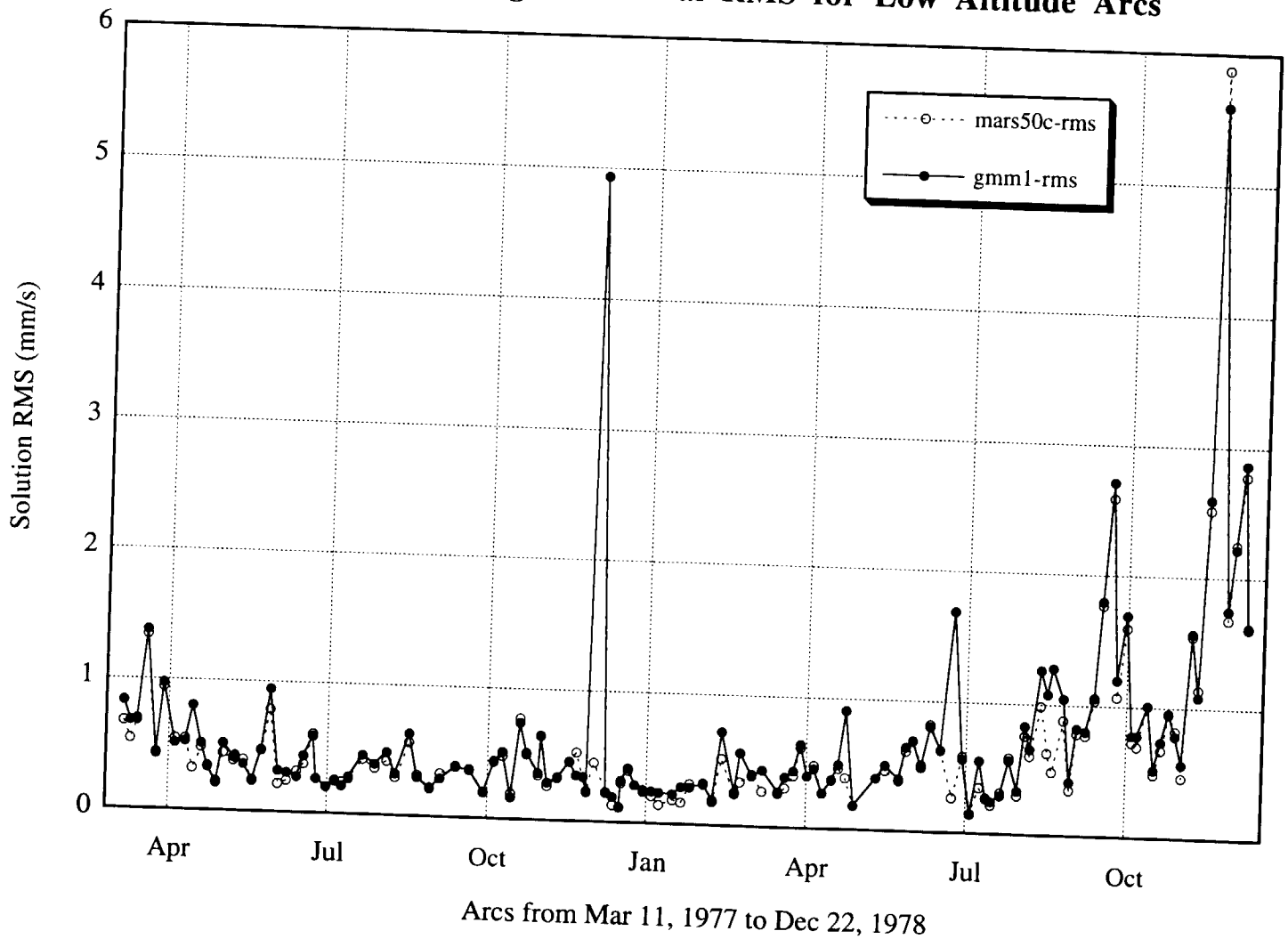

Figure 17: Viking 2 Residual RMS for High Altitude Arcs

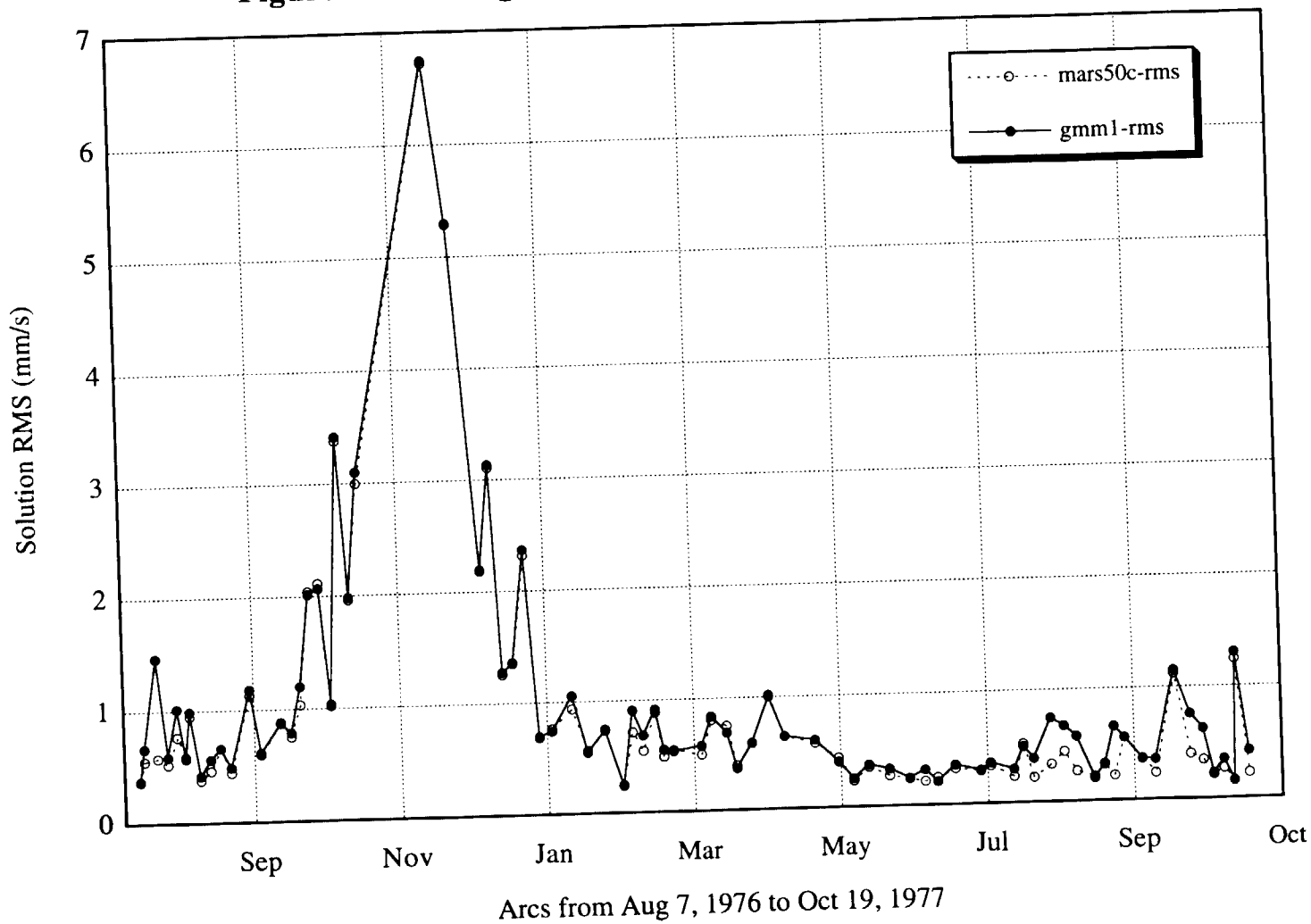

Figure 18: Viking 2 Residual RMS for Low Altitude Arcs

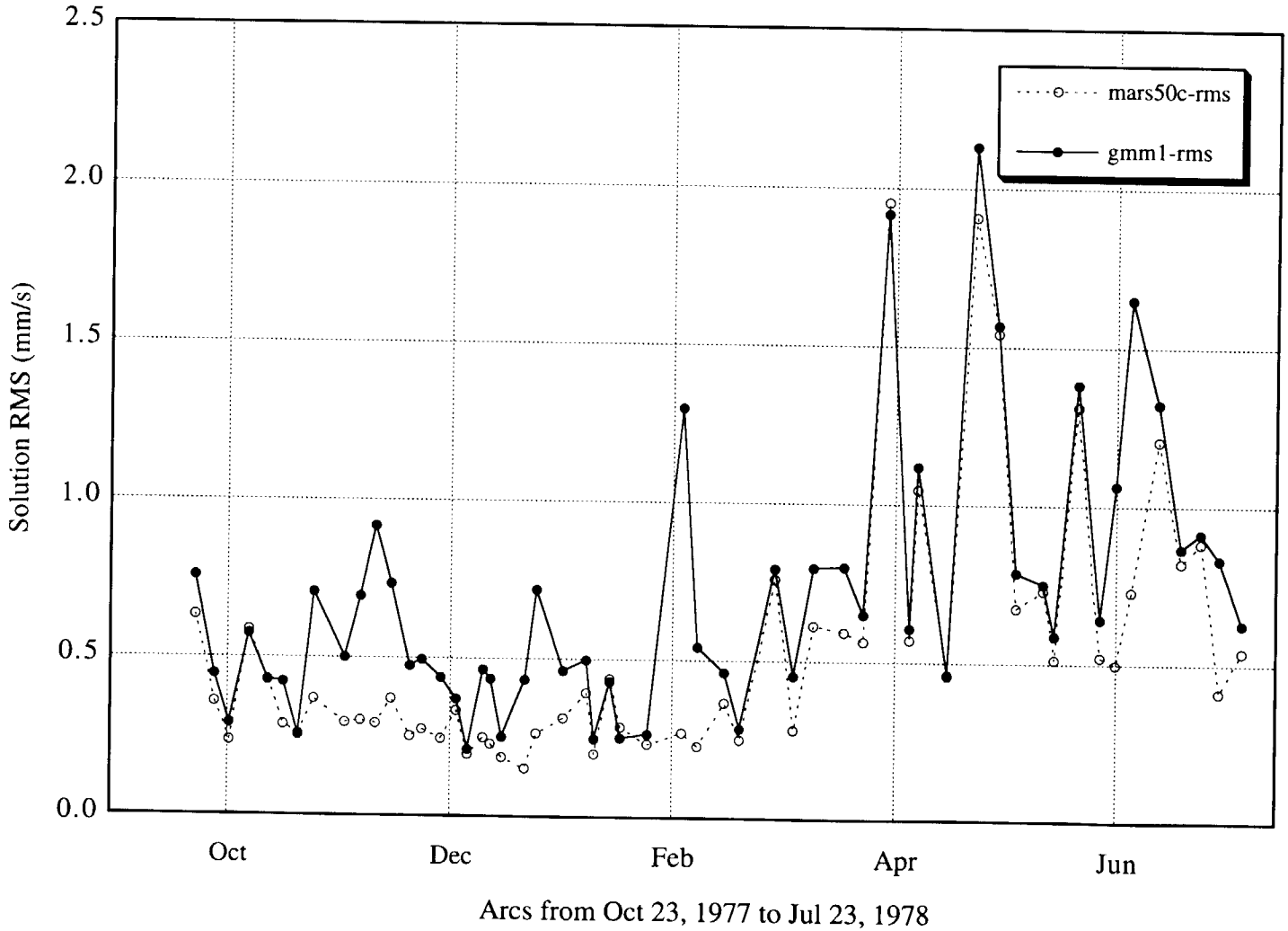

Figure 19: Mariner 9 Residual RMS

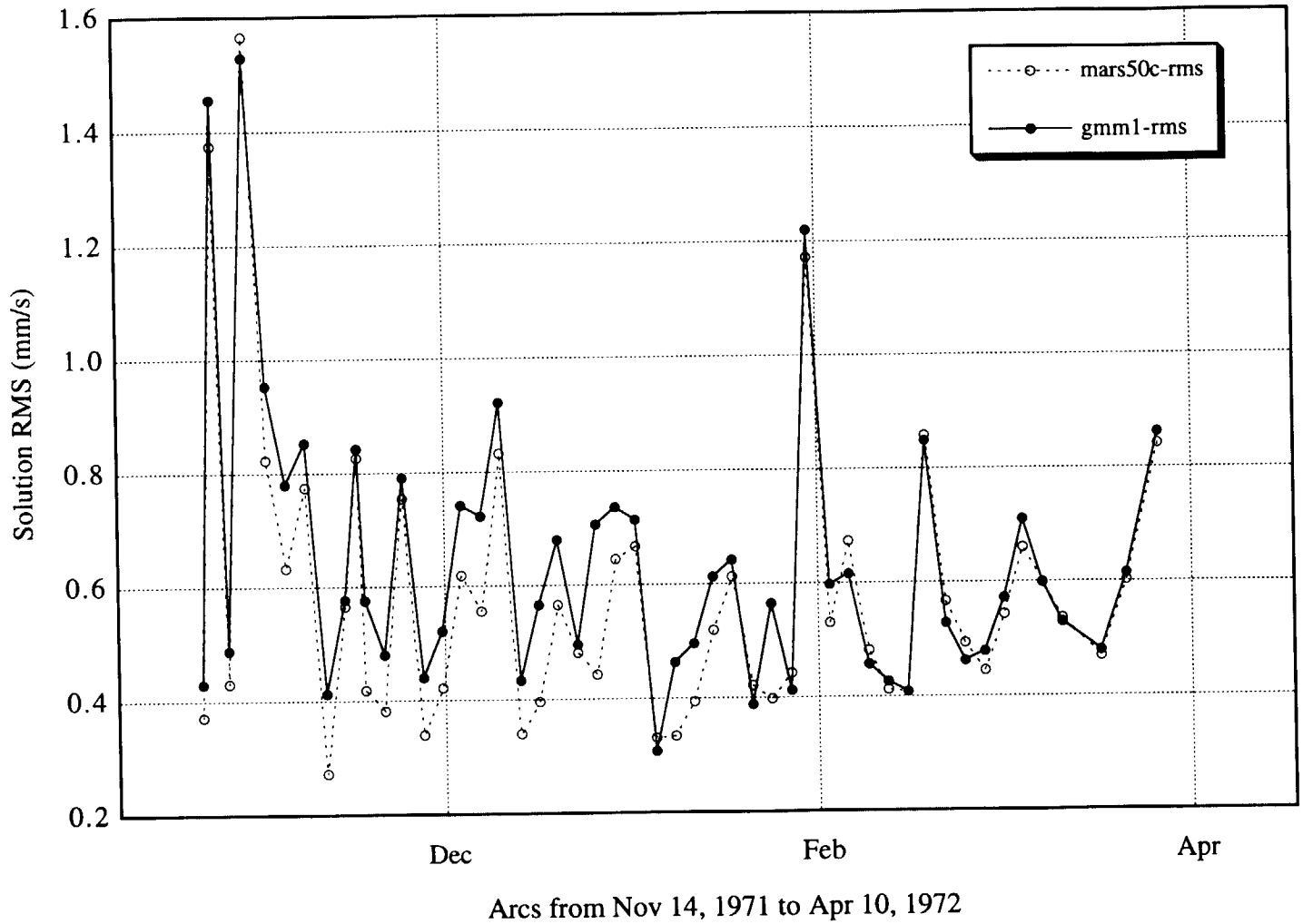

Figure 20: Viking 1 Groundtrack Over Tharsis

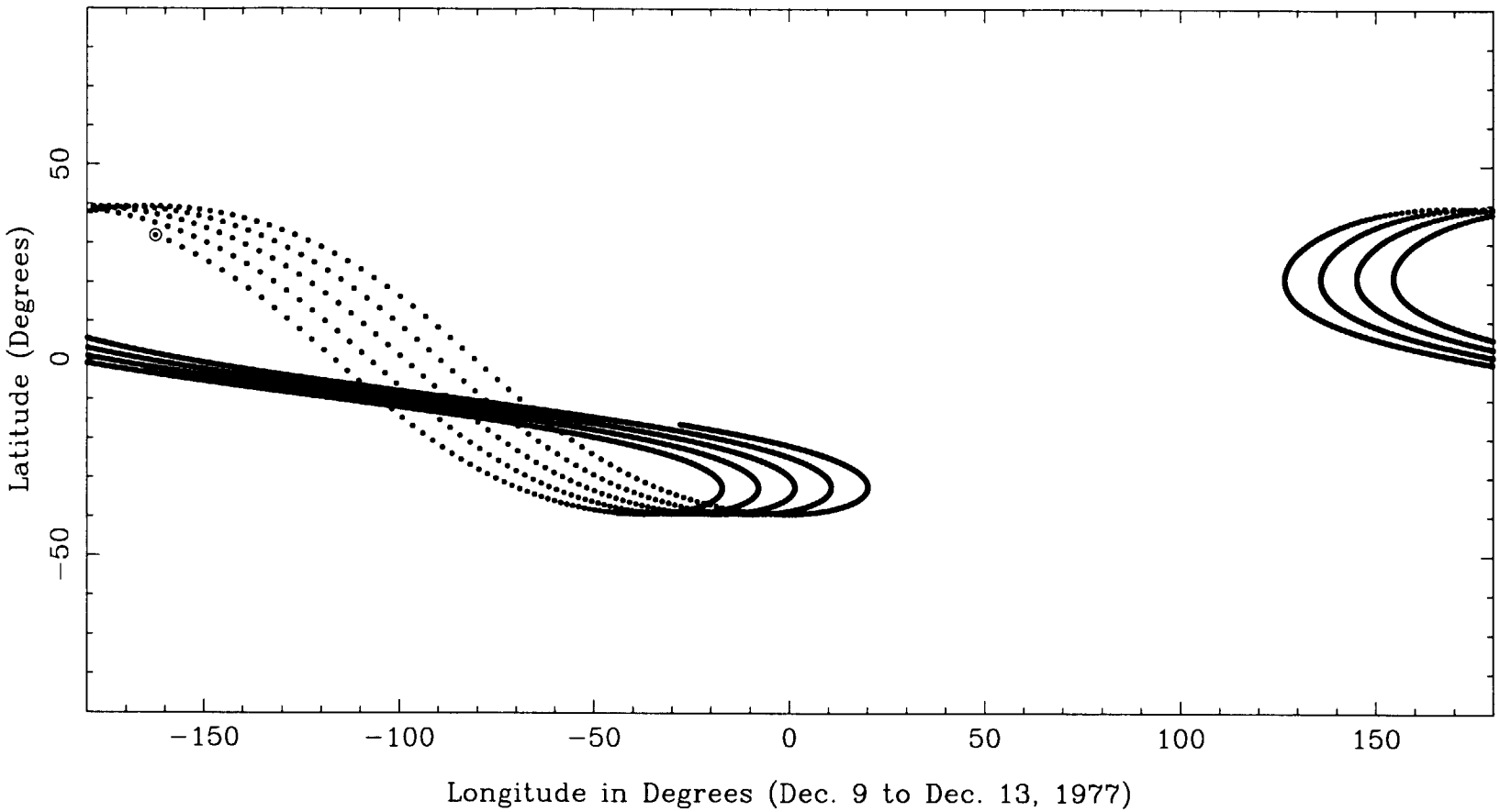

Figure 21: Viking 1 Tharsis Resids for Mars50c

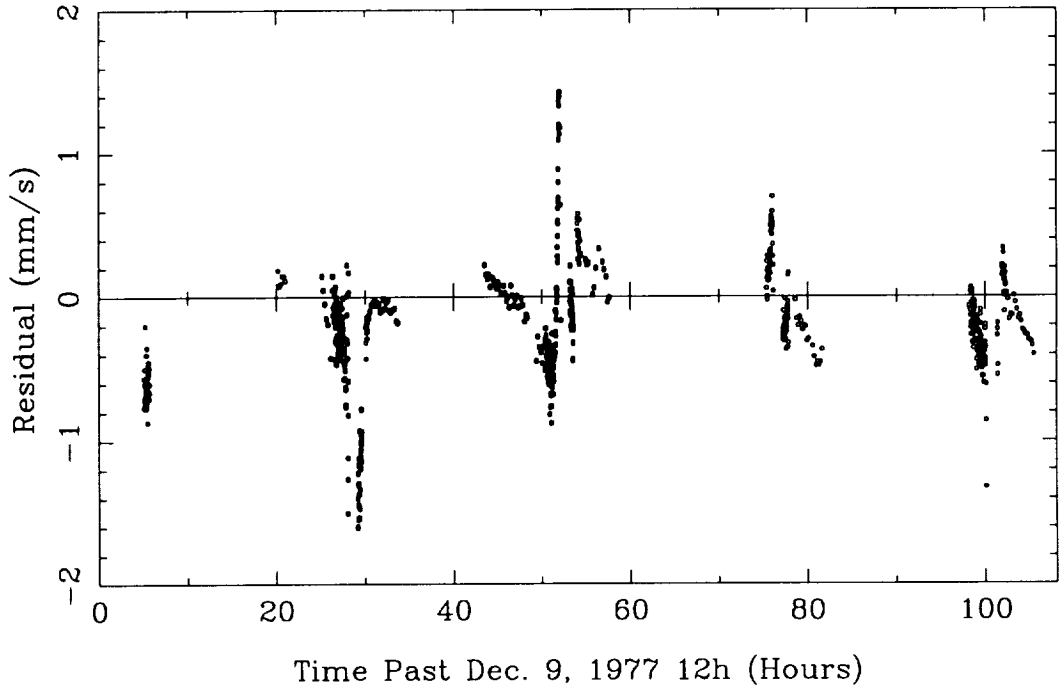

Figure 22: Viking 1 Tharsis Resids for GMM1

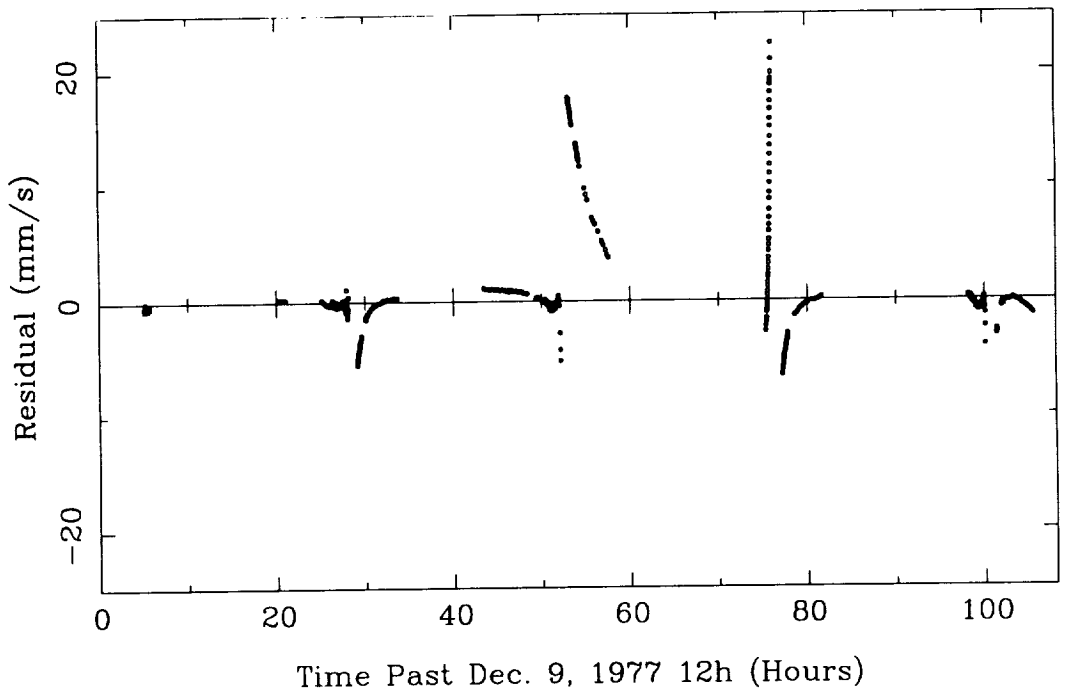

Figure 23: Tharsis Montes for Mars50c

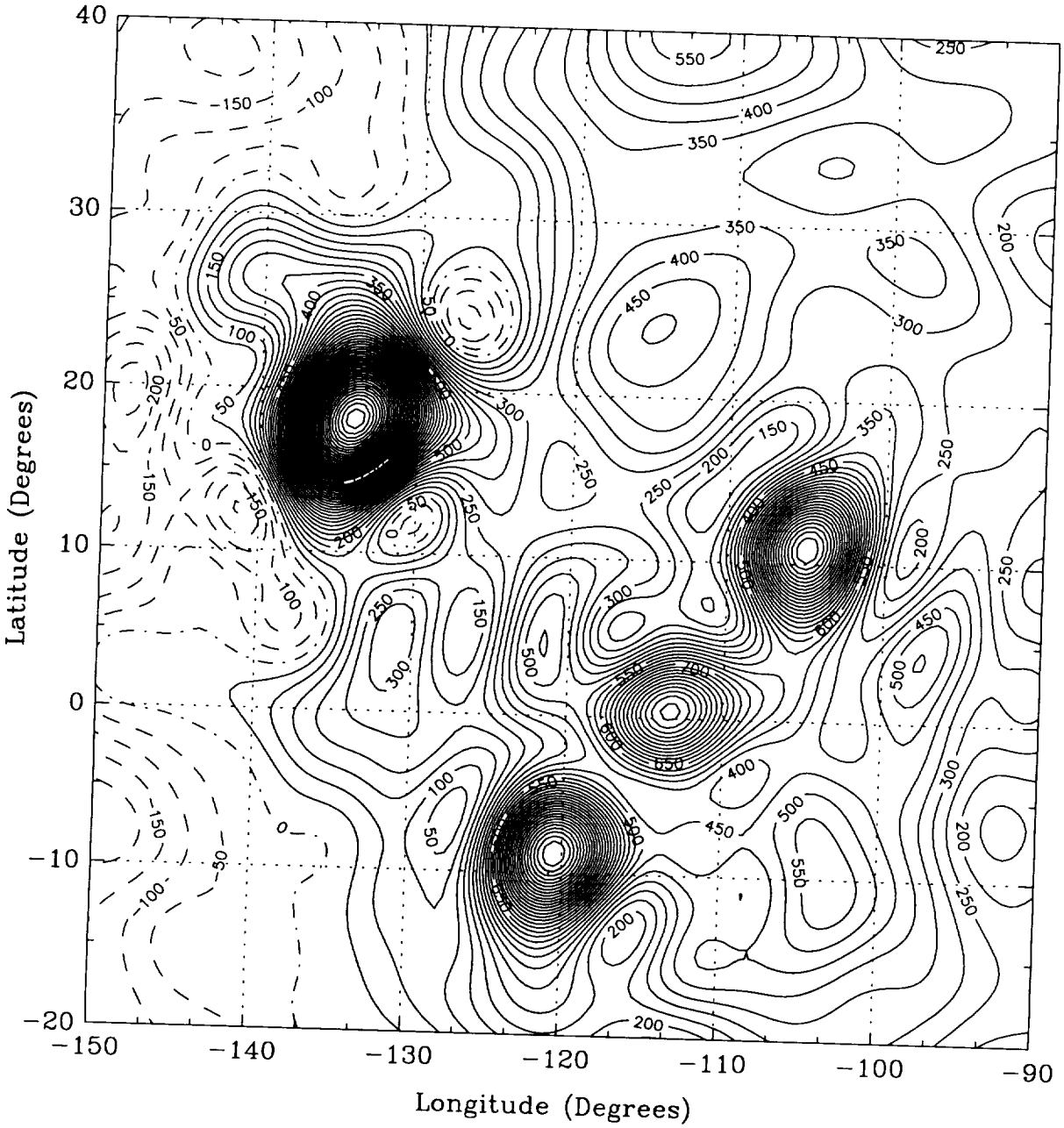

Figure 24: Tharsis Montes for GMM1

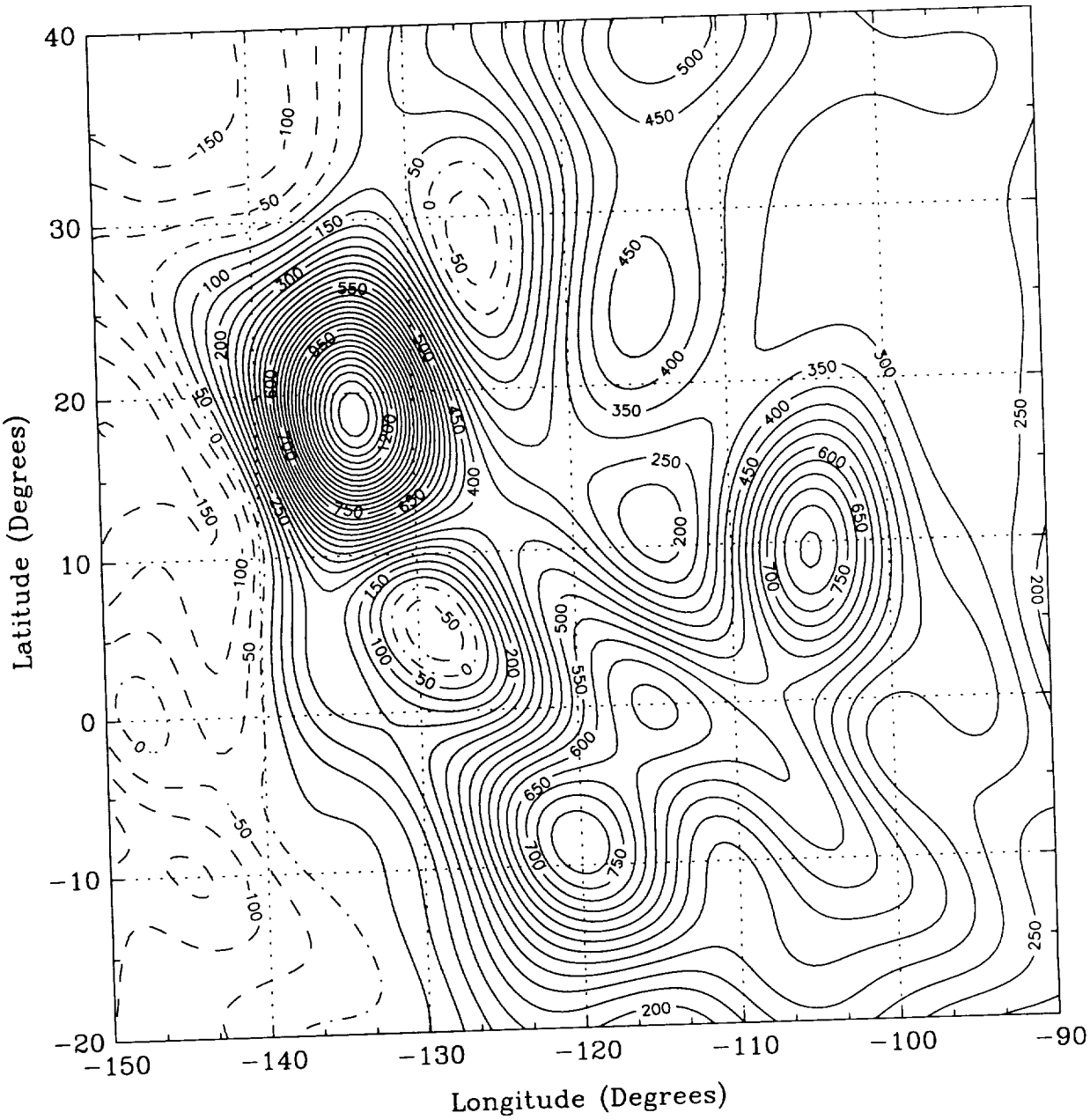

Figure 25: Viking 2 Groundtrack Over Olympus and Arsia

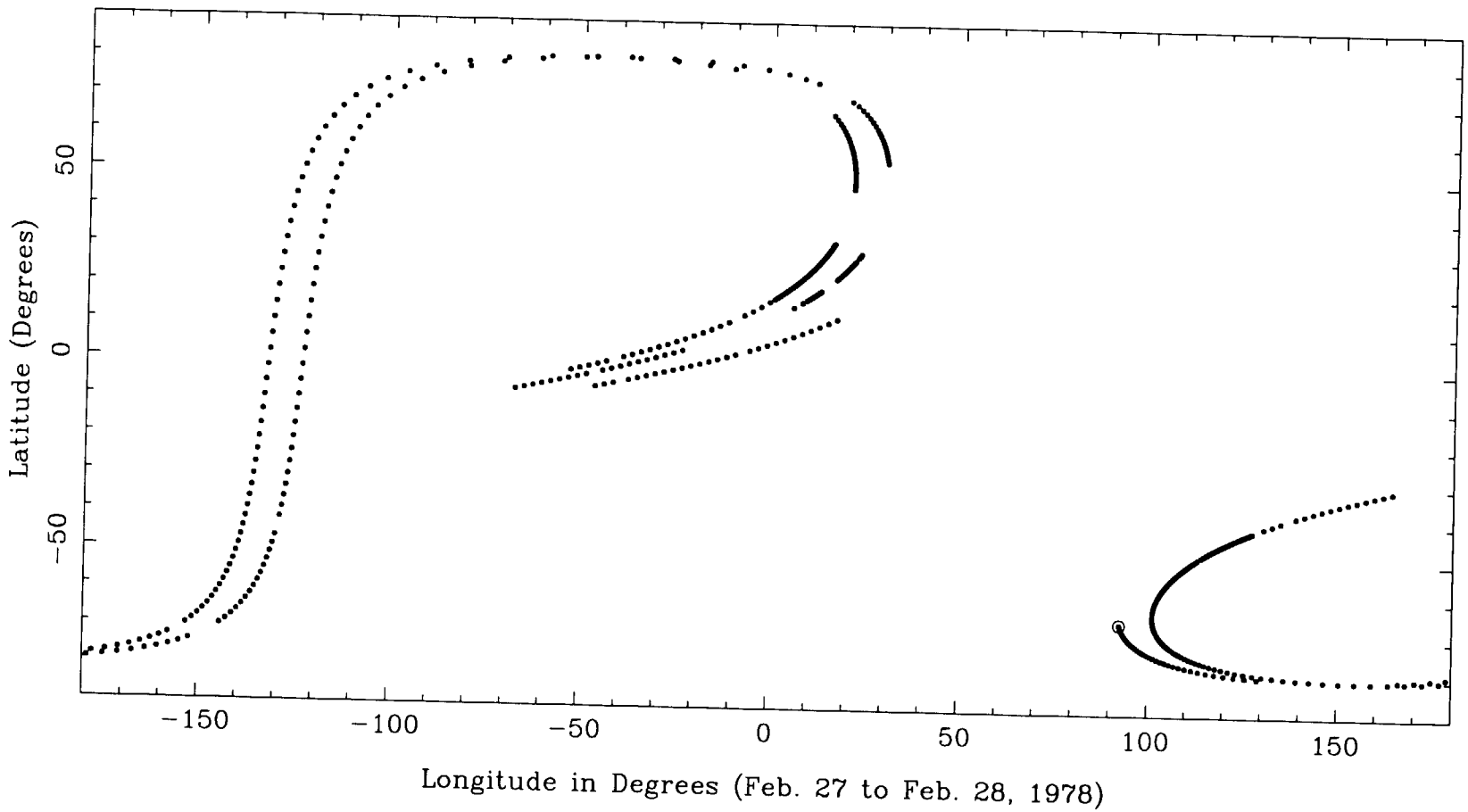

Figure 26: Viking 2 Olympus Resids for Mars50c

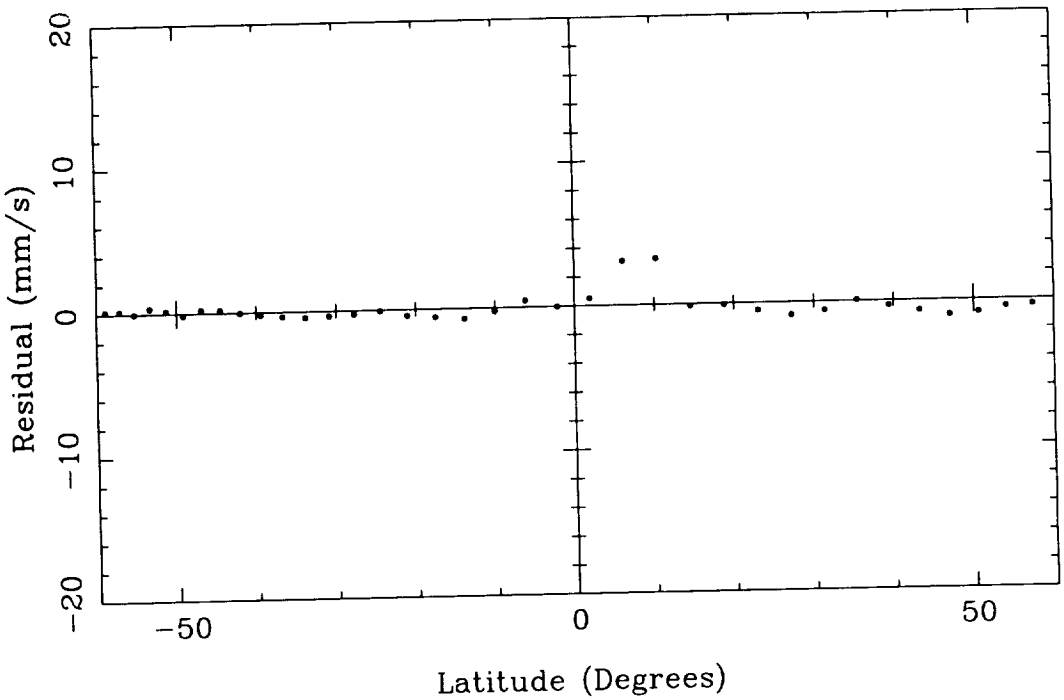

Figure 27: Viking 2 Olympus Resids for GMM1

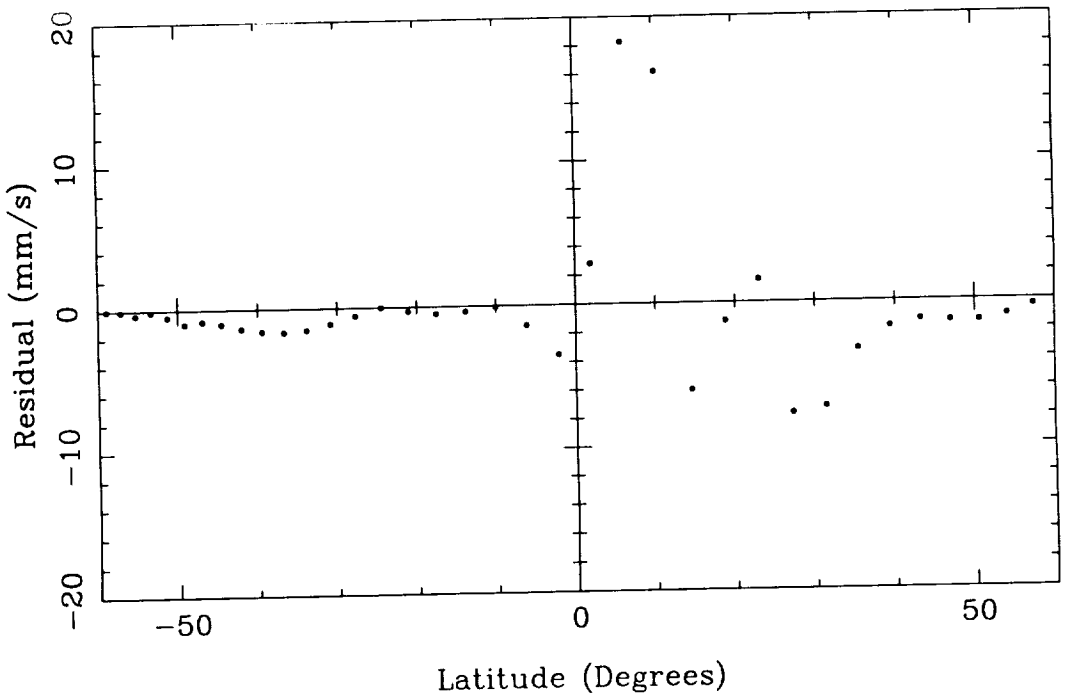

Figure 28: Viking 2 Arsia Resids for Mars50c

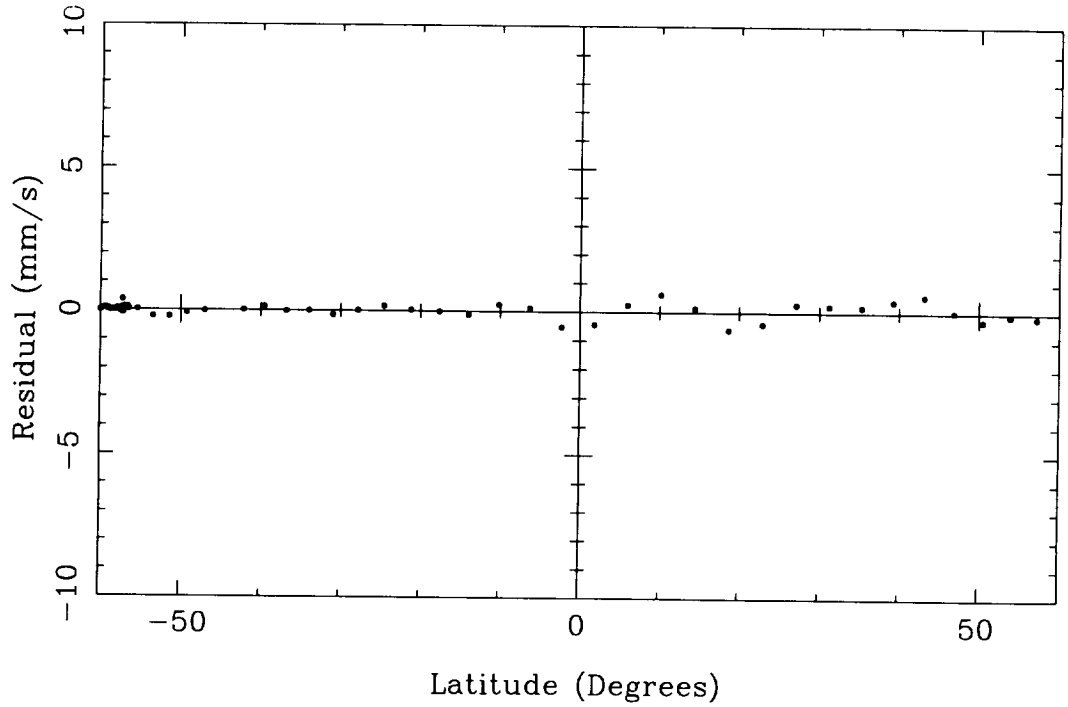

Figure 29: Viking 2 Arsia Resids for GMM1

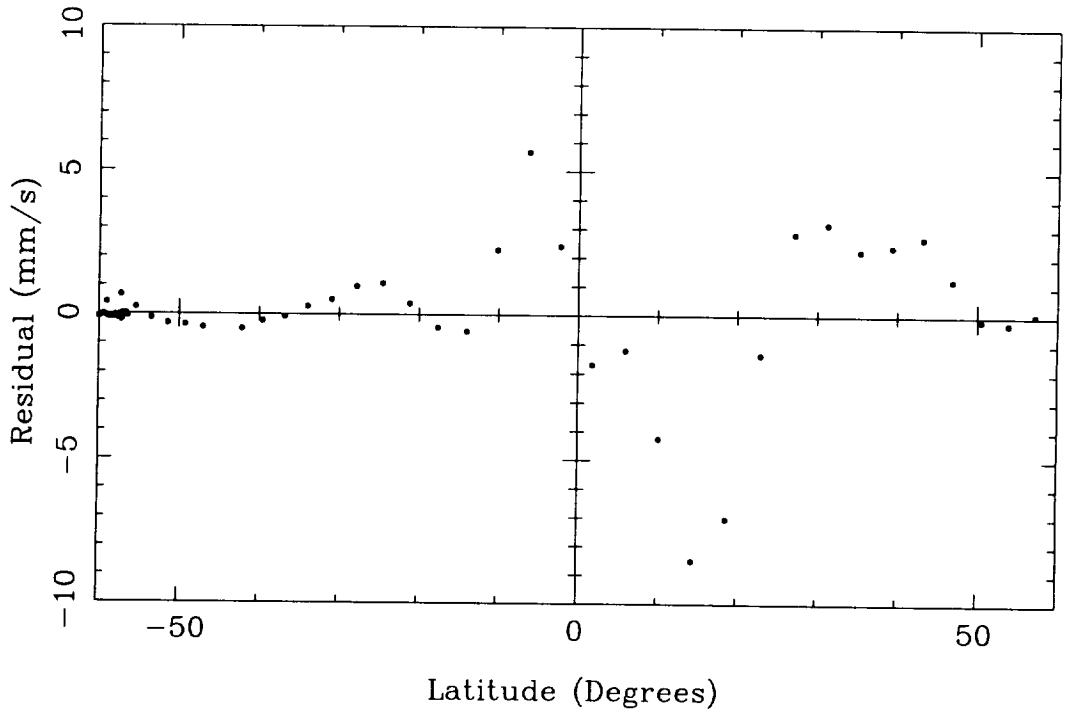

Figure 30: Viking 2 Groundtrack Over Pavonis and Ascraeus

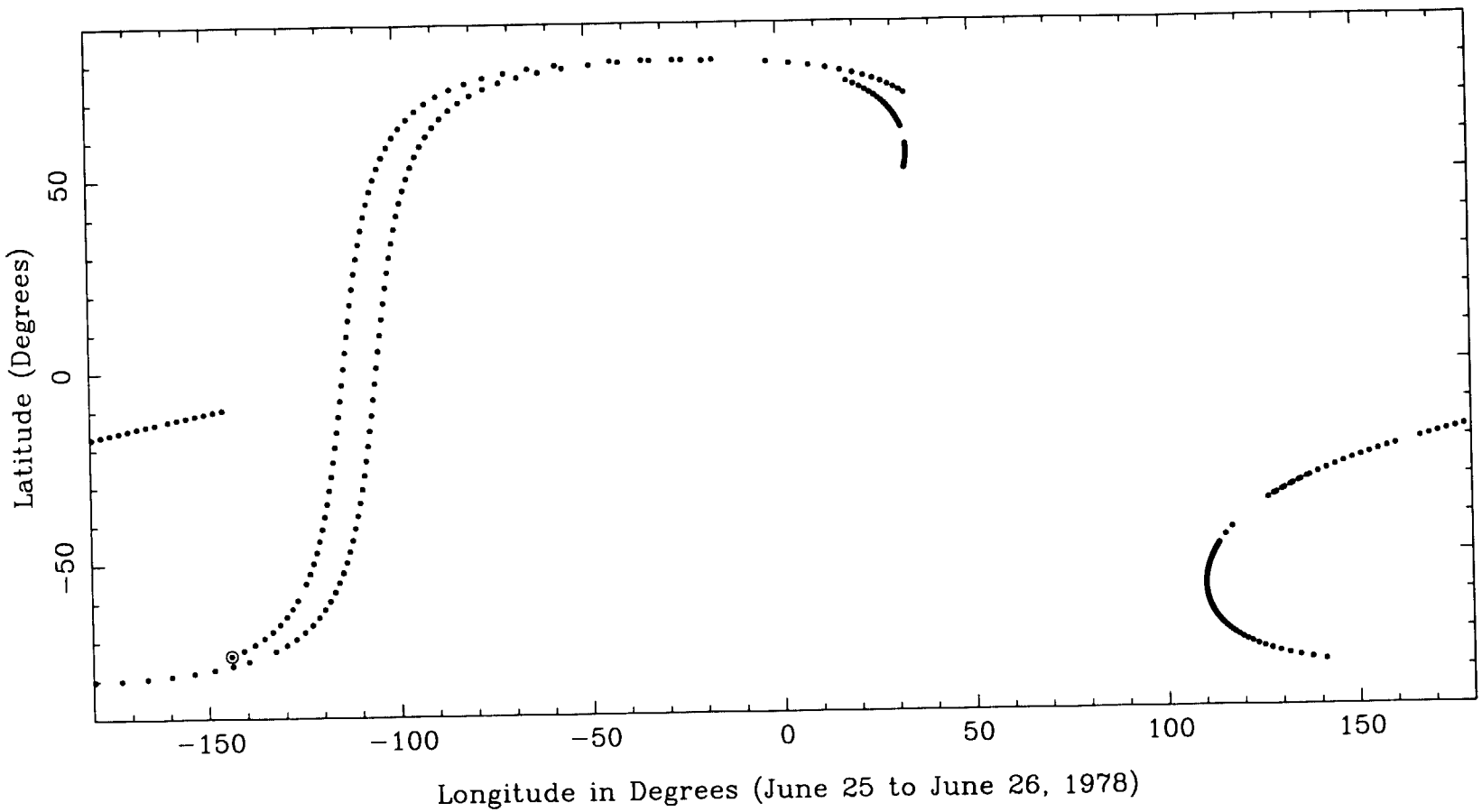

Figure 31: Viking 2 Pavonis Resids for Mars50c

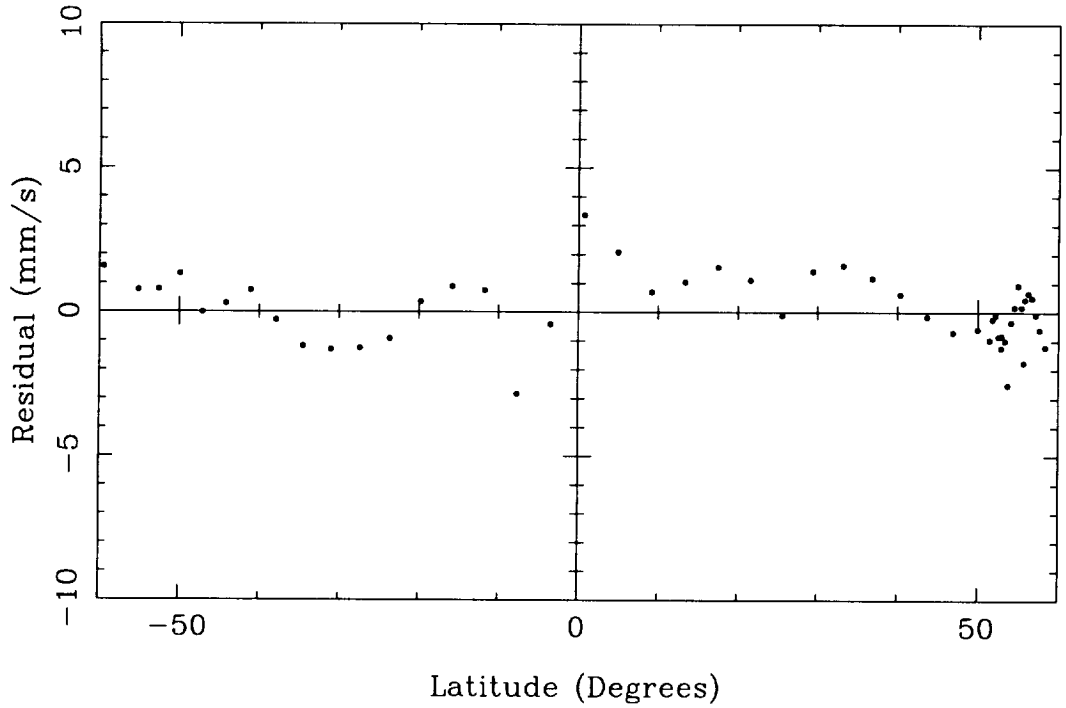

Figure 32: Viking 2 Pavonis Resids for GMM1

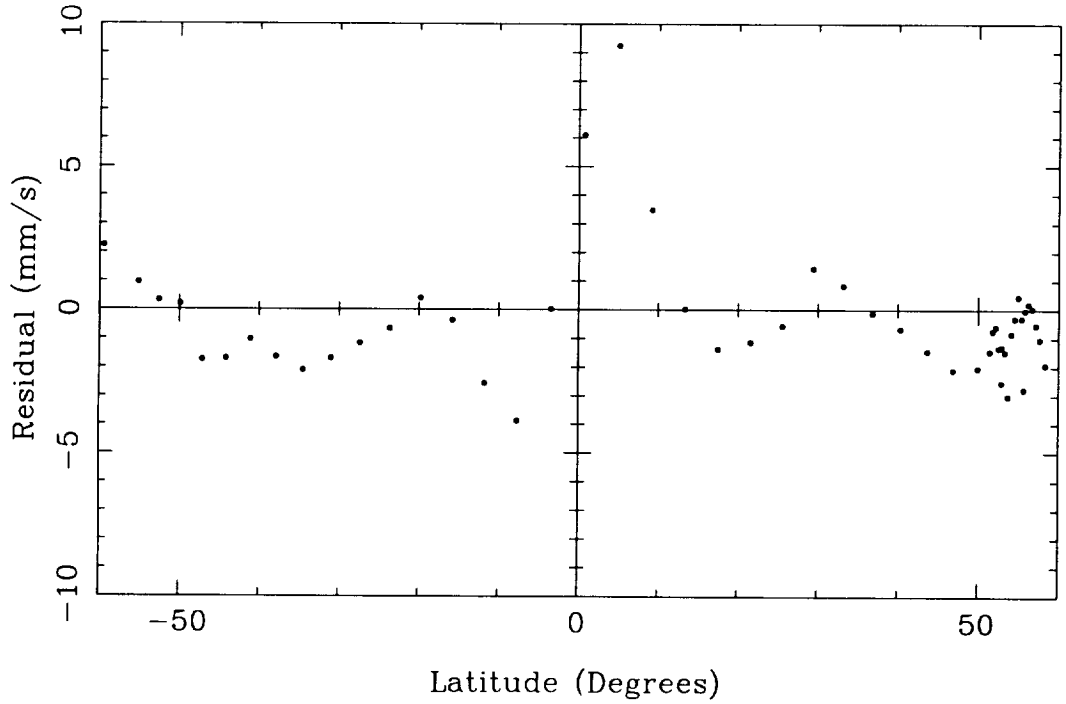

Figure 33: Viking 2 Ascraeus Resids for Mars50c

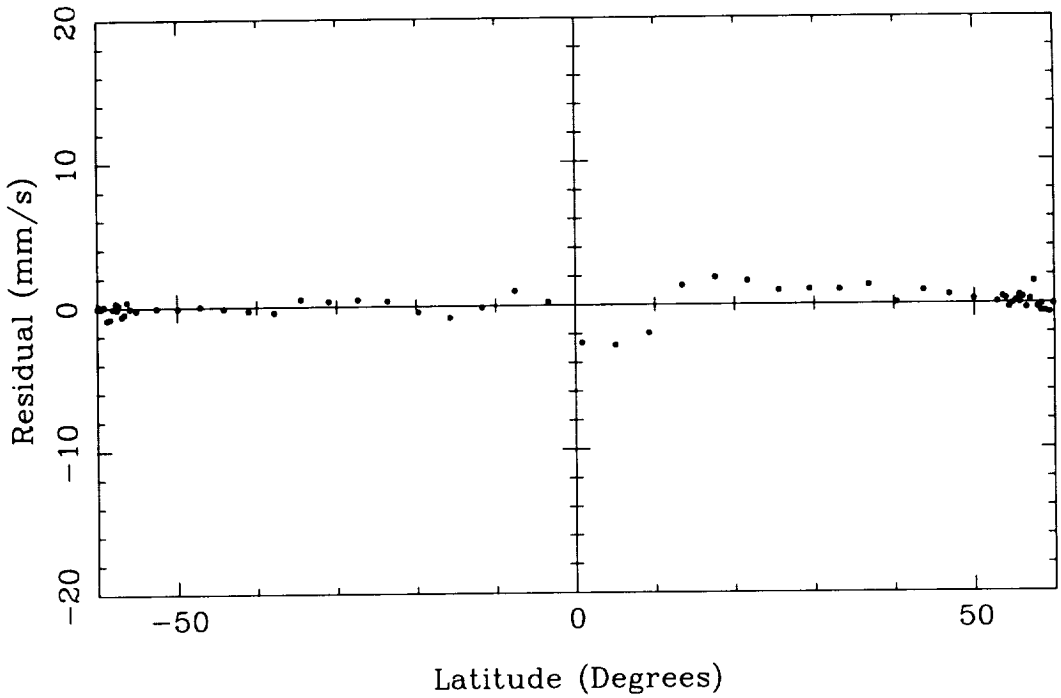

Figure 34: Viking 2 Ascraeus Resids for GMM1

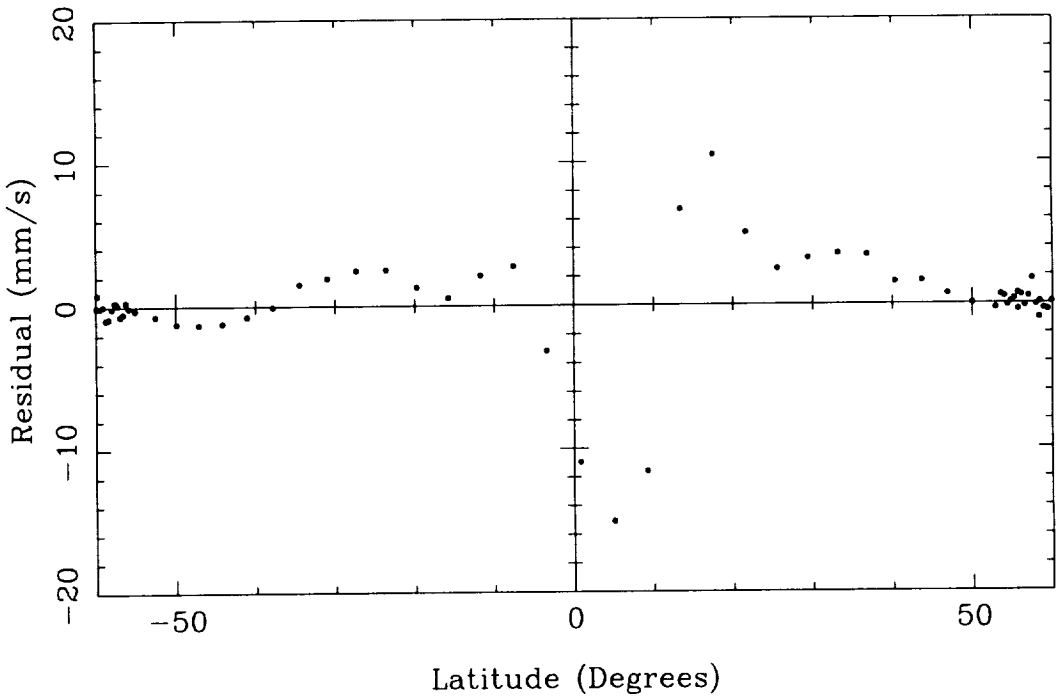

Figure 35: Tharsis Total Peak Value vs. Degree

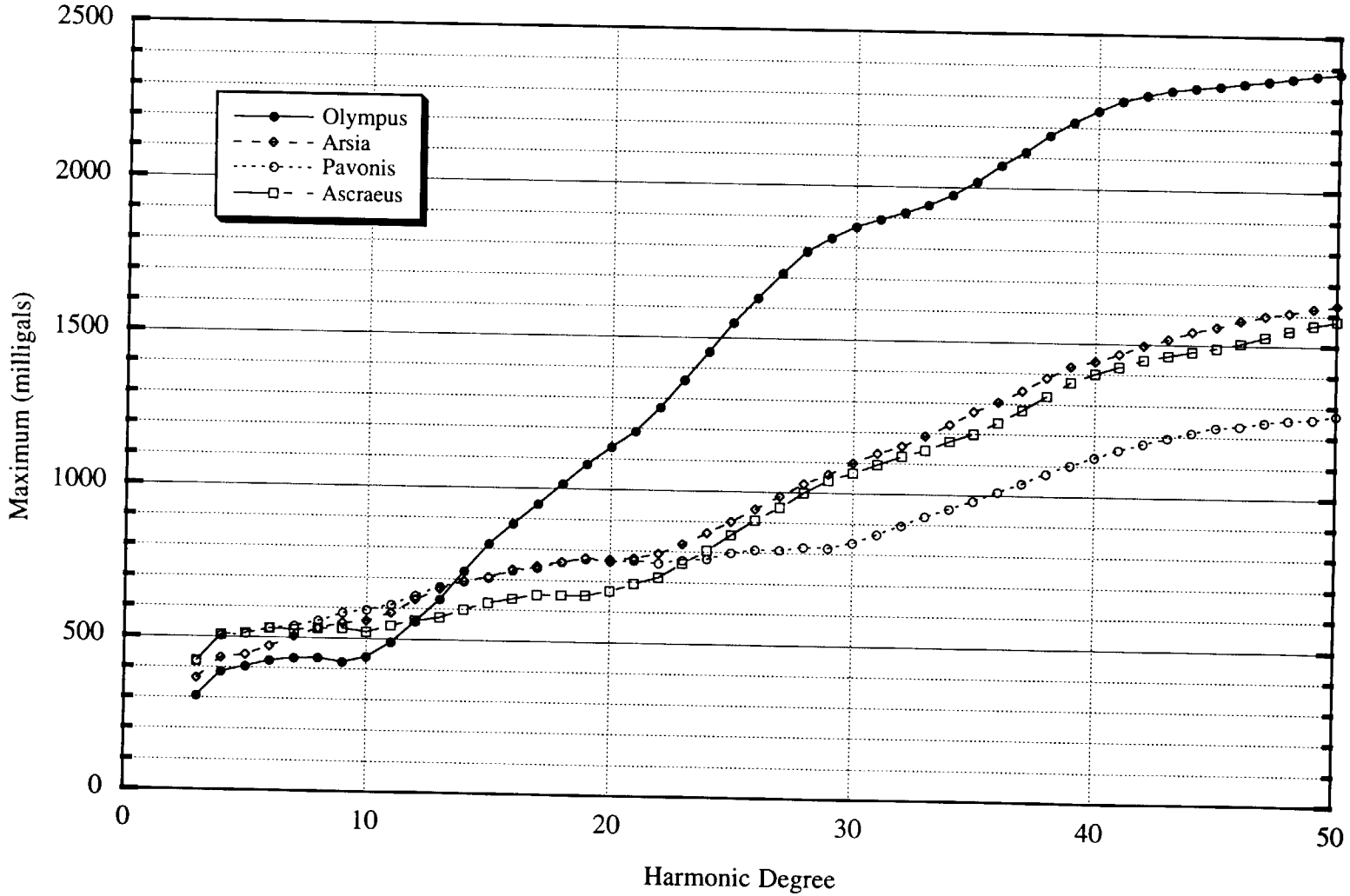

Figure 36: Tharsis Total Peak Uncertainty vs. Degree

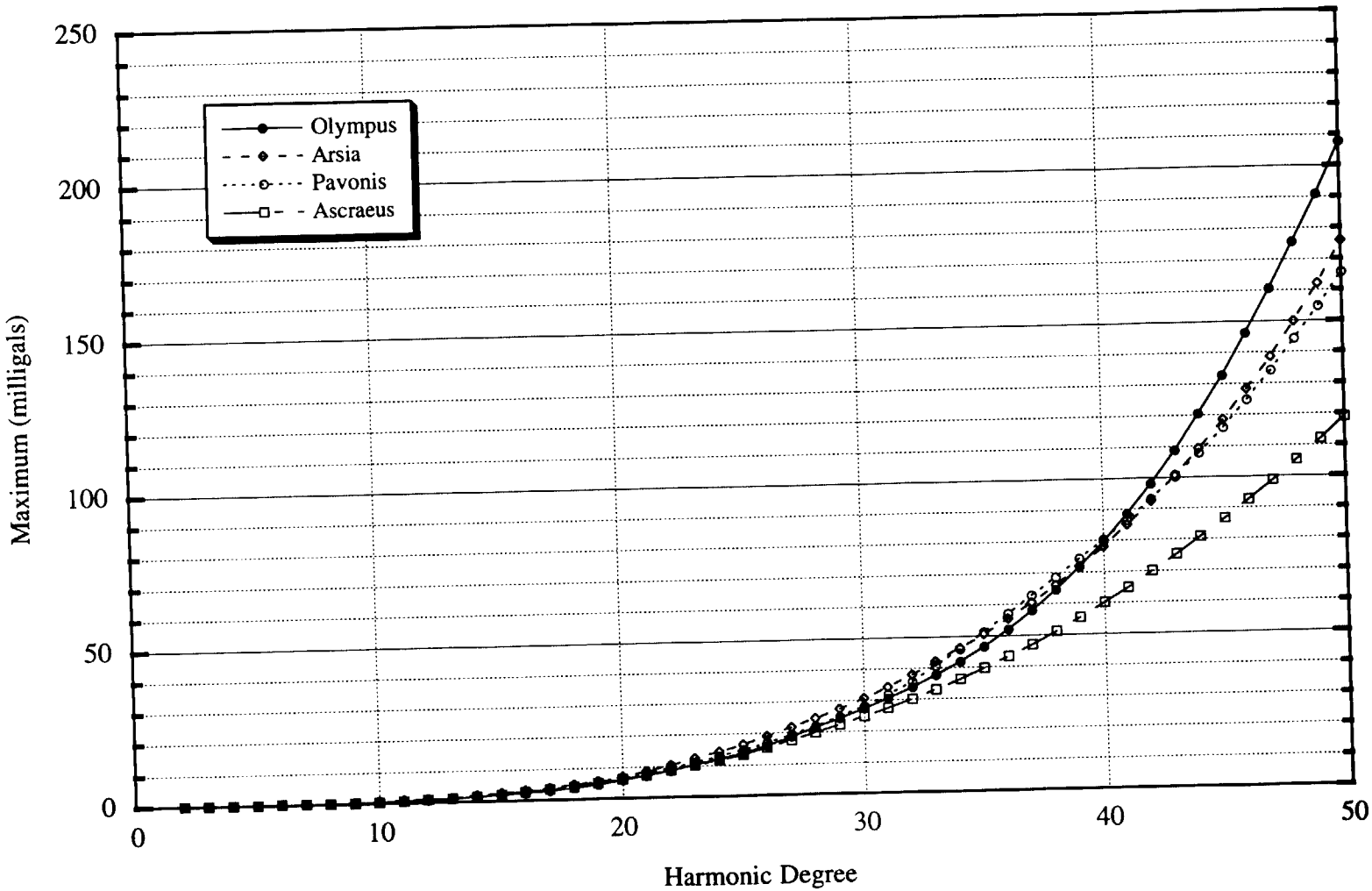

Figure 37: Olympus Gravity From Topography

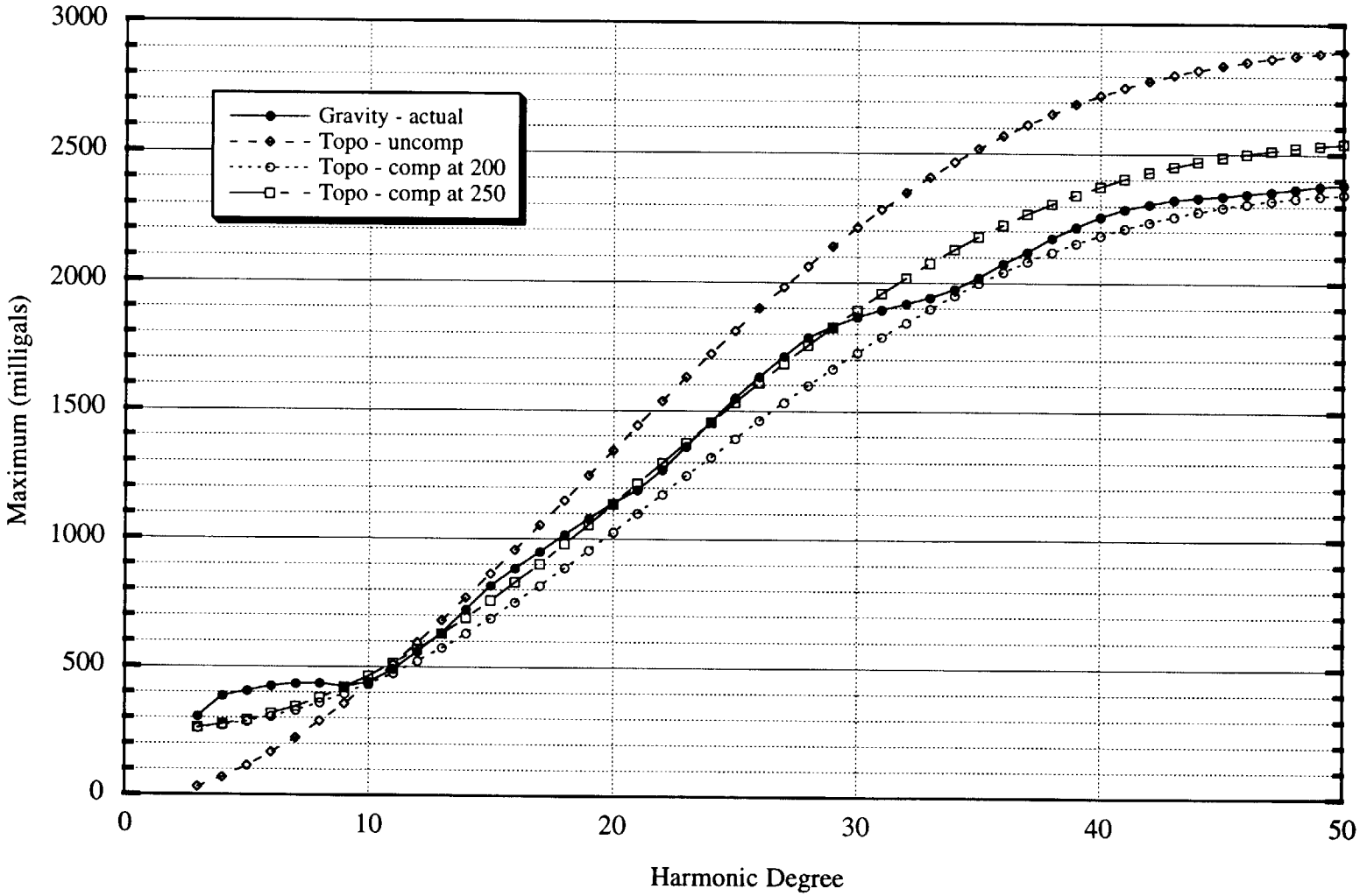

Figure 38: Olympus Gravity with Partial Compensation

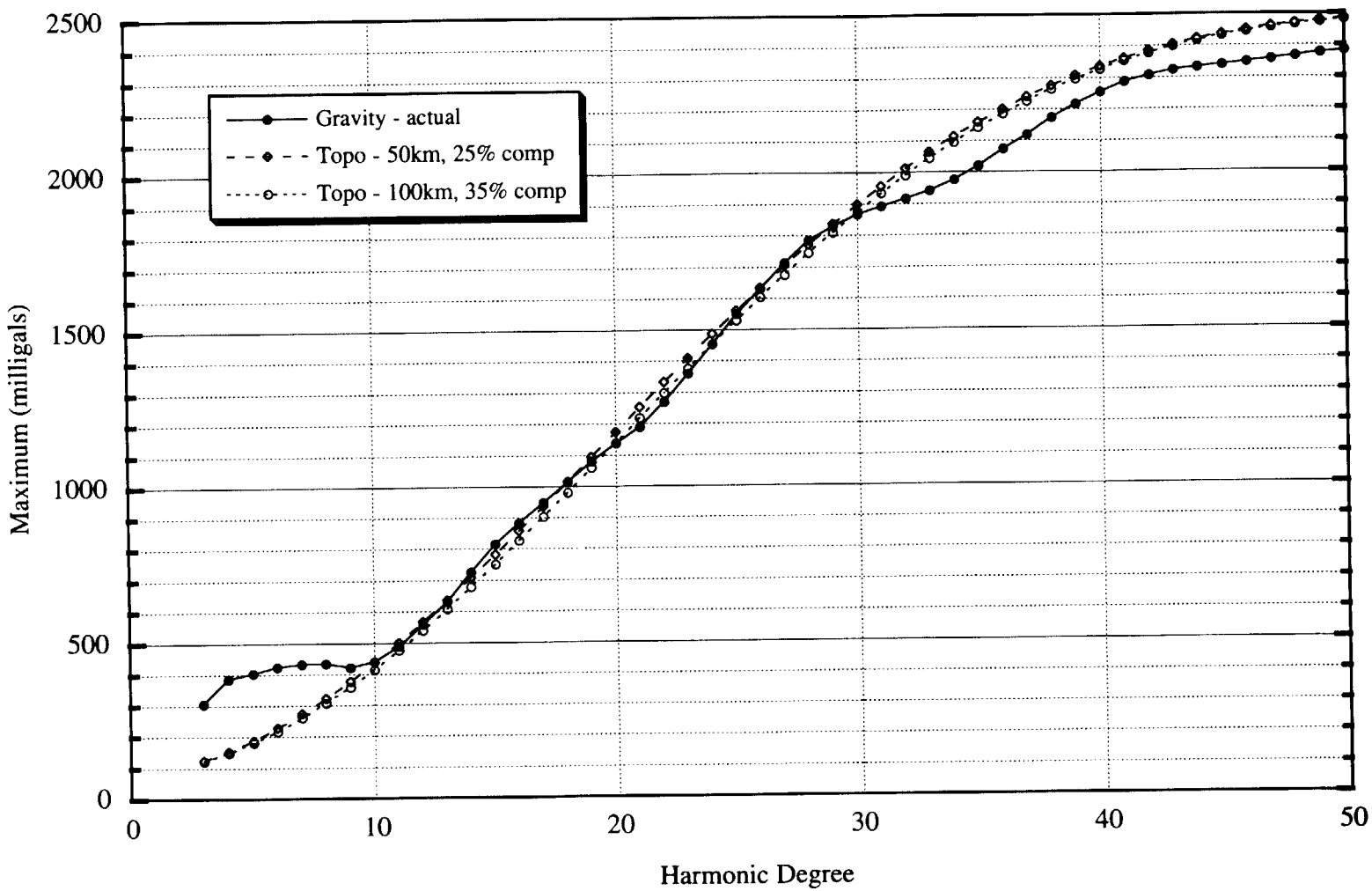

References

Balmino, G., B. Moynot, and N. Vales, Gravity field model of Mars in spherical harmonics up to degree and order eighteen. *J. Geophys. Res., 87,* 9735-9746, 1982.

Bierman, G.J., *Factorization Methods for Discrete Sequential Estimation*, Academic Press, New York, 1977.

Born, G. H., Mars physical parameters as determined from Mariner 9 observations of the natural satellites and Doppler tracking, *J. Geophys. Res., 79,* 4837-4844, 1974.

Chao, C.C. *The Tropospheric Calibration Model for Mariner Mars 1971*, Technical Report 32-1587, Jet Propulsion Laboratory, Pasadena, CA, 1972.

Christensen, E.J., and G. Balmino, Development and analysis of a twelfth degree and order gravity model for Mars, *J. Geophys. Res., 84,* 7943-7953, 1979.

Christensen, E.J., and B.G. Williams, Mars gravity field derived from Viking -1 and Viking -2: The navigation result, *J. Guid. Control, 3,* 179-183, 1979.

Davies, M.E., V.K. Abalakin, A. Brahic, M. Bursa, B.H. Chovitz, J.H. Lieske, P.K. Seidelmann, A.T. Sinclair, and Y.S. Tjuflin, Report of the IAU/IAG/COSPAR Working Group on Cartographic Coordinates and Rotational Elements of the Planets and Satellites: 1991, *Celes. Mech. 53*, 377-397, 1992.

Ellis, J., Large scale estimation algorithms for DSN tracking station location determination, *J. Astronaut. Sci., 28*, 15-30, 1980.

Folkner, W.M., C.S. Jacobs, O.J. Sovers, Radio Source Catalog for the Mars Observer Project, IOM 335.1-91-034 (internal document), Jet Propulsion Laboratory, Pasadena, CA, November 27, 1991.

Gapcynski, J.P., R.H. Tolson, and W.H. Michael, Jr., Mars gravity field: Combined Viking and Mariner 9 results, *J. Geophys. Res., 82*, 4325-4327, 1977.

Gross, R.S., A Combination of Earth Orientation Data: Space91, In *IERS Technical Note 11: Eath Oreientation Reference Frames and Atmosphere Excitation Functions Submitted for 1991 IERS Annual Report*, P. Charlot, Ed., IERS, Paris, 1992.

Hanover, G.A., VEM 1 Year Report - VO-1/VO-2 Propulsive and Non-propulsive Maneuver Performance, IOM OGCPAU-21091-GAH (internal document), Jet Propulsion Laboratory, Pasadena, CA, Nov. 15, 1977.

Hanover, G.A., (private communication), Avionic Systems Engineering Section, Jet Propulsion Laboratory, 1993.

Jacobson, R.A., (private communication), Navigations Systems Section, Jet Propulsion Laboratory, 1995.

Jordan, J.F., and J. Lorell, Mariner 9: An instrument of dynamical science, *Icarus, 25,* 146-165, 1975.

Kaula, W.M., *Theory of Satelltte Geodesy*, Blaisdell, Waltham, MA, 1966.

Konopliv, A.S., and W.L. Sjogren, Venus Spherical Harmonic Gravity Model to Degree and Order 60, *Icarus,* in press, 1995a.

Konopliv, A.S., and W.L. Sjogren, (private communication), Navigations Systems Section, Jet Propulsion Laboratory, 1995b.

Konopliv, A.S., N.J. Borderies, P.W. Chodas, E.J. Christensen, W.L. Sjogren and B.G. Williams, Venus Gravity and Topography: 60th Degree and Order Model, *Geophys. Res. Lett.* **20**, 2403-2406, 1993a.

Konopliv, A. S., W. L. Sjogren, R. N. Wimberly, R. A. Cook, A. Vijayaraghavan, "A High Resolution Lunar Gravity Field and Predicted Orbit Behavior," AAS Paper 93-622 in *Proceedings of the AAS/AIAA Astrodynamics Specialist Conference held August 16-19, 1993, Victoria, British Columbia, Canada*, Univelt, San Diego, 1275-1294, 1993b.

Lemoine, F.G., Mars: The dynamics of orbiting satellites and gravity model development, Ph.D. thesis, Univ. of Colorado, Boulder, 1992.

Lorell, J., G.H. Born, E.J. Christensen, J.F. Jordan, P.A. Laing. W.A. Martin, W.L. Sjogren, I.I. Shapiro, R.D. Reasenberg, and G.L. Slater, Mariner 9 celestial mechanics experiment, *Science, 175,* 317-320, 1972.

Lorell, J., G.H. Born, E.J. Christensen, P.B. Espositio, J.F. Jordan, P.A. Laing. W.L. Sjogren, S.K. Wong, R.D. Reasenberg, I.I. Shapiro, and G.L. Slater, Gravity field of Mars from Mariner 9 tracking data, *Icarus, 18,* 304-316, 1973.

McNamee, J.B., N.J. Borderies and W.L. Sjogren, Venus: Global Gravity and Topography, *J. Geophys. Res. Planets 98*, 9113-9128, 1993.

Miller, J.K. and T.C. Duxbury, "The Phobos Gravity Field and Internal Properties," Television Investigation of Phobos, Genry Avanesov, Ed., USSR Academy of Sciences, Moscow, USSR, October 1990.

Moyer, T.D., *Mathematical Formulation of the Double-Precision Orbit Determination Program (DPODP)*, Technical Report 32-1527, Jet Propulsion Laboratory, Pasadena, CA, 1971.

Moyer, T.D., Solid Earth Tides and Analytic Partials for Troposphere and Ionosphere Parameters in Link Regres for Galileo, IOM 314.5-786 (internal document), Jet Propulsion Laboratory, Pasadena, CA, May 17, 1984.

Nerem, R.S., B.G. Bills and J.B. McNamee, A High Resolution Gravity Model for Venus: GVM-1, *Geophys. Res. Lett. 20*, 599-602, 1993.

Nicholson, F.T., (private communication), Navigations Systems Section, Jet Propulsion Laboratory, 1995.

Null, G.W., A solution for the mass and dynamical oblateness of Mars using Mariner IV Doppler data, *Bull. Am. Astron. Soc.* 356, 1969.

O'Neil, W.J., J.F. Jordan, J.W. Zielenbach, S.K. Wong, R.T. Mitchell, W.A. Webb, P.E. Koskela, et al., *Mariner 9 Navigation*, JPL Technical Report 32-1586, Pasadena, CA, Nov. 13, 1973.

Reasenberg, R.D., I.I. Shapiro, and R.D. White, The gravity field of Mars, *Geophys. Res., Lett., 2,* 89-92, 1975.

Reasenberg, R.D., The moment of inertia and isostasy of Mars, *J. Geophys. Res., 82,* 369-375, 1977.

Sjogren, W.L., J. Lorell, L. Wong, and W. Downs, Mars gravity field based on a short arc technique, *J. Geophys. Res., 80,* 2899-2908, 1975.

Sjogren, W.L., Mars Gravity: High-Resolution Results from Viking Orbiter 2, *Science,* 203, 1006-1010, 1979.

Smith, D.E., F.J. Lerch, R.S. Nerem, M.T. Zuber, G.B. Patel, S.K. Fricke, and F.G. Lemoine, An Improved Gravity Model for Mars: Goddard Mars Model 1, *J. Geophys. Res., 98,* 20871-20889, 1993.

Standish, E. M., The observational basis for JPL's DE200, the planetary ephemeris of the Astronomical Almanac. *Astron. Astrophys. 233*, 252-271, 1980.

Standish, E.M., JPL Planetary and Lunar Ephemerides, DE400/LE400, IOM 314.10-108 (internal document), Jet Propulsion Laboratory, Pasadena, CA, Jan. 1995.

USGS, Topographic Contour Map of Olympus Mons of Mars, Map number "M 1M 19/134.T", Flagstaff, AZ, 1982.

Wu, S.S.C., P.A. Garcia, R. Jordan, F.J. Schafer, and B.A. Skiff, Topography of the Shield Volcano, Olympus Mons on Mars, *Nature, 309*, 5697, 432-435, 1984.

Wu, S.S.C., P.A. Garcia, A. Howington-Kraus, and C.T. Kelly, Proceedings of Lunar and Planetary Conference XIX, 1298-1299, 1988.

Appendix 1

Viking 1 Data Arcs

Arc Start Time (hh:mm:ss)	Arc Stop Time (hh:mm:ss)	Total Points	Perispse Altitude (km)	Periapse Latitude (deg)
NOTE: Inclination for all Viking 1 arcs is 39 degrees				
21-JUN-1976 20:39:50	25-JUN-1976 20:00:00	1242	1510.1	23.2
25-JUN-1976 20:00:00	29-JUN-1976 20:00:00	976	1508.1	23.6
29-JUN-1976 20:00:00	03-JUL-1976 20:00:00	1020	1508.9	23.8
03-JUL-1976 20:00:00	08-JUL-1976 22:00:00	1509	1508.6	24.2
09-JUL-1976 01:30:00	14-JUL-1976 06:00:00	1485	1509.4	25.5
14-JUL-1976 08:00:00	17-JUL-1976 14:00:00	781	1504.2	25.9
17-JUL-1976 14:00:00	20-JUL-1976 08:50:00	875	1505.1	26.2
23-JUL-1976 14:00:00	27-JUL-1976 14:00:00	1178	1503.6	26.7
27-JUL-1976 14:00:00	30-JUL-1976 14:00:00	735	1504.1	27.0
30-JUL-1976 14:00:00	01-AUG-1976 14:00:00	581	1503.3	27.3
01-AUG-1976 14:00:00	03-AUG-1976 02:00:00	416	1502.8	27.4
03-AUG-1976 02:00:00	06-AUG-1976 00:00:00	681	1502.1	27.6
06-AUG-1976 00:00:00	09-AUG-1976 14:00:00	861	1501.2	27.9
09-AUG-1976 14:00:00	12-AUG-1976 14:00:00	961	1499.9	28.2
12-AUG-1976 14:00:00	15-AUG-1976 14:00:00	895	1499.1	28.4
15-AUG-1976 14:00:00	18-AUG-1976 14:00:00	937	1498.2	28.7
18-AUG-1976 14:00:00	22-AUG-1976 04:00:00	751	1497.3	28.9
22-AUG-1976 11:00:00	26-AUG-1976 00:00:00	764	1496.1	29.2
26-AUG-1976 04:00:00	30-AUG-1976 04:00:00	1101	1494.2	29.5
30-AUG-1976 04:00:00	02-SEP-1976 21:00:00	1067	1492.8	29.8
02-SEP-1976 21:00:00	07-SEP-1976 00:00:00	1140	1491.8	30.1
07-SEP-1976 00:00:00	11-SEP-1976 18:40:00	1199	1490.1	30.4
11-SEP-1976 19:50:00	16-SEP-1976 20:00:00	1566	1487.3	30.7
16-SEP-1976 20:00:00	20-SEP-1976 22:00:00	1314	1486.5	31.1
20-SEP-1976 22:40:00	24-SEP-1976 14:50:00	1119	1488.7	31.5
24-SEP-1976 17:10:00	29-SEP-1976 14:00:00	1111	1512.6	32.2
29-SEP-1976 14:00:00	03-OCT-1976 19:00:00	908	1510.6	32.5
03-OCT-1976 19:00:00	07-OCT-1976 19:00:00	591	1509.8	32.8
07-OCT-1976 19:00:00	11-OCT-1976 10:00:00	740	1508.6	33.1
11-OCT-1976 10:00:00	15-OCT-1976 08:00:00	996	1508.2	33.3
15-OCT-1976 08:00:00	19-OCT-1976 10:00:00	940	1507.4	33.5
19-OCT-1976 20:00:00	23-OCT-1976 12:00:00	753	1505.8	33.8
23-OCT-1976 12:00:00	27-OCT-1976 15:00:00	531	1505.3	34.1
27-OCT-1976 15:00:00	31-OCT-1976 09:00:00	949	1504.1	34.3
31-OCT-1976 16:00:00	04-NOV-1976 22:00:00	770	1503.0	34.5
05-NOV-1976 03:00:00	09-NOV-1976 05:00:00	951	1501.2	34.8
09-NOV-1976 05:00:00	12-NOV-1976 18:00:00	398	1499.7	35.0
13-NOV-1976 14:00:00	16-NOV-1976 17:00:00	324	1497.6	35.3
06-DEC-1976 08:00:00	10-DEC-1976 23:00:00	902	1487.9	36.3
12-DEC-1976 18:00:00	17-DEC-1976 18:00:00	829	1485.9	36.6
18-DEC-1976 12:00:00	23-DEC-1976 02:00:00	533	1483.8	36.7
25-DEC-1976 03:00:00	30-DEC-1976 07:00:00	655	1484.8	36.9
01-JAN-1977 16:00:00	02-JAN-1977 22:00:00	272	1484.7	37.1

05-JAN-1977	16:00:00	08-JAN-1977	03:00:00	626	1484.8	37.2
09-JAN-1977	21:00:00	12-JAN-1977	16:00:00	651	1485.2	37.3
14-JAN-1977	20:00:00	18-JAN-1977	08:00:00	809	1485.3	37.4
21-JAN-1977	12:00:00	22-JAN-1977	09:00:00	202	1486.3	37.5
22-JAN-1977	12:30:00	25-JAN-1977	07:00:00	590	1471.8	38.1
28-JAN-1977	03:00:00	31-JAN-1977	17:00:00	653	1472.7	38.3
01-FEB-1977	03:00:00	04-FEB-1977	23:00:00	595	1473.4	38.3
05-FEB-1977	01:50:00	08-FEB-1977	07:00:00	610	1474.2	38.5
08-FEB-1977	12:00:00	12-FEB-1977	03:00:00	725	1475.2	38.6
12-FEB-1977	04:00:00	15-FEB-1977	11:00:00	873	1482.0	38.8
15-FEB-1977	13:00:00	19-FEB-1977	13:00:00	966	1483.3	38.8
19-FEB-1977	13:00:00	24-FEB-1977	06:00:00	1288	1484.2	38.9
24-FEB-1977	06:00:00	01-MAR-1977	06:00:00	1028	1485.4	39.0
02-MAR-1977	12:00:00	07-MAR-1977	13:00:00	1157	1488.2	39.1
10-MAR-1977	12:00:00	11-MAR-1977	14:00:00	138	1489.9	39.2
NOTE: Periapse altitude lowered on Mar. 11, 15h 58m						
11-MAR-1977	17:10:00	15-MAR-1977	05:00:00	1119	295.6	39.2
15-MAR-1977	05:00:00	18-MAR-1977	19:00:00	3172	296.9	39.2
19-MAR-1977	02:00:00	21-MAR-1977	15:00:00	862	297.9	39.2
24-MAR-1977	22:50:00	29-MAR-1977	14:00:00	651	300.5	39.1
30-MAR-1977	18:00:00	03-APR-1977	01:00:00	345	301.7	39.0
03-APR-1977	09:00:00	07-APR-1977	08:00:00	605	302.1	38.9
10-APR-1977	10:00:00	14-APR-1977	06:00:00	362	305.2	38.7
16-APR-1977	12:00:00	20-APR-1977	11:00:00	387	307.1	38.5
20-APR-1977	22:00:00	25-APR-1977	11:00:00	554	306.9	38.3
25-APR-1977	20:00:00	29-APR-1977	14:00:00	440	307.7	38.1
29-APR-1977	14:00:00	03-MAY-1977	01:00:00	238	308.5	37.8
04-MAY-1977	15:00:00	08-MAY-1977	15:00:00	725	309.4	37.6
08-MAY-1977	15:00:00	12-MAY-1977	21:00:00	693	310.7	37.4
14-MAY-1977	07:00:00	15-MAY-1977	22:00:00	139	309.8	37.0
15-MAY-1977	23:30:00	19-MAY-1977	06:00:00	471	320.8	36.8
20-MAY-1977	02:00:00	23-MAY-1977	06:00:00	224	321.0	36.5
25-MAY-1977	22:00:00	30-MAY-1977	06:00:00	786	321.0	36.1
30-MAY-1977	19:00:00	03-JUN-1977	07:00:00	52	321.5	35.7
04-JUN-1977	00:00:00	08-JUN-1977	08:00:00	755	320.0	35.4
09-JUN-1977	14:00:00	13-JUN-1977	17:00:00	648	319.3	34.9
14-JUN-1977	15:00:00	20-JUN-1977	03:00:00	863	318.6	34.4
20-JUN-1977	22:00:00	23-JUN-1977	19:00:00	110	318.3	33.8
24-JUN-1977	15:00:00	28-JUN-1977	14:00:00	772	316.2	33.4
29-JUN-1977	14:00:00	01-JUL-1977	18:20:00	425	314.6	32.9
01-JUL-1977	20:40:00	06-JUL-1977	04:00:00	625	319.7	32.7
07-JUL-1977	15:00:00	10-JUL-1977	06:00:00	736	317.3	32.1
12-JUL-1977	12:00:00	16-JUL-1977	16:00:00	1083	315.4	31.6
16-JUL-1977	23:00:00	20-JUL-1977	08:00:00	305	314.4	31.0
20-JUL-1977	22:00:00	24-JUL-1977	03:00:00	1154	313.7	30.5
28-JUL-1977	20:00:00	02-AUG-1977	04:00:00	1440	309.2	29.6
04-AUG-1977	00:00:00	09-AUG-1977	15:00:00	1323	305.8	28.8
11-AUG-1977	11:00:00	14-AUG-1977	03:00:00	1427	302.5	27.9
16-AUG-1977	18:00:00	20-AUG-1977	07:00:00	1160	299.7	27.2
24-AUG-1977	14:00:00	28-AUG-1977	18:00:00	670	297.2	26.2
29-AUG-1977	03:00:00	02-SEP-1977	09:00:00	233	296.3	25.4
05-SEP-1977	00:00:00	08-SEP-1977	19:00:00	863	291.3	24.4

Appendix 1: Viking 1 data arcs -- *continued*

11-SEP-1977	04:00:00	15-SEP-1977	12:00:00	240	288.8	23.6
20-SEP-1977	06:00:00	25-SEP-1977	13:00:00	763	285.0	22.2
28-SEP-1977	16:00:00	03-OCT-1977	22:00:00	720	281.8	21.0
06-OCT-1977	23:00:00	08-OCT-1977	19:00:00	387	280.9	19.6
12-OCT-1977	16:00:00	13-OCT-1977	10:00:00	165	277.7	18.8
17-OCT-1977	03:00:00	21-OCT-1977	00:00:00	1060	276.4	18.0
22-OCT-1977	04:00:00	23-OCT-1977	23:00:00	382	276.4	17.2
27-OCT-1977	06:00:00	30-OCT-1977	20:00:00	443	274.4	16.4
31-OCT-1977	15:00:00	05-NOV-1977	17:00:00	433	272.5	15.7
07-NOV-1977	10:00:00	08-NOV-1977	00:00:00	206	272.0	14.6
08-NOV-1977	12:10:00	10-NOV-1977	20:00:00	266	272.1	14.4
12-NOV-1977	14:00:00	17-NOV-1977	18:00:00	1366	272.8	13.7
18-NOV-1977	09:00:00	19-NOV-1977	22:00:00	154	271.4	12.8
25-NOV-1977	13:00:00	28-NOV-1977	23:00:00	672	270.5	11.6
29-NOV-1977	04:00:00	02-DEC-1977	20:00:00	713	271.5	10.9
03-DEC-1977	16:00:00	05-DEC-1977	16:40:00	219	269.3	10.2
05-DEC-1977	17:30:00	09-DEC-1977	00:00:00	528	268.9	9.7
09-DEC-1977	16:00:00	13-DEC-1977	23:00:00	1157	268.1	9.1
16-DEC-1977	05:00:00	19-DEC-1977	20:00:00	473	270.0	8.0
20-DEC-1977	10:00:00	23-DEC-1977	21:00:00	505	271.4	7.3
24-DEC-1977	01:00:00	25-DEC-1977	16:00:00	184	271.4	6.5
25-DEC-1977	17:30:00	26-DEC-1977	19:00:00	42	270.3	6.2
29-DEC-1977	03:00:00	01-JAN-1978	16:00:00	558	270.4	5.7
02-JAN-1978	04:00:00	05-JAN-1978	21:00:00	190	271.3	5.1
07-JAN-1978	02:00:00	11-JAN-1978	23:00:00	495	273.3	4.2
12-JAN-1978	09:00:00	16-JAN-1978	14:20:00	793	272.4	3.3
16-JAN-1978	15:40:00	21-JAN-1978	19:00:00	830	271.1	2.5
24-JAN-1978	06:00:00	29-JAN-1978	01:00:00	521	274.1	1.2
29-JAN-1978	09:00:00	03-FEB-1978	00:00:00	1004	275.9	.3
03-FEB-1978	22:00:00	07-FEB-1978	10:30:00	176	275.0	-.6
11-FEB-1978	08:20:00	13-FEB-1978	02:00:00	169	278.1	-1.8
16-FEB-1978	01:00:00	19-FEB-1978	21:00:00	964	279.8	-2.7
21-FEB-1978	11:00:00	26-FEB-1978	03:00:00	937	278.4	-3.5
01-MAR-1978	01:00:00	02-MAR-1978	14:00:00	270	280.3	-4.9
04-MAR-1978	01:00:00	07-MAR-1978	12:00:00	827	281.8	-5.5
11-MAR-1978	02:00:00	16-MAR-1978	02:00:00	748	283.5	-6.7
17-MAR-1978	19:00:00	22-MAR-1978	12:00:00	1306	284.4	-7.8
26-MAR-1978	20:00:00	29-MAR-1978	07:00:00	294	288.2	-9.3
30-MAR-1978	07:00:00	03-APR-1978	03:00:00	778	287.5	-9.8
04-APR-1978	03:00:00	08-APR-1978	04:00:00	709	287.8	-10.6
08-APR-1978	12:00:00	12-APR-1978	15:00:00	1117	288.8	-11.3
12-APR-1978	20:00:00	15-APR-1978	10:00:00	346	291.2	-12.2
16-APR-1978	08:00:00	18-APR-1978	15:00:00	806	292.0	-12.7
21-APR-1978	22:00:00	26-APR-1978	13:00:00	1208	292.0	-13.7
26-APR-1978	20:00:00	30-APR-1978	14:00:00	691	294.2	-14.5
30-APR-1978	17:00:00	04-MAY-1978	16:00:00	1006	296.4	-15.1
04-MAY-1978	14:00:00	07-MAY-1978	16:00:00	632	296.2	-15.8
09-MAY-1978	07:00:00	11-MAY-1978	09:00:00	133	295.3	-16.3
22-MAY-1978	06:00:00	24-MAY-1978	16:00:00	363	298.8	-18.4
27-MAY-1978	11:00:00	01-JUN-1978	08:00:00	1280	298.4	-19.2
04-JUN-1978	00:00:00	07-JUN-1978	02:00:00	858	300.4	-20.4
08-JUN-1978	14:00:00	11-JUN-1978	16:00:00	1108	302.8	-21.1

12-JUN-1978	20:00:00	16-JUN-1978	11:00:00	529	302.0	-21.7
17-JUN-1978	09:00:00	20-JUN-1978	21:00:00	276	302.6	-22.3
22-JUN-1978	11:00:00	26-JUN-1978	02:00:00	654	302.8	-23.0
28-JUN-1978	00:00:00	02-JUL-1978	12:00:00	7479	301.9	-23.9
05-JUL-1978	11:00:00	07-JUL-1978	12:00:00	519	300.7	-25.0
11-JUL-1978	11:00:00	15-JUL-1978	12:00:00	783	300.7	-25.8
16-JUL-1978	20:00:00	18-JUL-1978	09:00:00	144	303.8	-26.4
21-JUL-1978	10:00:00	25-JUL-1978	22:00:00	1746	303.1	-27.1
25-JUL-1978	22:00:00	27-JUL-1978	23:00:00	610	301.0	-27.7
28-JUL-1978	19:00:00	01-AUG-1978	00:00:00	911	301.5	-28.0
02-AUG-1978	21:00:00	07-AUG-1978	05:00:00	818	301.3	-28.7
07-AUG-1978	17:00:00	11-AUG-1978	14:00:00	277	300.5	-29.3
12-AUG-1978	00:00:00	15-AUG-1978	13:00:00	552	298.9	-29.8
16-AUG-1978	02:00:00	18-AUG-1978	22:00:00	591	297.9	-30.3
19-AUG-1978	21:00:00	24-AUG-1978	12:00:00	1353	298.4	-30.7
25-AUG-1978	00:00:00	29-AUG-1978	03:00:00	1053	298.8	-31.3
29-AUG-1978	03:00:00	01-SEP-1978	16:00:00	851	296.3	-31.8
01-SEP-1978	18:00:00	06-SEP-1978	13:00:00	1227	294.5	-32.2
07-SEP-1978	00:00:00	11-SEP-1978	07:00:00	760	294.1	-32.7
11-SEP-1978	07:00:00	14-SEP-1978	23:00:00	772	292.7	-33.1
15-SEP-1978	19:00:00	20-SEP-1978	21:00:00	996	290.5	-33.6
20-SEP-1978	21:00:00	25-SEP-1978	16:00:00	1158	287.9	-34.1
25-SEP-1978	16:00:00	29-SEP-1978	20:00:00	836	287.1	-34.5
29-SEP-1978	20:00:00	04-OCT-1978	03:00:00	626	286.9	-34.9
04-OCT-1978	23:00:00	08-OCT-1978	13:00:00	346	284.2	-35.3
08-OCT-1978	11:00:00	13-OCT-1978	00:00:00	504	281.7	-35.7
13-OCT-1978	04:00:00	16-OCT-1978	12:00:00	327	280.2	-36.0
17-OCT-1978	00:00:00	20-OCT-1978	12:00:00	400	278.9	-36.2
20-OCT-1978	23:00:00	25-OCT-1978	20:00:00	420	276.4	-36.6
26-OCT-1978	17:00:00	30-OCT-1978	15:00:00	338	272.6	-37.0
30-OCT-1978	15:00:00	02-NOV-1978	10:00:00	118	270.7	-37.2
03-NOV-1978	07:00:00	06-NOV-1978	10:00:00	237	270.2	-37.4
07-NOV-1978	08:00:00	10-NOV-1978	18:00:00	103	268.5	-37.7
11-NOV-1978	08:00:00	14-NOV-1978	19:00:00	99	265.7	-37.9
15-NOV-1978	09:00:00	18-NOV-1978	12:00:00	284	263.5	-38.1
20-NOV-1978	06:00:00	24-NOV-1978	10:00:00	396	262.0	-38.2
24-NOV-1978	23:00:00	27-NOV-1978	11:00:00	558	259.8	-38.4
29-NOV-1978	09:00:00	02-DEC-1978	08:00:00	252	256.8	-38.6
03-DEC-1978	00:59:54	04-DEC-1978	10:00:00	312	258.7	-38.4
10-DEC-1978	06:00:00	13-DEC-1978	08:00:00	386	253.6	-38.7
14-DEC-1978	23:00:00	18-DEC-1978	14:00:00	194	250.0	-38.8
19-DEC-1978	00:00:00	22-DEC-1978	18:00:00	351	247.1	-38.9
22-DEC-1978	18:00:00	25-DEC-1978	06:00:00	380	244.2	-38.9

Appendix 2

Viking 2 Data Arcs

Arc Start Time (hh:mm:ss)	Arc Stop Time (hh:mm:ss)	Total Points	Perispse Altitude (km)	Periapse Latitude (deg)
07-AUG-1976 12:10:14	09-AUG-1976 17:35:00	511	1514.4	50.1
09-AUG-1976 17:40:00	14-AUG-1976 07:30:00	1000	1496.6	50.3
14-AUG-1976 09:10:00	18-AUG-1976 10:00:00	989	1498.3	50.5
18-AUG-1976 10:00:00	22-AUG-1976 00:00:00	869	1498.0	50.5
22-AUG-1976 00:00:00	25-AUG-1976 16:45:00	1000	1498.3	50.6
25-AUG-1976 18:30:00	27-AUG-1976 19:20:00	667	1419.9	51.9
27-AUG-1976 21:25:00	31-AUG-1976 21:00:00	1046	1485.8	52.1
31-AUG-1976 21:00:00	03-SEP-1976 19:00:00	877	1485.7	52.2
04-SEP-1976 21:00:00	08-SEP-1976 21:00:00	1243	1488.7	52.2
08-SEP-1976 21:00:00	12-SEP-1976 21:00:00	810	1490.0	52.3
12-SEP-1976 21:00:00	16-SEP-1976 21:00:00	1300	1491.8	52.4
20-SEP-1976 21:00:00	24-SEP-1976 21:00:00	814	1495.7	52.6
24-SEP-1976 21:00:00	28-SEP-1976 13:30:00	1106	1497.7	52.7
NOTE: Inclination change from 50 to 75 degrees on Sep. 30, 21h 7m				
02-OCT-1976 02:23:00	06-OCT-1976 02:23:00	664	1505.3	63.7
06-OCT-1976 02:23:00	10-OCT-1976 02:23:00	885	1505.0	63.6
10-OCT-1976 02:23:00	14-OCT-1976 02:23:00	1033	1505.4	63.4
14-OCT-1976 02:23:00	18-OCT-1976 02:23:00	911	1506.6	63.3
18-OCT-1976 02:23:00	22-OCT-1976 02:23:00	770	1505.6	63.1
22-OCT-1976 02:23:00	26-OCT-1976 02:23:00	368	1506.8	62.9
26-OCT-1976 02:23:00	30-OCT-1976 02:23:00	778	1506.4	62.8
30-OCT-1976 02:23:00	03-NOV-1976 02:00:00	864	1507.1	62.6
03-NOV-1976 02:00:00	07-NOV-1976 02:00:00	902	1509.0	62.5
03-DEC-1976 08:00:00	08-DEC-1976 09:00:00	608	1513.2	61.3
11-DEC-1976 01:00:00	14-DEC-1976 23:00:00	761	1514.4	61.0
NOTE: Inclination change from 75 to 80 degrees on Dec. 21, 8h 54m				
NOTE: Periapse altitude lowered on Dec. 21, 8h 54m				
21-DEC-1976 09:00:00	25-DEC-1976 09:00:00	868	774.7	60.5
25-DEC-1976 09:00:00	29-DEC-1976 09:00:00	1040	773.9	60.3
29-DEC-1976 09:00:00	01-JAN-1977 16:00:00	711	773.8	59.9
02-JAN-1977 18:00:00	06-JAN-1977 00:00:00	673	773.4	59.6
07-JAN-1977 13:00:00	11-JAN-1977 17:00:00	517	773.3	59.3
12-JAN-1977 17:00:00	16-JAN-1977 20:00:00	606	772.7	58.8
17-JAN-1977 11:00:00	20-JAN-1977 00:00:00	489	771.5	58.4
25-JAN-1977 09:00:00	29-JAN-1977 00:00:00	587	770.3	57.8
31-JAN-1977 21:00:00	04-FEB-1977 16:00:00	454	768.0	57.3
07-FEB-1977 12:00:00	12-FEB-1977 08:00:00	598	766.4	56.8
14-FEB-1977 14:00:00	16-FEB-1977 13:00:00	231	763.9	56.2
18-FEB-1977 04:00:00	22-FEB-1977 08:00:00	637	762.6	55.9
22-FEB-1977 08:00:00	26-FEB-1977 14:00:00	484	760.8	55.5
27-FEB-1977 02:00:00	02-MAR-1977 21:00:00	378	757.9	55.2
02-MAR-1977 22:40:00	05-MAR-1977 05:00:00	379	747.9	54.4
06-MAR-1977 12:00:00	10-MAR-1977 12:00:00	341	747.3	54.1
17-MAR-1977 03:00:00	20-MAR-1977 19:00:00	257	744.9	53.2
21-MAR-1977 04:00:00	25-MAR-1977 12:00:00	501	744.2	52.8

27-MAR-1977	03:00:00	31-MAR-1977	06:00:00	459	743.4	52.2
31-MAR-1977	17:00:00	03-APR-1977	17:00:00	86	743.6	51.7
06-APR-1977	10:00:00	10-APR-1977	21:00:00	490	740.9	51.2
13-APR-1977	11:00:00	17-APR-1977	07:00:00	563	738.5	50.5
19-APR-1977	06:00:00	23-APR-1977	07:00:00	755	720.2	50.4
01-MAY-1977	23:00:00	04-MAY-1977	18:00:00	551	713.9	49.2
10-MAY-1977	07:00:00	15-MAY-1977	20:00:00	256	710.6	48.4
16-MAY-1977	16:00:00	21-MAY-1977	11:00:00	502	709.3	47.7
22-MAY-1977	18:00:00	27-MAY-1977	05:00:00	777	706.6	47.1
30-MAY-1977	03:00:00	03-JUN-1977	16:00:00	874	706.0	46.4
07-JUN-1977	02:00:00	11-JUN-1977	01:00:00	576	704.1	45.7
13-JUN-1977	15:00:00	16-JUN-1977	19:00:00	634	703.3	45.0
18-JUN-1977	02:00:00	21-JUN-1977	13:00:00	687	703.5	44.5
25-JUN-1977	00:00:00	29-JUN-1977	20:00:00	1131	703.2	43.9
05-JUL-1977	08:00:00	09-JUL-1977	02:00:00	789	703.2	42.8
09-JUL-1977	17:00:00	12-JUL-1977	17:00:00	1586	703.8	42.3
18-JUL-1977	22:00:00	22-JUL-1977	01:00:00	1603	706.8	41.5
22-JUL-1977	22:00:00	24-JUL-1977	19:00:00	254	704.8	41.0
26-JUL-1977	05:00:00	30-JUL-1977	18:00:00	1228	704.9	40.7
02-AUG-1977	00:00:00	05-AUG-1977	15:00:00	1501	704.8	40.1
07-AUG-1977	07:00:00	11-AUG-1977	22:00:00	1068	706.2	39.4
12-AUG-1977	08:00:00	16-AUG-1977	20:00:00	1071	705.9	39.0
19-AUG-1977	04:00:00	23-AUG-1977	07:00:00	193	707.7	38.3
23-AUG-1977	07:00:00	27-AUG-1977	16:00:00	324	706.6	37.8
27-AUG-1977	21:00:00	31-AUG-1977	21:00:00	656	706.7	37.3
31-AUG-1977	20:00:00	05-SEP-1977	16:00:00	779	706.9	37.0
07-SEP-1977	05:00:00	10-SEP-1977	12:00:00	102	706.9	36.3
12-SEP-1977	04:00:00	16-SEP-1977	12:00:00	1276	706.0	35.8
20-SEP-1977	17:00:00	24-SEP-1977	14:00:00	519	705.1	34.9
26-SEP-1977	02:30:00	30-SEP-1977	23:00:00	900	705.1	34.1
01-OCT-1977	00:00:00	05-OCT-1977	22:00:00	1054	704.7	33.7
05-OCT-1977	22:00:00	09-OCT-1977	17:00:00	489	702.7	33.2
NOTE: Periapse altitude lowered on Oct. 9, 15h 4m						
09-OCT-1977	16:20:00	13-OCT-1977	16:00:00	665	589.4	32.5
13-OCT-1977	22:00:00	14-OCT-1977	21:00:00	281	587.8	32.2
14-OCT-1977	21:00:00	17-OCT-1977	10:00:00	955	587.8	32.1
19-OCT-1977	14:00:00	23-OCT-1977	20:00:00	349	588.5	31.7
NOTE: Periapse altitude lowered on Oct. 23, 19h 30m						
23-OCT-1977	20:30:00	27-OCT-1977	11:00:00	622	296.6	31.3
28-OCT-1977	06:00:00	30-OCT-1977	21:00:00	405	294.1	30.8
01-NOV-1977	05:00:00	05-NOV-1977	05:00:00	989	291.7	30.2
06-NOV-1977	07:00:00	09-NOV-1977	19:00:00	349	289.4	29.6
11-NOV-1977	05:00:00	13-NOV-1977	01:00:00	322	288.7	29.2
15-NOV-1977	05:00:00	19-NOV-1977	00:00:00	777	289.0	28.7
19-NOV-1977	06:00:00	22-NOV-1977	02:00:00	535	287.6	28.2
23-NOV-1977	04:00:00	27-NOV-1977	16:00:00	987	285.5	27.7
01-DEC-1977	01:00:00	03-DEC-1977	19:00:00	525	285.0	26.9
05-DEC-1977	23:00:00	09-DEC-1977	21:00:00	647	283.0	26.3
09-DEC-1977	21:00:00	12-DEC-1977	19:00:00	751	280.6	25.7
13-DEC-1977	22:00:00	16-DEC-1977	13:00:00	581	279.0	25.3
18-DEC-1977	05:00:00	20-DEC-1977	17:00:00	813	277.2	25.0
21-DEC-1977	06:00:00	25-DEC-1977	22:00:00	410	277.2	24.6
26-DEC-1977	02:00:00	29-DEC-1977	21:00:00	903	277.7	24.0
30-DEC-1977	02:00:00	02-JAN-1978	05:00:00	709	275.6	23.5

Appendix 2: Viking 2 data arcs -- *continued*

02-JAN-1978	08:00:00	05-JAN-1978	18:00:00	774	272.4	23.0
06-JAN-1978	03:00:00	08-JAN-1978	07:00:00	429	274.3	22.8
08-JAN-1978	09:00:00	11-JAN-1978	21:00:00	125	274.8	22.5
11-JAN-1978	21:00:00	15-JAN-1978	13:00:00	1296	274.4	22.1
17-JAN-1978	09:00:00	19-JAN-1978	08:00:00	706	271.1	21.2
20-JAN-1978	10:00:00	22-JAN-1978	07:00:00	436	270.7	20.9
27-JAN-1978	06:00:00	31-JAN-1978	07:00:00	274	268.9	20.4
02-FEB-1978	08:00:00	04-FEB-1978	04:00:00	466	270.2	19.5
04-FEB-1978	09:00:00	08-FEB-1978	02:00:00	335	270.2	19.2
08-FEB-1978	08:00:00	11-FEB-1978	04:00:00	530	268.2	18.6
11-FEB-1978	15:00:00	15-FEB-1978	21:00:00	504	271.1	18.5
18-FEB-1978	05:00:00	22-FEB-1978	18:00:00	524	271.7	17.9
27-FEB-1978	04:00:00	02-MAR-1978	16:00:00	643	269.4	16.6
03-MAR-1978	12:00:00	08-MAR-1978	05:00:00	661	270.6	16.2
10-MAR-1978	17:00:00	14-MAR-1978	15:00:00	987	273.0	15.4
14-MAR-1978	19:00:00	18-MAR-1978	03:00:00	824	273.0	14.9
23-MAR-1978	02:00:00	27-MAR-1978	11:00:00	936	272.4	14.0
28-MAR-1978	07:00:00	01-APR-1978	11:00:00	1099	273.4	13.4
02-APR-1978	19:00:00	07-APR-1978	15:00:00	970	273.3	12.7
10-APR-1978	01:00:00	13-APR-1978	12:00:00	686	273.3	11.9
15-APR-1978	03:00:00	18-APR-1978	10:00:00	754	274.6	11.4
21-APR-1978	00:00:00	22-APR-1978	10:00:00	97	277.3	10.7
27-APR-1978	21:00:00	29-APR-1978	03:00:00	427	276.7	9.9
29-APR-1978	10:00:00	30-APR-1978	10:00:00	176	277.9	9.6
07-MAY-1978	12:00:00	12-MAY-1978	09:00:00	280	279.9	8.8
14-MAY-1978	10:00:00	18-MAY-1978	09:00:00	461	279.2	7.8
20-MAY-1978	00:00:00	23-MAY-1978	05:00:00	459	280.7	7.4
25-MAY-1978	22:00:00	29-MAY-1978	13:00:00	701	283.4	6.7
01-JUN-1978	13:00:00	04-JUN-1978	10:00:00	1246	284.7	5.8
04-JUN-1978	22:00:00	07-JUN-1978	14:00:00	528	284.3	5.5
10-JUN-1978	19:00:00	15-JUN-1978	11:00:00	299	286.5	4.9
16-JUN-1978	21:00:00	20-JUN-1978	06:00:00	556	287.4	4.2
20-JUN-1978	16:00:00	24-JUN-1978	09:00:00	930	286.3	3.6
24-JUN-1978	23:00:00	27-JUN-1978	13:00:00	419	285.7	3.1
01-JUL-1978	13:00:00	05-JUL-1978	17:00:00	604	287.5	2.5
07-JUL-1978	17:00:00	11-JUL-1978	15:00:00	582	288.6	1.7
12-JUL-1978	16:00:00	16-JUL-1978	13:00:00	291	288.0	1.1
17-JUL-1978	17:00:00	21-JUL-1978	08:00:00	567	288.6	0.6
23-JUL-1978	19:00:00	25-JUL-1978	10:00:00	258	289.7	0.0

Appendix 3

Mariner 9 Data Arcs

Arc Start Time (hh:mm:ss)	Arc Stop Time (hh:mm:ss)	Total Points	Perispse Altitude (km)	Periapse Latitude (deg)
NOTE: Inclination for all Mariner 9 arcs is 64 degrees				
14-NOV-1971 01:30:00	16-NOV-1971 03:00:00	722	1392.7	-22.4
16-NOV-1971 03:00:00	18-NOV-1971 20:00:00	903	1383.8	-21.8
18-NOV-1971 20:00:00	21-NOV-1971 10:00:00	581	1382.3	-21.8
21-NOV-1971 10:00:00	24-NOV-1971 10:00:00	909	1384.1	-21.9
24-NOV-1971 10:00:00	27-NOV-1971 07:00:00	943	1386.8	-22.0
27-NOV-1971 07:00:00	30-NOV-1971 07:00:00	1083	1386.9	-22.2
30-NOV-1971 07:00:00	03-DEC-1971 07:30:00	1039	1384.8	-22.2
03-DEC-1971 07:30:00	06-DEC-1971 07:30:00	1063	1382.1	-22.1
06-DEC-1971 07:30:00	08-DEC-1971 09:00:00	692	1380.9	-22.1
08-DEC-1971 09:00:00	09-DEC-1971 20:00:00	524	1381.6	-22.2
09-DEC-1971 20:00:00	12-DEC-1971 20:00:00	1071	1382.3	-22.2
12-DEC-1971 20:00:00	15-DEC-1971 20:00:00	1043	1384.9	-22.3
15-DEC-1971 20:00:00	18-DEC-1971 20:00:00	1152	1385.5	-22.4
18-DEC-1971 20:00:00	21-DEC-1971 08:00:00	839	1383.2	-22.5
21-DEC-1971 08:00:00	24-DEC-1971 08:00:00	1154	1380.8	-22.5
24-DEC-1971 08:00:00	27-DEC-1971 08:00:00	1325	1379.1	-22.4
27-DEC-1971 08:00:00	30-DEC-1971 20:00:00	1626	1379.8	-22.5
30-DEC-1971 20:00:00	02-JAN-1972 20:00:00	1307	1645.1	-23.3
02-JAN-1972 20:00:00	05-JAN-1972 20:00:00	997	1646.2	-23.3
05-JAN-1972 20:00:00	08-JAN-1972 20:00:00	1391	1644.7	-23.4
08-JAN-1972 20:00:00	11-JAN-1972 20:00:00	1486	1641.7	-23.4
11-JAN-1972 20:00:00	14-JAN-1972 20:00:00	1425	1639.6	-23.3
14-JAN-1972 20:00:00	17-JAN-1972 20:00:00	1257	1639.7	-23.3
17-JAN-1972 20:00:00	20-JAN-1972 20:00:00	1296	1642.0	-23.4
20-JAN-1972 20:00:00	23-JAN-1972 20:00:00	1332	1644.4	-23.5
23-JAN-1972 20:00:00	25-JAN-1972 20:00:00	1201	1644.3	-23.6
26-JAN-1972 20:00:00	29-JAN-1972 20:00:00	1367	1641.7	-23.6
29-JAN-1972 20:00:00	01-FEB-1972 20:00:00	1407	1639.0	-23.6
01-FEB-1972 20:00:00	04-FEB-1972 20:00:00	1366	1638.0	-23.6
04-FEB-1972 20:00:00	07-FEB-1972 20:00:00	1319	1639.4	-23.6
07-FEB-1972 20:00:00	10-FEB-1972 20:00:00	1060	1642.1	-23.7
10-FEB-1972 20:00:00	13-FEB-1972 20:00:00	1145	1643.6	-23.8
13-FEB-1972 20:00:00	16-FEB-1972 20:00:00	1053	1642.3	-23.8
16-FEB-1972 20:00:00	19-FEB-1972 20:00:00	974	1639.7	-23.8
19-FEB-1972 20:00:00	22-FEB-1972 20:00:00	838	1637.8	-23.7
22-FEB-1972 20:00:00	25-FEB-1972 20:00:00	688	1638.1	-23.8
25-FEB-1972 20:00:00	28-FEB-1972 20:00:00	878	1640.6	-23.8
28-FEB-1972 20:00:00	02-MAR-1972 20:00:00	813	1643.4	-23.9
02-MAR-1972 20:00:00	05-MAR-1972 20:00:00	931	1643.6	-24.0
05-MAR-1972 20:00:00	08-MAR-1972 20:00:00	785	1641.4	-24.0
08-MAR-1972 20:00:00	11-MAR-1972 20:00:00	630	1639.0	-24.0
11-MAR-1972 20:00:00	14-MAR-1972 20:00:00	1042	1638.3	-23.9
14-MAR-1972 20:00:00	17-MAR-1972 20:00:00	904	1639.9	-24.0
17-MAR-1972 20:00:00	20-MAR-1972 20:00:00	961	1642.9	-24.0

20-MAR-1972 20:00:00	23-MAR-1972 20:00:00	758	1644.7	-24.2
23-MAR-1972 20:00:00	26-MAR-1972 20:00:00	500	1643.8	-24.2
26-MAR-1972 20:00:00	29-MAR-1972 20:00:00	442	1641.5	-24.2
01-APR-1972 20:00:00	04-APR-1972 03:00:00	648	1640.3	-24.1
05-APR-1972 16:00:00	09-APR-1972 06:00:00	556	1643.6	-24.2
10-APR-1972 15:00:00	14-APR-1972 06:00:00	548	1646.0	-24.4

Appendix 4

Viking 1 Uncoupled Attitude Maneuvers and Gas Leaks

Attitude Maneuver Times

03-JUL-1977 21:50:00
03-JUL-1977 23:01:00
08-JUL-1977 21:38:00
08-JUL-1977 22:50:00
11-JUL-1977 21:36:00
11-JUL-1977 22:52:00
14-JUL-1977 18:15:00
18-JUL-1977 19:19:00
18-JUL-1977 20:04:00
24-JUL-1977 17:56:00
24-JUL-1977 19:23:00
29-JUL-1977 18:11:00
29-JUL-1977 18:54:00
04-AUG-1977 17:11:00
04-AUG-1977 18:14:00
05-AUG-1977 16:09:00
05-AUG-1977 18:09:00
16-AUG-1977 16:07:00
16-AUG-1977 18:32:00
17-AUG-1977 18:37:00
17-AUG-1977 19:59:00
19-AUG-1977 20:32:00
20-AUG-1977 01:17:00
21-AUG-1977 13:06:00
21-AUG-1977 18:42:00
21-AUG-1977 19:52:00
22-AUG-1977 20:47:00
22-AUG-1977 21:52:00
29-AUG-1977 18:28:00
29-AUG-1977 21:35:00
31-AUG-1977 18:33:00
01-SEP-1977 07:43:00
02-SEP-1977 20:04:00
02-SEP-1977 21:15:00
04-SEP-1977 16:46:00
04-SEP-1977 18:18:00
06-SEP-1977 20:00:00
07-SEP-1977 07:40:00
10-SEP-1977 17:18:00
10-SEP-1977 18:24:00
11-SEP-1977 06:09:00
13-SEP-1977 06:28:00
13-SEP-1977 07:24:00
14-SEP-1977 19:45:00
14-SEP-1977 20:56:00
16-SEP-1977 13:01:00
16-SEP-1977 17:04:00
19-SEP-1977 06:26:00
19-SEP-1977 16:58:00
21-SEP-1977 12:52:00
21-SEP-1977 17:04:00
23-SEP-1977 18:04:00
24-SEP-1977 05:18:00
24-SEP-1977 13:48:00
24-SEP-1977 16:58:00
26-SEP-1977 15:37:00
26-SEP-1977 16:22:00
27-SEP-1977 12:51:00
27-SEP-1977 16:57:00
27-SEP-1977 22:49:00
28-SEP-1977 05:39:00
29-SEP-1977 18:05:00
30-SEP-1977 05:20:00
30-SEP-1977 12:40:00
30-SEP-1977 23:40:00
03-OCT-1977 12:38:00
03-OCT-1977 17:05:00
06-OCT-1977 12:28:00
06-OCT-1977 23:25:00
09-OCT-1977 12:25:00
09-OCT-1977 17:45:00
10-OCT-1977 03:45:00
12-OCT-1977 12:20:00
12-OCT-1977 16:32:00
14-OCT-1977 17:45:00
15-OCT-1977 04:00:00
15-OCT-1977 10:55:00
15-OCT-1977 16:26:00
16-OCT-1977 06:30:00
16-OCT-1977 16:45:00
18-OCT-1977 12:20:00
18-OCT-1977 16:20:00
21-OCT-1977 05:43:00
21-OCT-1977 16:45:00
24-OCT-1977 12:05:00
24-OCT-1977 17:28:00
26-OCT-1977 15:00:00
26-OCT-1977 17:18:00
28-OCT-1977 09:18:00
30-OCT-1977 18:09:00
31-OCT-1977 01:34:00
01-NOV-1977 15:20:00
01-NOV-1977 16:52:00
03-NOV-1977 14:45:00
03-NOV-1977 16:46:00
04-NOV-1977 03:37:00

06-NOV-1977 14:34:00
06-NOV-1977 16:47:00
06-NOV-1977 23:34:00
07-NOV-1977 16:10:00
11-NOV-1977 13:07:00
11-NOV-1977 16:35:00
11-NOV-1977 18:15:00
12-NOV-1977 09:05:00
15-NOV-1977 14:36:00
15-NOV-1977 16:38:00
18-NOV-1977 15:15:00
18-NOV-1977 17:15:00
19-NOV-1977 14:32:00
19-NOV-1977 16:03:00
20-NOV-1977 17:35:00
20-NOV-1977 18:52:00
21-NOV-1977 18:30:00
23-NOV-1977 14:15:00
23-NOV-1977 16:05:00
28-NOV-1977 14:07:00
28-NOV-1977 17:48:00
03-DEC-1977 14:00:00
03-DEC-1977 16:20:00
05-DEC-1977 16:50:00
05-DEC-1977 17:13:00
07-DEC-1977 13:55:00
07-DEC-1977 17:36:00
09-DEC-1977 14:04:00
09-DEC-1977 15:14:00
10-DEC-1977 13:52:00
10-DEC-1977 15:49:00
14-DEC-1977 12:54:00
14-DEC-1977 16:19:00
18-DEC-1977 12:20:00
18-DEC-1977 16:22:00
24-DEC-1977 12:02:00
24-DEC-1977 16:02:00
25-DEC-1977 16:32:00
25-DEC-1977 17:12:00
27-DEC-1977 05:26:00
27-DEC-1977 16:01:00
30-DEC-1977 11:28:00
30-DEC-1977 15:48:00
01-JAN-1978 16:59:00
01-JAN-1978 18:14:00
04-JAN-1978 09:30:00
06-JAN-1978 16:07:00
06-JAN-1978 16:47:00
12-JAN-1978 10:08:00
12-JAN-1978 11:01:00
14-JAN-1978 09:32:00
14-JAN-1978 10:55:00
16-JAN-1978 09:29:00
16-JAN-1978 10:52:00
16-JAN-1978 14:28:00
16-JAN-1978 15:25:00
19-JAN-1978 09:30:00
19-JAN-1978 10:53:00
19-JAN-1978 13:14:00
19-JAN-1978 14:54:00
21-JAN-1978 09:47:00
21-JAN-1978 10:41:00
24-JAN-1978 09:21:00
24-JAN-1978 10:15:00
27-JAN-1978 08:49:00
27-JAN-1978 09:42:00
27-JAN-1978 14:15:00
27-JAN-1978 15:03:00
29-JAN-1978 06:15:00
29-JAN-1978 08:12:00
29-JAN-1978 08:33:00
30-JAN-1978 08:22:00
30-JAN-1978 11:45:00
02-FEB-1978 07:47:00
02-FEB-1978 08:41:00
04-FEB-1978 07:32:00
04-FEB-1978 11:15:00
06-FEB-1978 07:17:00
06-FEB-1978 11:32:00
06-FEB-1978 12:38:00
06-FEB-1978 13:57:00
07-FEB-1978 10:46:00
07-FEB-1978 13:31:00
08-FEB-1978 09:46:00
08-FEB-1978 11:10:00
11-FEB-1978 05:49:00
11-FEB-1978 07:58:00
14-FEB-1978 15:03:00
14-FEB-1978 16:03:00
15-FEB-1978 11:45:00
15-FEB-1978 12:18:00
25-FEB-1978 12:30:00
25-FEB-1978 14:07:00
28-FEB-1978 01:56:00
28-FEB-1978 07:20:00
07-MAR-1978 12:19:00
07-MAR-1978 13:40:00
17-MAR-1978 11:08:00
17-MAR-1978 13:13:00
07-APR-1978 01:28:00
07-APR-1978 11:12:00
11-APR-1978 01:50:00
11-APR-1978 02:18:00
14-APR-1978 01:10:00
14-APR-1978 10:55:00
16-APR-1978 01:10:00

16-APR-1978 02:15:00
20-APR-1978 01:30:00
20-APR-1978 11:25:00
23-APR-1978 01:32:00
23-APR-1978 02:09:00
29-APR-1978 01:28:00
29-APR-1978 02:02:00
02-MAY-1978 01:23:00
02-MAY-1978 01:57:00
05-MAY-1978 01:16:00
05-MAY-1978 01:52:00
08-MAY-1978 00:37:00
08-MAY-1978 10:55:00
11-MAY-1978 13:35:00
11-MAY-1978 14:28:00
14-MAY-1978 00:55:00
14-MAY-1978 10:55:00
19-MAY-1978 03:15:00
19-MAY-1978 11:23:00
22-MAY-1978 08:52:00
22-MAY-1978 11:18:00
25-MAY-1978 00:44:00
25-MAY-1978 12:08:00
28-MAY-1978 08:38:00
28-MAY-1978 23:41:00
01-JUN-1978 07:56:00
01-JUN-1978 10:37:00
04-JUN-1978 05:26:00
04-JUN-1978 10:30:00
07-JUN-1978 05:26:00
07-JUN-1978 10:30:00
09-JUN-1978 10:42:00
09-JUN-1978 11:43:00
09-JUN-1978 22:50:00
10-JUN-1978 10:23:00
13-JUN-1978 05:14:00
13-JUN-1978 10:15:00
16-JUN-1978 05:03:00
16-JUN-1978 10:06:00
16-JUN-1978 16:23:00
19-JUN-1978 04:54:00
19-JUN-1978 10:10:00
21-JUN-1978 23:47:00
22-JUN-1978 17:36:00
25-JUN-1978 06:20:00
25-JUN-1978 10:00:00
28-JUN-1978 06:29:00
28-JUN-1978 17:48:00
01-JUL-1978 05:32:00
01-JUL-1978 09:47:00
04-JUL-1978 06:06:00
04-JUL-1978 17:51:00
07-JUL-1978 05:20:00
07-JUL-1978 15:45:00
10-JUL-1978 05:55:00
10-JUL-1978 16:40:00
12-JUL-1978 23:33:00
13-JUL-1978 11:38:00
16-JUL-1978 05:50:00
16-JUL-1978 18:07:00
18-JUL-1978 09:27:00
18-JUL-1978 11:04:00
19-JUL-1978 05:07:00
19-JUL-1978 16:11:00
22-JUL-1978 05:43:00
22-JUL-1978 16:53:00
25-JUL-1978 05:40:00
25-JUL-1978 16:10:00
28-JUL-1978 00:33:00
28-JUL-1978 16:47:00
30-JUL-1978 23:07:00
31-JUL-1978 16:12:00
02-AUG-1978 05:07:00
02-AUG-1978 16:12:00
05-AUG-1978 23:00:00
06-AUG-1978 15:30:00
09-AUG-1978 05:25:00
09-AUG-1978 20:17:00
11-AUG-1978 22:48:00
12-AUG-1978 15:18:00
15-AUG-1978 04:42:00
15-AUG-1978 19:04:00
18-AUG-1978 08:10:00
18-AUG-1978 09:44:00
19-AUG-1978 05:02:00
19-AUG-1978 14:14:00
22-AUG-1978 03:46:00
15-SEP-1978 08:59:00
15-SEP-1978 10:38:00
29-SEP-1978 09:20:00
29-SEP-1978 10:45:00
02-OCT-1978 06:48:00
02-OCT-1978 08:33:00
02-OCT-1978 09:35:00
14-OCT-1978 07:28:00
14-OCT-1978 08:29:00
18-OCT-1978 07:00:00
18-OCT-1978 07:30:00
02-NOV-1978 09:00:00
02-NOV-1978 11:00:00
03-NOV-1978 08:43:00
03-NOV-1978 10:20:00
07-NOV-1978 10:20:00
07-NOV-1978 12:21:00
09-NOV-1978 06:01:00
09-NOV-1978 07:28:00

09-NOV-1978 08:29:00
19-NOV-1978 07:28:00
19-NOV-1978 08:17:00
21-NOV-1978 08:09:00
21-NOV-1978 10:23:00
26-NOV-1978 05:45:00
26-NOV-1978 11:48:00
06-DEC-1978 22:10:00

Gas Leak Times

13-FEB-1978 11:00:00
14-FEB-1978 12:15:00
19-FEB-1978 11:00:00
21-FEB-1978 23:00:00
10-APR-1978 00:00:00
11-APR-1978 14:40:00
12-APR-1978 07:00:00
12-APR-1978 23:00:00
15-APR-1978 07:00:00
16-APR-1978 19:00:00
17-APR-1978 05:00:00
18-APR-1978 10:00:00
19-APR-1978 02:00:00
23-APR-1978 10:15:00
28-APR-1978 18:00:00
29-APR-1978 09:20:00
21-DEC-1978 21:00:00
22-DEC-1978 12:00:00
23-DEC-1978 00:00:00
23-DEC-1978 12:00:00
24-DEC-1978 00:00:00
24-DEC-1978 16:30:00
25-DEC-1978 02:00:00

Appendix 5

Viking 2 Uncoupled Attitude Maneuvers and Gas Leaks

Attitude Maneuver Times

02-NOV-1977 10:31:00
02-NOV-1977 13:24:00
04-NOV-1977 08:49:00
04-NOV-1977 09:22:00
04-NOV-1977 13:21:00
07-NOV-1977 05:46:00
07-NOV-1977 07:42:00
07-NOV-1977 09:01:00
07-NOV-1977 13:31:00
11-NOV-1977 08:22:00
11-NOV-1977 09:33:00
13-NOV-1977 08:12:00
13-NOV-1977 09:22:00
14-NOV-1977 05:32:00
14-NOV-1977 08:02:00
16-NOV-1977 08:57:00
16-NOV-1977 09:56:00
19-NOV-1977 05:17:00
19-NOV-1977 07:47:00
21-NOV-1977 07:56:00
21-NOV-1977 09:08:00
22-NOV-1977 07:48:00
22-NOV-1977 09:33:00
27-NOV-1977 05:06:00
27-NOV-1977 07:49:00
27-NOV-1977 09:03:00
29-NOV-1977 08:28:00
29-NOV-1977 10:03:00
30-NOV-1977 08:08:00
30-NOV-1977 08:58:00
03-DEC-1977 05:03:00
03-DEC-1977 07:48:00
03-DEC-1977 08:38:00
03-DEC-1977 09:35:00
05-DEC-1977 08:35:00
05-DEC-1977 09:55:00
07-DEC-1977 07:53:00
07-DEC-1977 09:09:00
10-DEC-1977 04:38:00
10-DEC-1977 07:24:00
16-DEC-1977 04:39:00
16-DEC-1977 07:33:00
17-DEC-1977 07:54:00
17-DEC-1977 09:30:00
22-DEC-1977 04:32:00
22-DEC-1977 07:27:00
23-DEC-1977 07:21:00
23-DEC-1977 09:04:00
28-DEC-1977 04:15:00
28-DEC-1977 07:08:00
28-DEC-1977 08:34:00
01-JAN-1978 06:52:00
01-JAN-1978 08:25:00
02-JAN-1978 05:57:00
02-JAN-1978 07:22:00
04-JAN-1978 04:09:00
04-JAN-1978 07:21:00
04-JAN-1978 08:07:00
08-JAN-1978 07:29:00
08-JAN-1978 08:11:00
10-JAN-1978 04:03:00
10-JAN-1978 07:47:00
10-JAN-1978 08:41:00
13-JAN-1978 06:45:00
13-JAN-1978 08:30:00
16-JAN-1978 03:52:00
16-JAN-1978 07:05:00
17-JAN-1978 07:28:00
17-JAN-1978 08:42:00
20-JAN-1978 07:07:00
20-JAN-1978 08:48:00
21-JAN-1978 04:30:00
21-JAN-1978 06:53:00
22-JAN-1978 07:13:00
22-JAN-1978 08:16:00
27-JAN-1978 04:50:00
27-JAN-1978 06:55:00
30-JAN-1978 07:15:00
30-JAN-1978 08:15:00
02-FEB-1978 04:28:00
02-FEB-1978 06:54:00
02-FEB-1978 08:00:00
04-FEB-1978 06:54:00
04-FEB-1978 08:16:00
08-FEB-1978 04:20:00
08-FEB-1978 06:37:00
08-FEB-1978 07:42:00
11-FEB-1978 05:00:00
11-FEB-1978 06:14:00
12-FEB-1978 06:07:00
12-FEB-1978 07:16:00
14-FEB-1978 04:47:00
14-FEB-1978 10:36:00
19-FEB-1978 06:55:00
19-FEB-1978 07:51:00
20-FEB-1978 04:46:00

20-FEB-1978 06:22:00
20-FEB-1978 08:52:00
21-FEB-1978 20:35:00
25-FEB-1978 06:29:00
25-FEB-1978 10:06:00
01-MAR-1978 06:11:00
01-MAR-1978 08:42:00
02-MAR-1978 06:19:00
02-MAR-1978 09:22:00
07-MAR-1978 06:14:00
07-MAR-1978 08:49:00
09-MAR-1978 06:26:00
09-MAR-1978 07:31:00
11-MAR-1978 05:55:00
11-MAR-1978 07:04:00
12-MAR-1978 05:53:00
12-MAR-1978 07:18:00
15-MAR-1978 05:31:00

Gas Leak Times

01-NOV-1977 12:00:00
02-NOV-1977 04:00:00
08-FEB-1978 21:00:00
10-FEB-1978 03:35:00
11-FEB-1978 22:36:00
12-FEB-1978 00:55:00
12-FEB-1978 19:30:00
14-FEB-1978 19:40:00
21-FEB-1978 10:00:00
21-FEB-1978 16:00:00
11-MAR-1978 13:40:00
11-MAR-1978 17:40:00
14-MAR-1978 07:53:00
14-MAR-1978 12:23:00
14-MAR-1978 17:53:00
15-MAR-1978 09:53:00
15-MAR-1978 13:53:00
15-MAR-1978 18:53:00
16-MAR-1978 02:00:00
16-MAR-1978 02:45:00
16-MAR-1978 03:30:00
16-MAR-1978 05:30:00
17-MAR-1978 08:30:00

Appendix 6

Mars50c Gravity Coefficents

(Degree n, Order m, C_{nm}, S_{nm}, Sigma C_{nm}, Sigma S_{nm})
Normalized coefficients x 10^{-10}

2	0	-8759197.6	.0	134.6	.0
2	1	132.0	6.8	30.7	31.7
2	2	-843122.0	496785.3	22.3	22.9
3	0	-119340.7	.0	208.9	.0
3	1	38656.8	252774.2	77.7	78.4
3	2	-159257.9	84668.7	79.7	77.8
3	3	354141.3	251996.6	36.7	35.9
4	0	51505.2	.0	311.4	.0
4	1	42392.1	37475.6	139.5	150.3
4	2	-11164.7	-89633.9	116.0	116.5
4	3	65141.9	-2723.5	85.9	81.7
4	4	1130.0	-128953.9	64.0	65.2
5	0	-18240.3	.0	465.8	.0
5	1	4833.2	20971.1	232.8	239.5
5	2	-42495.1	-12248.1	176.6	184.1
5	3	33031.5	2541.9	154.0	159.2
5	4	-46875.9	-33259.2	118.4	115.3
5	5	-44218.0	38360.5	77.8	79.0
6	0	14566.6	.0	719.0	.0
6	1	18929.2	-16257.6	377.9	386.2
6	2	9528.8	16124.7	269.7	259.6
6	3	9513.1	2440.5	260.8	256.2
6	4	10349.7	26518.5	181.3	179.7
6	5	17817.5	16289.7	151.9	152.6
6	6	27853.0	7853.5	100.8	97.8
7	0	8401.3	.0	1117.4	.0
7	1	11439.3	-1214.2	564.6	572.3
7	2	27991.4	-7319.2	469.9	449.5
7	3	8403.9	-4237.2	384.9	380.7
7	4	23982.0	-5259.8	292.6	285.9
7	5	-3087.7	-13347.4	215.7	223.2
7	6	-5723.0	-19362.7	179.0	179.2
7	7	4192.0	-17712.2	132.0	122.8
8	0	4983.2	.0	1640.9	.0
8	1	2028.6	6261.5	850.7	873.5
8	2	16676.0	6591.3	769.5	740.3
8	3	-10871.2	-13273.0	544.1	542.6
8	4	16265.1	415.4	434.7	435.0
8	5	-27955.4	-16262.9	345.9	340.9
8	6	-10069.2	-17674.1	251.2	245.2
8	7	-4937.1	16561.8	213.3	218.3
8	8	-3060.7	-2638.7	149.4	143.3
9	0	-7386.3	.0	2314.0	.0
9	1	140.4	-2075.2	1217.0	1229.2
9	2	11984.4	1547.0	1213.8	1180.6
9	3	-11677.3	-8942.2	804.8	814.7
9	4	4037.7	16965.4	672.6	661.4
9	5	-23714.7	-15066.9	494.8	506.2
9	6	8909.1	5676.2	374.7	386.3
9	7	-5441.8	9272.9	281.9	284.1
9	8	11962.3	-1763.3	239.9	242.8
9	9	-12239.8	-6218.0	171.2	184.1
10	0	13777.9	.0	2989.5	.0
10	1	15878.6	-2557.6	1648.6	1665.5
10	2	-491.8	-9796.9	1790.6	1752.8
10	3	-279.7	3215.2	1166.7	1179.7
10	4	-12144.5	-339.0	997.6	1011.3
10	5	4880.1	-8166.0	749.2	740.9
10	6	5242.0	11369.9	548.2	571.5
10	7	2418.9	-7111.8	420.3	415.0
10	8	5420.8	8104.4	321.1	312.9
10	9	-15754.7	-14585.3	277.1	279.9
10	10	-2146.7	8040.5	210.0	185.3
11	0	-8998.4	.0	3621.8	.0
11	1	-17039.2	2359.7	2100.6	2141.6
11	2	-3174.2	-11116.1	2367.8	2331.7
11	3	-17809.0	8747.0	1583.6	1593.2
11	4	-16842.8	-5269.7	1433.9	1455.7
11	5	9849.5	4991.2	1077.3	1057.0
11	6	-395.9	135.6	803.2	837.0
11	7	8659.3	-8835.2	625.0	625.8
11	8	-11046.8	8284.7	461.9	457.5
11	9	-3531.2	-3903.7	355.9	353.8
11	10	4025.6	19127.3	305.9	290.7
11	11	-19.8	-3517.7	219.5	241.9
12	0	9656.0	.0	3857.5	.0
12	1	-3205.2	-5438.8	2552.8	2577.8
12	2	-2295.2	8030.3	2783.7	2752.6
12	3	-9349.2	1594.1	2016.0	2024.9
12	4	-2086.0	-880.1	1847.3	1870.8
12	5	13088.1	14056.2	1482.9	1476.2
12	6	-6731.8	-15708.3	1135.0	1130.6
12	7	2945.2	-1582.3	921.6	909.4
12	8	-17022.7	-3964.5	679.8	703.5
12	9	8034.8	4899.9	502.4	514.8
12	10	5389.4	14379.0	398.6	361.9
12	11	7504.5	-15625.3	325.5	330.5
12	12	-108.4	-1276.3	258.9	257.9
13	0	-8796.4	.0	3747.7	.0
13	1	-11615.8	7271.7	2840.8	2809.5
13	2	1994.1	6307.7	2902.4	2879.0
13	3	-1703.1	5283.3	2347.3	2358.8
13	4	3574.9	8342.7	2157.2	2181.4
13	5	-6718.2	-9087.9	1837.9	1861.2
13	6	3299.5	-9362.3	1500.7	1486.7
13	7	-5459.5	5408.9	1215.6	1206.2
13	8	-121.4	900.9	979.0	994.0
13	9	10180.6	9250.5	780.1	770.9
13	10	-832.3	-7406.3	544.1	518.2
13	11	8188.3	-9316.5	409.9	413.5
13	12	-14861.4	-3375.9	347.8	355.8
13	13	4904.2	8543.9	286.4	302.6
14	0	6987.3	.0	3165.6	.0
14	1	11398.9	836.4	2804.5	2766.2
14	2	3965.7	-3591.6	2719.8	2715.3
14	3	7380.3	-5897.8	2412.1	2423.9
14	4	-647.6	-9536.5	2279.7	2302.9
14	5	3776.3	-4609.6	2042.4	2100.2
14	6	-3910.1	-61.6	1799.9	1781.1
14	7	-8806.5	2360.0	1490.0	1502.9
14	8	5664.8	3684.4	1262.3	1269.6
14	9	2155.8	9184.6	1100.9	1109.1
14	10	-2461.6	-14420.9	789.6	797.6
14	11	-8893.8	1866.5	558.0	553.1

14	12	-4935.7	-3612.7	445.5	430.2
14	13	9435.1	19837.8	386.9	392.5
14	14	-251.0	-7695.2	335.8	318.2
15	0	5442.6	.0	2651.4	.0
15	1	488.4	2750.0	2471.5	2437.7
15	2	-4199.4	-8494.4	2372.6	2382.7
15	3	-8238.1	-1458.1	2225.1	2239.7
15	4	-6840.9	-7933.4	2213.8	2214.2
15	5	-16303.3	-6984.3	2025.4	2074.2
15	6	678.3	5487.0	1948.2	1934.3
15	7	12884.4	2019.3	1675.9	1662.2
15	8	13756.0	4640.1	1482.2	1479.0
15	9	-3083.1	-3432.8	1397.1	1407.0
15	10	-500.5	-4142.6	1091.5	1119.4
15	11	-9150.0	6574.9	790.3	794.7
15	12	9980.5	7184.3	577.7	578.8
15	13	-195.3	6971.3	488.4	474.6
15	14	895.4	-13735.9	431.4	422.9
15	15	-3919.0	1096.5	351.1	378.6
16	0	7927.2	.0	2260.1	.0
16	1	-1465.7	-4779.9	2041.7	2065.5
16	2	-4338.4	-919.3	2031.5	2040.5
16	3	-5197.9	2429.6	1936.1	1943.8
16	4	-8954.6	487.6	1994.3	1971.2
16	5	2071.5	6958.9	1881.5	1915.1
16	6	2314.3	1589.6	1896.9	1869.7
16	7	2123.4	2602.6	1733.6	1718.4
16	8	697.3	3200.0	1557.8	1558.0
16	9	-2162.7	-10653.6	1557.4	1564.1
16	10	-5900.9	4714.8	1378.4	1414.0
16	11	103.9	-4612.9	1086.1	1086.5
16	12	4956.6	7243.1	782.6	773.4
16	13	973.2	-6695.0	616.4	623.1
16	14	-1349.5	-8527.0	528.7	522.7
16	15	-7639.2	3787.9	465.7	485.2
16	16	2681.4	660.9	443.9	364.7
17	0	3032.1	.0	2137.5	.0
17	1	-1239.5	-8961.4	1945.9	2011.6
17	2	-575.1	1754.3	1812.7	1788.5
17	3	675.9	1371.6	1794.5	1810.6
17	4	5312.1	444.6	1764.3	1724.0
17	5	5506.6	3439.9	1709.9	1743.9
17	6	7316.0	-1711.7	1716.6	1698.7
17	7	5820.7	-3557.5	1664.6	1685.3
17	8	-1330.7	-2478.0	1552.9	1554.5
17	9	-1810.8	-1222.3	1563.7	1552.3
17	10	-3308.8	929.0	1531.2	1537.0
17	11	3155.9	665.1	1365.5	1351.0
17	12	1387.0	-375.2	1031.8	1023.4
17	13	-4889.0	-6250.8	793.7	784.4
17	14	-3577.9	-4104.7	683.7	654.9
17	15	-3558.6	5277.1	578.9	593.1
17	16	11309.4	5519.0	555.5	510.3
17	17	1079.0	3378.2	436.8	452.9
18	0	-3030.1	.0	2183.7	.0
18	1	-3224.3	-1449.0	2068.6	2159.5
18	2	-1654.9	1675.8	1792.2	1771.1
18	3	-4505.8	-4193.2	1824.2	1849.0
18	4	7704.1	3049.9	1659.2	1616.1
18	5	2724.7	-7059.3	1650.1	1682.6
18	6	1120.5	-6030.6	1557.5	1562.6
18	7	-2672.8	194.7	1552.8	1586.9
18	8	-532.7	-2423.3	1487.9	1491.8
18	9	-358.8	2274.5	1500.3	1479.7
18	10	5336.3	2021.6	1483.5	1501.8
18	11	3844.4	-2347.7	1463.3	1477.7
18	12	571.9	-412.0	1246.4	1260.6
18	13	-3486.3	-1752.9	995.9	989.4
18	14	-4998.0	2167.0	830.9	800.5
18	15	3479.3	7730.8	702.4	755.8
18	16	4246.3	1559.5	673.5	638.1
18	17	-1602.3	-10825.0	587.0	586.6
18	18	5025.3	3068.8	518.8	459.5
19	0	3083.7	.0	2225.5	.0
19	1	4316.5	3607.5	2108.0	2215.1
19	2	-975.7	1362.2	1964.5	1956.2
19	3	142.9	-2180.2	1897.8	1917.4
19	4	-437.2	4297.7	1783.6	1733.0
19	5	543.1	-3568.1	1664.1	1679.9
19	6	-1594.7	-826.6	1553.7	1574.3
19	7	-4276.5	1274.8	1468.6	1502.0
19	8	2937.2	-1448.7	1456.9	1460.9
19	9	1423.0	3721.6	1409.9	1405.9
19	10	6373.3	-1880.2	1406.2	1401.8
19	11	-2834.1	-3984.2	1440.6	1441.3
19	12	-2391.4	-1451.7	1359.0	1356.0
19	13	-2457.1	-846.0	1175.1	1183.5
19	14	2127.9	4478.5	1002.3	977.6
19	15	6835.3	4383.7	843.4	885.6
19	16	-1461.0	-1886.4	835.0	778.8
19	17	-1548.7	-7490.9	727.3	729.1
19	18	-6151.2	5357.9	708.7	630.5
19	19	-4122.4	-8134.4	537.7	513.8
20	0	3662.6	.0	2178.2	.0
20	1	1949.0	4374.3	2010.3	2105.2
20	2	610.9	-2894.1	1993.9	1959.8
20	3	1183.9	2043.7	1862.1	1884.7
20	4	-2228.9	4006.3	1878.6	1831.5
20	5	-677.2	-761.3	1736.2	1757.9
20	6	2875.9	6297.3	1681.9	1688.4
20	7	2452.8	-3255.7	1511.5	1567.8
20	8	4261.4	1666.5	1463.3	1469.1
20	9	-462.6	936.7	1407.0	1405.5
20	10	-3736.0	-336.9	1352.0	1355.0
20	11	-119.0	-847.5	1358.1	1353.4
20	12	-4406.4	-59.8	1365.5	1361.6
20	13	609.4	2162.4	1277.0	1291.9
20	14	3751.0	1685.5	1142.6	1153.2
20	15	2842.5	-4230.7	987.3	1039.6
20	16	2357.5	-2527.2	923.9	935.2
20	17	-2093.9	-297.6	881.6	890.1
20	18	518.2	7226.2	856.8	819.6
20	19	2659.0	-1389.5	714.6	730.7
20	20	-4324.2	1852.8	562.5	581.7
21	0	1361.6	.0	1989.0	.0
21	1	-1973.4	-924.2	1956.2	1993.4
21	2	1724.7	-3023.6	1906.2	1877.8
21	3	-1204.0	1017.9	1884.5	1892.9
21	4	-1840.0	248.6	1843.6	1793.8
21	5	5066.6	1403.4	1747.4	1771.7
21	6	970.0	2105.1	1674.6	1681.8
21	7	1523.1	-3890.7	1606.7	1651.0
21	8	-182.8	2208.5	1515.6	1515.3
21	9	-1263.7	-1953.5	1484.1	1471.5
21	10	-3650.1	2003.3	1384.2	1409.4
21	11	-1772.1	-2341.2	1328.9	1325.3
21	12	1758.6	-537.1	1330.6	1302.5
21	13	1169.1	1687.0	1308.4	1313.7
21	14	1115.8	-3652.1	1243.7	1247.0
21	15	-3571.8	-5199.8	1129.0	1138.2
21	16	-4001.9	.0	1035.1	1055.7
21	17	-3174.9	-3005.5	998.6	992.6

21	18	3516.5	5838.2	1003.4	997.1
21	19	193.8	-5026.9	903.1	908.9
21	20	-2495.8	-4394.3	829.9	787.8
21	21	7391.3	2296.8	626.5	597.2
22	0	1587.7	.0	1828.4	.0
22	1	-1638.4	-2080.9	1820.1	1872.9
22	2	1584.7	1747.6	1784.2	1765.4
22	3	-2477.7	731.0	1794.8	1807.2
22	4	1708.9	-2393.7	1747.4	1707.7
22	5	1060.3	1525.2	1735.0	1772.2
22	6	-783.2	-2701.8	1665.7	1684.7
22	7	4013.1	-365.3	1622.4	1678.6
22	8	-1819.9	-2569.3	1545.2	1559.7
22	9	-40.0	1772.6	1502.3	1483.2
22	10	-587.8	3923.8	1436.7	1458.2
22	11	925.4	-519.5	1385.7	1385.6
22	12	3715.1	1332.6	1315.7	1305.0
22	13	-1638.1	-1552.7	1283.5	1297.3
22	14	-52.0	-5434.9	1268.8	1292.3
22	15	-3334.0	2427.1	1210.6	1217.6
22	16	-1311.7	-665.0	1104.6	1146.9
22	17	1867.5	2049.2	1063.8	1080.2
22	18	-1506.1	1323.0	1067.3	1075.1
22	19	2813.2	-6868.4	1074.5	1059.5
22	20	-3768.4	1888.7	1030.8	987.5
22	21	2352.2	6514.3	813.3	894.1
22	22	-2266.3	-4135.0	639.1	660.4
23	0	126.4	.0	1735.1	.0
23	1	1231.7	2801.7	1645.6	1699.8
23	2	1101.5	4184.3	1718.3	1705.9
23	3	-212.5	-780.3	1639.6	1651.8
23	4	3214.2	18.1	1690.7	1650.4
23	5	-3376.5	396.6	1592.7	1629.4
23	6	1977.5	-2842.1	1605.0	1630.8
23	7	-1300.6	1365.6	1541.7	1577.3
23	8	-1979.2	-2323.5	1557.3	1554.2
23	9	-98.8	1218.5	1494.2	1482.6
23	10	-1605.5	29.9	1438.1	1435.8
23	11	3259.5	-663.3	1380.6	1397.8
23	12	-2361.7	472.1	1343.3	1316.6
23	13	-1011.7	35.2	1268.4	1280.3
23	14	-1435.0	-1810.5	1256.4	1262.4
23	15	-1864.3	6041.5	1253.3	1232.2
23	16	4488.3	1397.3	1170.1	1179.9
23	17	4189.8	7324.1	1130.6	1087.7
23	18	-2277.2	-5894.9	1062.1	1109.6
23	19	5233.5	879.3	1099.8	1067.9
23	20	-5051.0	791.0	1127.0	1090.6
23	21	3626.6	6676.8	1003.8	1019.8
23	22	-171.7	-1280.5	908.3	866.6
23	23	-6386.8	2936.0	663.7	689.8
24	0	575.3	.0	1620.1	.0
24	1	845.3	1718.4	1574.4	1607.8
24	2	342.4	464.8	1577.5	1597.9
24	3	2025.4	-2551.8	1570.1	1567.8
24	4	-1036.2	1479.3	1569.3	1549.9
24	5	-1576.1	-1792.3	1518.5	1548.1
24	6	1782.5	818.4	1516.6	1543.5
24	7	-4206.0	1848.1	1464.2	1508.2
24	8	1553.0	-102.0	1466.4	1489.2
24	9	-1080.0	1878.3	1437.7	1423.0
24	10	-908.6	-3917.2	1400.8	1395.8
24	11	-359.9	1300.0	1359.8	1373.8
24	12	-3251.5	-2184.9	1338.6	1313.2
24	13	451.1	488.0	1255.6	1262.3
24	14	-618.5	3546.6	1214.5	1231.2
24	15	1650.2	-93.3	1220.0	1226.8
24	16	5271.0	2646.6	1180.5	1219.9
24	17	-670.3	-1640.3	1145.7	1132.4
24	18	2809.9	-6460.5	1060.0	1123.3
24	19	-3909.7	3760.3	1092.8	1076.6
24	20	-396.4	-3182.0	1110.5	1065.0
24	21	1180.3	4703.9	1055.2	1096.4
24	22	-204.2	-5853.9	1002.9	1001.8
24	23	-5354.4	1624.6	873.4	896.2
24	24	4493.4	1016.0	703.0	680.5
25	0	237.0	.0	1543.9	.0
25	1	-509.1	-2485.7	1546.6	1567.9
25	2	-662.8	-2560.1	1492.6	1498.5
25	3	587.3	-662.0	1532.9	1527.9
25	4	-3102.1	-56.8	1481.2	1457.1
25	5	552.0	-2066.6	1477.1	1502.3
25	6	-1989.1	3123.4	1418.5	1443.5
25	7	668.4	275.2	1437.8	1454.4
25	8	3090.2	1028.4	1402.3	1396.4
25	9	-61.4	-201.1	1406.5	1391.1
25	10	1624.0	-869.4	1358.9	1345.3
25	11	-2809.2	2148.9	1321.3	1323.2
25	12	-880.5	-1808.1	1311.3	1285.4
25	13	1685.6	351.9	1268.4	1277.0
25	14	353.7	904.9	1208.1	1233.3
25	15	2608.6	-2320.7	1191.1	1178.6
25	16	1506.2	448.7	1171.0	1201.5
25	17	-2835.1	-7083.1	1167.3	1159.9
25	18	551.4	-1016.7	1087.7	1149.1
25	19	-5053.6	-653.8	1083.1	1095.6
25	20	3214.5	567.8	1103.7	1080.2
25	21	-5454.1	2697.2	1059.7	1082.8
25	22	2141.5	-4487.4	1049.9	1055.3
25	23	-3910.1	4667.8	977.6	976.4
25	24	4030.5	-31.7	877.9	877.3
25	25	1149.7	-3821.4	711.4	689.9
26	0	-1831.0	.0	1513.4	.0
26	1	-1160.8	-2641.5	1482.2	1512.6
26	2	-1407.6	-298.6	1473.9	1491.7
26	3	-926.7	1845.7	1466.6	1465.5
26	4	-396.1	195.2	1475.2	1449.8
26	5	2277.4	1804.3	1428.6	1430.3
26	6	-1731.4	529.2	1404.8	1423.2
26	7	2876.1	-1579.0	1387.9	1407.8
26	8	795.4	1073.8	1373.7	1363.8
26	9	1206.3	-3838.4	1356.7	1360.7
26	10	1592.4	1204.9	1327.3	1310.4
26	11	-2347.6	-1080.1	1300.7	1297.8
26	12	1049.2	22.9	1271.4	1260.5
26	13	85.3	-522.0	1251.4	1246.6
26	14	1151.7	-1406.1	1212.6	1229.2
26	15	-28.9	-364.6	1189.0	1189.1
26	16	-3045.5	-1267.1	1162.3	1171.0
26	17	-520.8	-1777.4	1156.1	1155.4
26	18	-2181.7	4307.6	1119.2	1156.1
26	19	450.4	-1526.5	1081.8	1129.2
26	20	2562.0	3755.7	1104.8	1075.7
26	21	-2992.2	-3725.7	1081.8	1097.5
26	22	4247.1	427.3	1062.1	1063.4
26	23	-1872.8	2100.7	1036.9	1020.3
26	24	5356.5	-553.7	974.8	962.2
26	25	1744.6	-3595.5	880.2	872.2
26	26	-2071.3	4909.9	642.7	774.5
27	0	-2026.9	.0	1445.5	.0
27	1	276.5	108.9	1411.5	1452.0
27	2	-997.7	1657.7	1425.9	1438.2

27	3	-177.6	1552.2	1419.6	1407.0
27	4	2697.9	-12.6	1427.8	1413.4
27	5	876.3	2291.5	1385.1	1393.5
27	6	539.3	-2280.4	1382.2	1402.1
27	7	1127.4	-1191.9	1348.6	1378.4
27	8	-1033.3	-1215.2	1363.5	1358.7
27	9	380.4	-2580.7	1334.4	1319.5
27	10	-1446.7	103.9	1317.2	1308.3
27	11	-1994.7	-1684.0	1277.7	1279.7
27	12	725.6	1295.1	1253.1	1237.9
27	13	-1510.0	-1410.6	1227.7	1224.4
27	14	539.7	768.3	1199.1	1222.8
27	15	-1072.8	574.0	1180.4	1181.3
27	16	-963.3	-799.7	1151.3	1160.0
27	17	1427.8	3684.6	1145.8	1154.0
27	18	-839.6	1566.1	1123.2	1121.4
27	19	4666.2	1333.0	1086.1	1106.9
27	20	-828.2	-263.7	1083.6	1065.3
27	21	1689.4	-2777.5	1060.4	1085.9
27	22	672.8	3201.4	1068.7	1072.1
27	23	429.8	-2734.2	1047.5	1028.8
27	24	1278.3	34.2	1028.4	1002.4
27	25	-1268.8	-4966.4	960.8	974.2
27	26	-2475.5	2703.2	861.1	909.6
27	27	4380.1	-1604.2	758.3	719.0
28	0	429.1	.0	1386.1	.0
28	1	1311.5	1492.4	1363.3	1406.8
28	2	672.2	609.4	1356.2	1388.5
28	3	1180.7	-779.5	1386.8	1370.2
28	4	1759.6	-1118.8	1369.2	1357.8
28	5	-806.9	-894.0	1360.3	1366.5
28	6	1051.2	-1843.0	1335.0	1357.2
28	7	-1690.4	228.5	1328.5	1344.1
28	8	-1723.5	-1464.7	1331.0	1330.4
28	9	-477.8	1556.0	1323.0	1305.7
28	10	-1975.6	545.5	1304.7	1301.8
28	11	1475.6	1120.7	1273.6	1279.3
28	12	-119.8	1077.0	1265.4	1249.6
28	13	310.2	506.2	1225.2	1214.8
28	14	231.9	1610.3	1195.2	1207.2
28	15	-295.5	358.0	1184.2	1184.7
28	16	1794.9	-25.1	1164.7	1162.1
28	17	1359.9	2271.9	1125.9	1148.6
28	18	1264.3	-2341.6	1119.0	1141.3
28	19	2307.2	386.5	1105.2	1112.0
28	20	-1267.3	-3699.8	1086.7	1074.9
28	21	1616.1	-108.8	1058.0	1054.8
28	22	-2649.0	-259.5	1056.6	1057.7
28	23	3447.6	-670.5	1068.3	1048.3
28	24	-2356.6	478.5	1057.0	1022.8
28	25	155.1	-2883.5	1013.8	1040.3
28	26	-2189.2	5220.1	976.2	1005.0
28	27	2603.8	-44.3	927.3	896.1
28	28	-3236.0	-3354.9	775.4	762.4
29	0	731.8	.0	1360.7	.0
29	1	-293.0	657.0	1334.6	1386.3
29	2	513.1	-919.5	1327.6	1371.2
29	3	-156.6	-1690.8	1368.4	1337.4
29	4	-1043.6	-357.8	1349.2	1329.3
29	5	-1702.6	-1431.7	1340.5	1341.3
29	6	-433.0	420.8	1307.0	1335.3
29	7	-1615.5	1113.0	1319.7	1328.9
29	8	-123.1	1190.6	1303.1	1295.5
29	9	-158.0	2110.5	1309.6	1299.3
29	10	761.4	572.3	1280.0	1271.3
29	11	2071.0	382.9	1271.2	1275.6
29	12	-173.4	-551.5	1258.9	1248.0
29	13	1518.0	623.3	1234.1	1226.0
29	14	325.4	-631.1	1191.0	1213.6
29	15	259.6	-35.8	1184.1	1188.6
29	16	561.1	268.3	1169.6	1165.7
29	17	35.5	-782.6	1153.6	1145.3
29	18	146.4	-2058.8	1133.7	1135.0
29	19	-2439.2	-922.5	1122.4	1125.6
29	20	-592.5	-2048.3	1101.1	1105.6
29	21	-1109.4	1724.2	1065.6	1096.5
29	22	-959.8	-427.6	1066.6	1066.2
29	23	1232.1	2278.5	1088.2	1052.8
29	24	-918.8	-1210.7	1088.3	1061.8
29	25	2181.8	2298.0	1036.7	1067.8
29	26	-957.4	1413.0	1029.0	1050.8
29	27	3560.7	-597.7	1013.4	991.6
29	28	263.9	-1459.7	918.0	935.7
29	29	-1848.6	2758.7	788.2	807.1
30	0	385.7	.0	1341.0	.0
30	1	-598.7	-713.5	1305.6	1357.1
30	2	-246.2	-121.3	1310.5	1354.2
30	3	-676.6	129.6	1335.2	1309.6
30	4	-1570.2	352.9	1325.4	1322.4
30	5	-453.7	436.5	1308.4	1304.7
30	6	-214.8	1531.6	1303.0	1315.3
30	7	270.5	521.2	1286.2	1300.4
30	8	1869.9	1132.2	1292.8	1285.1
30	9	190.8	74.8	1279.5	1266.9
30	10	1514.2	-1498.5	1266.8	1263.4
30	11	-506.5	-511.5	1242.2	1255.8
30	12	-472.2	-1264.6	1240.4	1236.8
30	13	-686.6	-301.3	1232.7	1210.8
30	14	-644.9	-1034.4	1196.1	1204.7
30	15	198.3	142.8	1178.3	1184.6
30	16	95.4	-128.4	1170.9	1167.1
30	17	-740.6	1.6	1140.6	1159.7
30	18	-632.2	167.3	1139.1	1125.8
30	19	-2188.1	956.7	1127.4	1116.7
30	20	669.1	1766.8	1119.7	1108.5
30	21	-660.3	1088.2	1086.7	1108.4
30	22	1818.9	186.2	1087.4	1072.3
30	23	-204.0	1526.3	1080.1	1068.0
30	24	1007.0	-1197.2	1089.1	1079.3
30	25	-62.7	1779.7	1070.5	1100.3
30	26	470.1	-3823.7	1062.1	1056.2
30	27	1365.6	-881.7	1063.8	1029.7
30	28	-2297.7	-2166.7	1018.5	1008.8
30	29	-693.7	-104.5	949.7	932.5
30	30	2673.1	-1076.8	791.0	849.9
31	0	-44.9	.0	1328.3	.0
31	1	-504.2	-269.8	1279.0	1331.5
31	2	-366.9	375.2	1284.1	1343.3
31	3	-167.9	1490.0	1315.5	1281.9
31	4	-94.2	523.3	1311.3	1296.4
31	5	1516.8	437.8	1286.0	1285.2
31	6	439.7	472.4	1277.9	1300.4
31	7	1799.1	-658.1	1255.2	1275.5
31	8	464.3	-735.3	1277.4	1269.6
31	9	225.3	-1089.0	1254.3	1240.5
31	10	-867.9	-517.0	1250.3	1250.0
31	11	-657.7	98.3	1228.3	1232.0
31	12	-1068.9	182.9	1223.4	1218.1
31	13	-773.7	978.7	1217.1	1206.1
31	14	-779.1	435.1	1185.8	1199.5
31	15	156.7	-28.7	1172.2	1178.3
31	16	-642.5	362.7	1167.5	1152.7

31	17	-156.1	946.9	1155.5	1142.0
31	18	606.5	389.7	1125.2	1138.0
31	19	346.7	1087.9	1119.6	1117.3
31	20	1950.7	1306.7	1108.8	1114.1
31	21	1252.5	-385.4	1095.9	1104.3
31	22	788.8	-438.7	1104.8	1074.0
31	23	-396.3	-1001.5	1082.7	1072.6
31	24	747.0	331.1	1082.7	1075.1
31	25	-1591.7	-259.3	1065.0	1117.5
31	26	1182.0	-1699.0	1095.5	1078.3
31	27	-706.8	-825.2	1081.8	1043.2
31	28	-858.5	-1017.8	1054.1	1043.2
31	29	-214.3	1910.4	1019.0	1020.2
31	30	-1177.5	1198.0	933.0	973.1
31	31	-1074.9	632.3	846.7	833.7
32	0	-99.4	.0	1290.2	.0
32	1	35.8	54.6	1272.1	1331.4
32	2	853.5	145.9	1247.9	1301.5
32	3	171.8	387.2	1321.3	1274.2
32	4	1270.3	-962.2	1268.8	1265.7
32	5	869.3	.0	1286.2	1287.8
32	6	-406.8	-1855.3	1247.9	1262.2
32	7	854.0	-620.1	1262.4	1272.5
32	8	-1992.4	-307.8	1246.9	1238.6
32	9	-58.6	-923.3	1254.5	1237.2
32	10	-859.3	972.8	1221.9	1224.9
32	11	-703.4	100.6	1211.1	1228.2
32	12	108.3	820.7	1209.0	1206.6
32	13	1039.9	779.8	1210.0	1181.5
32	14	795.6	369.5	1180.8	1192.5
32	15	599.8	-486.5	1161.0	1179.8
32	16	-854.8	93.2	1156.1	1155.5
32	17	772.1	71.9	1138.3	1147.2
32	18	116.8	-301.9	1139.1	1125.2
32	19	912.5	-892.0	1120.8	1111.7
32	20	591.9	-315.4	1106.3	1108.3
32	21	624.1	-1372.9	1086.2	1110.9
32	22	-1189.9	-708.4	1099.4	1070.5
32	23	-640.5	196.3	1093.8	1067.8
32	24	-1154.6	810.3	1076.0	1074.1
32	25	-8.8	-524.8	1063.9	1100.2
32	26	-184.5	7.8	1107.3	1082.3
32	27	-283.6	-36.3	1100.8	1070.8
32	28	144.1	1593.0	1060.6	1063.5
32	29	1201.7	1316.6	1042.5	1056.0
32	30	-177.2	-896.8	1015.2	1029.7
32	31	1560.0	602.7	972.5	952.7
32	32	404.8	202.0	849.8	871.7
33	0	-333.0	.0	1280.6	.0
33	1	320.5	-802.5	1235.5	1291.3
33	2	267.4	345.2	1232.6	1307.5
33	3	-111.2	-683.9	1277.6	1237.0
33	4	774.5	-500.2	1267.3	1262.4
33	5	-917.2	395.1	1253.7	1241.4
33	6	-644.8	-1142.5	1245.8	1260.8
33	7	-1108.3	1123.1	1223.8	1243.8
33	8	-427.7	-118.3	1241.0	1231.4
33	9	291.9	557.9	1229.7	1217.3
33	10	-23.3	436.3	1212.0	1216.3
33	11	621.2	21.7	1199.0	1209.5
33	12	1033.6	-57.1	1197.6	1194.7
33	13	388.1	-1295.5	1194.3	1174.7
33	14	573.4	-98.3	1171.2	1179.9
33	15	-365.8	-244.7	1159.3	1166.7
33	16	325.7	-653.1	1160.5	1138.1
33	17	135.8	122.7	1144.6	1131.3
33	18	-967.6	-407.3	1125.7	1125.3
33	19	57.6	-733.5	1107.4	1122.0
33	20	-893.1	-325.9	1097.3	1104.2
33	21	-437.5	-917.3	1090.9	1096.7
33	22	-862.7	159.5	1090.5	1075.1
33	23	-666.6	1027.7	1078.4	1068.7
33	24	322.4	1038.7	1063.6	1082.2
33	25	496.4	-3.1	1060.7	1082.4
33	26	206.3	-522.0	1093.0	1070.2
33	27	1724.1	570.7	1112.7	1070.5
33	28	266.9	272.7	1065.1	1096.0
33	29	1580.4	-31.9	1061.7	1052.9
33	30	109.1	-2436.5	1036.1	1059.9
33	31	-1742.2	-752.5	1036.4	1012.6
33	32	1621.0	-2180.9	966.5	979.5
33	33	650.1	-2125.1	891.7	865.2
34	0	-597.7	.0	1249.2	.0
34	1	215.2	-208.9	1208.3	1278.1
34	2	-1013.9	190.5	1201.3	1278.8
34	3	149.7	-908.8	1269.2	1205.4
34	4	-460.6	855.4	1238.9	1231.4
34	5	-931.3	-416.9	1228.9	1233.1
34	6	605.5	991.6	1214.3	1237.6
34	7	-514.6	906.0	1207.8	1226.9
34	8	1013.6	-444.1	1222.9	1201.4
34	9	822.1	979.6	1216.7	1193.3
34	10	158.3	-551.4	1189.0	1199.0
34	11	1240.3	-569.8	1181.8	1199.7
34	12	3.3	-643.9	1178.5	1171.1
34	13	-616.2	-1052.1	1190.5	1163.4
34	14	-350.0	506.3	1155.9	1166.3
34	15	-1381.7	103.1	1139.2	1172.4
34	16	490.6	-383.2	1140.2	1144.1
34	17	-842.5	587.6	1132.2	1123.7
34	18	62.9	-374.0	1119.5	1121.5
34	19	-287.4	1099.1	1108.9	1104.8
34	20	-226.0	-360.1	1100.4	1098.8
34	21	335.0	1082.6	1077.3	1093.4
34	22	302.2	434.4	1085.2	1076.5
34	23	-95.8	69.2	1074.7	1061.0
34	24	1274.7	-135.2	1052.1	1074.5
34	25	-349.0	-568.8	1046.9	1086.9
34	26	919.7	-1524.2	1075.8	1055.0
34	27	300.8	466.1	1103.6	1053.3
34	28	741.1	-1138.4	1074.0	1097.5
34	29	246.7	652.3	1080.1	1068.2
34	30	-393.7	-1396.6	1053.4	1052.6
34	31	-1710.7	-317.5	1056.4	1033.2
34	32	1650.4	564.2	1017.5	1035.2
34	33	-3212.5	386.3	983.4	978.3
34	34	254.2	879.7	905.2	883.7
35	0	-42.7	.0	1222.7	.0
35	1	60.4	1157.3	1190.5	1249.0
35	2	-613.5	-545.7	1177.0	1249.6
35	3	782.1	175.3	1240.8	1192.5
35	4	-753.3	605.4	1205.0	1212.5
35	5	901.9	-430.8	1216.4	1200.6
35	6	435.2	1166.8	1201.3	1205.5
35	7	177.0	-1467.0	1181.8	1209.3
35	8	880.3	236.6	1198.5	1192.5
35	9	-862.6	-847.9	1191.1	1170.7
35	10	725.8	-1006.5	1178.0	1191.8
35	11	-1165.3	53.6	1154.3	1171.6
35	12	-892.2	-620.2	1173.2	1164.7
35	13	-178.8	580.7	1158.4	1137.3
35	14	-383.5	834.3	1149.5	1156.7

35	15	316.4	377.0	1134.5	1141.7
35	16	230.1	397.6	1142.2	1123.9
35	17	-481.7	-523.3	1129.1	1115.2
35	18	1043.0	79.0	1105.0	1109.3
35	19	-143.6	529.5	1088.7	1117.3
35	20	623.7	-572.9	1080.5	1094.5
35	21	746.6	1074.2	1082.2	1082.8
35	22	349.7	-739.9	1082.1	1055.9
35	23	354.0	312.7	1080.0	1050.9
35	24	-419.9	-416.1	1048.5	1060.3
35	25	-2.7	-883.8	1049.0	1060.2
35	26	89.2	81.9	1065.7	1056.1
35	27	-1168.1	-822.5	1061.6	1056.3
35	28	1249.1	126.9	1055.0	1092.0
35	29	-1204.9	66.0	1071.5	1087.2
35	30	879.4	183.6	1080.5	1050.3
35	31	-649.9	55.7	1045.3	1047.5
35	32	1598.6	1446.6	1038.9	1037.6
35	33	-1337.8	-2336.8	1022.3	1030.4
35	34	2410.7	2516.2	1001.5	974.5
35	35	1432.3	2052.8	906.8	911.6
36	0	1320.0	.0	1201.8	.0
36	1	-332.3	249.9	1160.6	1229.1
36	2	852.1	-1048.1	1147.3	1237.3
36	3	45.6	1004.9	1224.0	1160.3
36	4	-580.7	-1081.3	1194.9	1179.7
36	5	1165.0	326.5	1190.1	1183.3
36	6	-904.8	-91.2	1162.2	1192.4
36	7	691.2	-982.7	1170.1	1189.6
36	8	-239.1	457.4	1179.4	1149.2
36	9	-974.6	-748.2	1179.7	1161.1
36	10	-11.5	293.8	1142.9	1160.2
36	11	-883.6	710.3	1150.3	1162.9
36	12	-104.8	219.7	1144.6	1132.4
36	13	66.2	920.6	1149.8	1128.5
36	14	-151.1	-126.2	1118.5	1131.3
36	15	1426.8	245.8	1109.6	1140.7
36	16	-258.8	326.3	1114.1	1114.0
36	17	151.4	-882.0	1114.3	1099.9
36	18	162.1	526.5	1104.6	1097.0
36	19	-285.7	-885.9	1085.7	1085.1
36	20	358.4	538.3	1098.1	1073.8
36	21	-84.4	-451.3	1060.4	1073.8
36	22	4.7	-151.3	1057.9	1072.3
36	23	13.1	165.3	1056.9	1050.3
36	24	-674.7	-240.1	1042.9	1056.1
36	25	583.0	-264.6	1031.5	1051.3
36	26	-715.9	479.5	1060.5	1026.1
36	27	413.0	-356.6	1071.3	1033.6
36	28	101.5	1062.8	1044.7	1055.4
36	29	-402.2	-818.3	1053.6	1079.4
36	30	748.5	1970.4	1075.3	1060.5
36	31	-317.7	-949.3	1045.9	1063.1
36	32	1270.5	1278.4	1036.0	1041.3
36	33	-266.3	-2516.6	1029.8	1036.8
36	34	337.5	1397.1	1041.5	1007.8
36	35	1715.3	-1550.1	1005.3	979.8
36	36	-32.5	-1154.0	922.2	920.8
37	0	156.0	.0	1175.0	.0
37	1	-826.8	-961.8	1138.1	1205.1
37	2	688.3	131.5	1127.3	1207.6
37	3	-1635.0	-5.5	1194.0	1138.3
37	4	510.0	-713.1	1162.3	1167.6
37	5	-730.8	766.7	1166.9	1153.7
37	6	-286.6	-1182.3	1156.6	1160.2
37	7	363.1	815.3	1141.6	1163.9
37	8	-1475.3	-74.6	1155.7	1143.3
37	9	775.3	559.2	1150.4	1132.6
37	10	-699.2	1398.3	1128.8	1147.1
37	11	877.0	-46.2	1118.9	1138.1
37	12	764.6	774.9	1131.3	1116.2
37	13	-13.4	291.2	1127.0	1104.2
37	14	303.3	-708.7	1105.0	1117.4
37	15	370.9	-135.7	1092.2	1110.5
37	16	-405.4	-235.5	1107.4	1093.6
37	17	193.1	201.9	1100.1	1080.1
37	18	-632.4	-39.3	1077.6	1090.9
37	19	337.3	-191.8	1062.1	1097.3
37	20	-196.8	1044.2	1058.2	1072.7
37	21	-217.2	-766.2	1068.9	1066.6
37	22	625.6	1094.3	1059.7	1036.2
37	23	-480.3	-869.3	1058.4	1035.8
37	24	104.7	-108.2	1025.4	1049.4
37	25	-243.5	223.6	1024.6	1038.1
37	26	193.8	-416.2	1031.0	1028.6
37	27	1269.6	297.2	1032.3	1029.5
37	28	-635.0	431.6	1041.1	1043.4
37	29	935.2	-551.2	1040.6	1037.7
37	30	-1192.2	1260.8	1067.5	1040.7
37	31	656.7	-973.2	1066.4	1040.9
37	32	-991.2	1118.8	1024.1	1059.6
37	33	360.6	-1768.0	1034.1	1022.5
37	34	-665.7	315.4	1029.0	1022.2
37	35	1390.3	-34.8	1029.7	1016.0
37	36	-2636.5	348.7	979.7	1008.1
37	37	-188.5	1190.9	924.0	934.5
38	0	-1016.3	.0	1149.4	.0
38	1	-104.2	-547.3	1111.2	1171.5
38	2	-476.2	1420.3	1101.1	1180.5
38	3	-340.1	-536.9	1165.8	1112.2
38	4	923.8	1268.0	1138.7	1137.9
38	5	-1120.7	-87.4	1141.5	1126.4
38	6	977.5	-137.1	1121.4	1145.2
38	7	-500.7	865.4	1108.9	1142.8
38	8	253.5	-208.2	1139.0	1115.7
38	9	482.1	722.9	1128.5	1104.5
38	10	247.6	-144.2	1107.7	1128.2
38	11	540.1	-337.6	1102.5	1110.6
38	12	192.1	-53.6	1111.7	1094.5
38	13	180.9	-274.5	1101.0	1090.5
38	14	150.9	-179.7	1083.5	1096.7
38	15	-469.4	-269.3	1077.7	1088.9
38	16	228.6	114.5	1078.4	1079.2
38	17	112.2	602.4	1080.7	1067.5
38	18	-27.7	-296.7	1071.6	1065.3
38	19	647.2	7.3	1059.1	1064.0
38	20	-135.4	-128.1	1073.7	1043.1
38	21	191.7	-140.5	1041.5	1047.9
38	22	61.8	-283.0	1038.9	1055.0
38	23	-629.1	-385.4	1033.1	1019.9
38	24	118.3	448.1	1030.8	1022.6
38	25	-659.6	206.6	1010.8	1029.1
38	26	674.0	-819.7	1016.2	1008.8
38	27	8.3	271.8	1026.5	1006.8
38	28	142.6	-913.1	1013.3	1022.2
38	29	659.6	1287.7	1014.7	1045.8
38	30	-1748.9	-444.9	1029.7	1023.9
38	31	1627.3	320.8	1055.0	1028.6
38	32	-1919.5	144.4	1023.9	1054.5
38	33	1619.3	-865.9	1045.0	1014.8
38	34	-341.2	256.8	1016.4	1020.8
38	35	1089.8	588.1	1023.9	1013.0

38	36	-1394.1	-992.1	1000.1	1038.6
38	37	1549.8	3399.4	986.2	998.4
38	38	1773.5	128.4	916.7	951.0
39	0	-411.2	.0	1120.2	.0
39	1	972.6	1104.7	1083.2	1151.6
39	2	-534.5	169.5	1067.1	1153.2
39	3	1388.0	-117.5	1143.4	1085.1
39	4	-236.9	724.7	1111.5	1104.4
39	5	388.6	-1066.8	1118.5	1102.5
39	6	506.5	726.7	1094.7	1109.6
39	7	-573.9	-329.8	1097.9	1112.0
39	8	1271.6	17.0	1107.1	1085.3
39	9	-315.0	29.6	1103.1	1092.3
39	10	333.0	-876.0	1076.3	1099.2
39	11	43.6	57.5	1081.4	1094.2
39	12	-113.1	-462.2	1085.6	1070.6
39	13	-.6	-315.7	1082.0	1064.1
39	14	-336.8	-87.6	1062.0	1074.8
39	15	-667.8	-5.3	1053.4	1069.5
39	16	547.3	435.4	1060.9	1051.9
39	17	-92.1	90.6	1065.0	1044.9
39	18	432.6	-336.8	1045.9	1049.6
39	19	-636.9	-142.2	1030.5	1060.7
39	20	18.8	-746.1	1041.7	1037.0
39	21	-58.7	298.5	1028.4	1042.4
39	22	-831.5	-706.7	1026.1	1023.2
39	23	-121.1	552.3	1036.0	1013.5
39	24	-82.0	373.1	995.0	1017.2
39	25	397.2	89.7	1001.0	1013.2
39	26	272.9	76.3	1010.9	992.6
39	27	-412.8	-303.8	995.4	992.4
39	28	820.1	-294.5	1003.9	1003.2
39	29	-470.8	715.1	1003.4	1004.1
39	30	373.8	-1098.1	1017.1	1017.1
39	31	225.7	1207.5	1022.3	1002.8
39	32	-731.0	-1546.7	1014.5	1037.9
39	33	1281.5	952.5	1024.9	1020.4
39	34	-654.5	-1265.4	1021.1	1009.3
39	35	63.6	523.7	999.1	1008.3
39	36	-349.2	-971.6	995.8	1020.7
39	37	114.6	2093.0	1014.0	1010.4
39	38	972.1	-2514.8	995.9	983.2
39	39	-51.4	-2409.7	934.1	937.4
40	0	838.5	.0	1097.2	.0
40	1	250.3	377.1	1058.3	1114.7
40	2	387.0	-1405.4	1053.2	1123.9
40	3	699.1	378.8	1107.1	1059.4
40	4	-945.7	-619.8	1081.6	1090.6
40	5	767.6	-69.0	1090.0	1071.3
40	6	-669.2	276.4	1073.5	1085.9
40	7	211.3	-613.2	1061.4	1092.6
40	8	-100.5	194.3	1079.1	1067.6
40	9	-178.8	-539.2	1083.2	1061.4
40	10	-81.3	13.8	1059.3	1072.6
40	11	-341.3	-275.3	1060.6	1066.8
40	12	-128.3	48.5	1066.5	1047.2
40	13	-197.4	-70.5	1055.2	1047.7
40	14	27.0	37.4	1038.8	1054.7
40	15	-278.6	-90.0	1036.8	1044.3
40	16	250.8	-171.8	1038.1	1033.8
40	17	-195.0	-93.7	1035.2	1025.7
40	18	146.2	-87.0	1032.4	1030.4
40	19	-509.5	298.8	1012.5	1033.2
40	20	-2.7	54.7	1033.1	1015.2
40	21	-280.2	270.6	1019.2	1016.9
40	22	5.0	271.4	1010.3	1016.4
40	23	351.1	432.7	1013.0	995.5
40	24	100.3	-146.0	1003.7	1000.7
40	25	624.7	-86.3	976.7	994.2
40	26	227.8	451.1	981.5	993.2
40	27	-29.4	-223.3	987.3	975.4
40	28	291.0	442.5	985.0	966.3
40	29	-661.2	-185.1	970.0	1006.0
40	30	964.5	-213.9	988.7	989.4
40	31	-969.7	25.5	1017.6	986.6
40	32	755.8	-944.7	986.8	1008.4
40	33	-643.8	1171.0	1008.3	1013.7
40	34	603.7	-1293.6	1012.1	1000.2
40	35	-361.8	1170.3	991.8	1009.8
40	36	245.7	-689.2	988.7	991.6
40	37	222.9	1453.6	1000.8	992.6
40	38	676.8	-919.6	1017.3	990.0
40	39	-1359.5	217.6	973.6	987.6
40	40	-216.3	159.9	949.6	917.9
41	0	332.8	.0	1064.7	.0
41	1	-640.0	-856.4	1031.1	1095.9
41	2	176.4	-357.5	1021.3	1093.9
41	3	-642.9	283.7	1086.3	1036.0
41	4	-51.0	-581.0	1057.9	1055.9
41	5	-19.5	828.4	1069.3	1046.7
41	6	-626.2	-274.7	1044.6	1062.5
41	7	420.4	181.3	1040.6	1063.0
41	8	-487.6	8.2	1062.4	1036.3
41	9	154.2	-106.9	1053.4	1037.9
41	10	-45.4	-50.7	1031.5	1056.0
41	11	-166.1	51.9	1033.8	1044.5
41	12	-145.0	42.7	1041.4	1028.3
41	13	272.5	-172.3	1034.0	1027.7
41	14	2.7	360.1	1020.1	1027.8
41	15	230.8	-93.6	1017.6	1026.5
41	16	-222.3	-187.3	1013.7	1016.1
41	17	45.8	-267.2	1017.9	1005.9
41	18	-135.8	355.3	1009.3	1007.1
41	19	214.1	39.3	1000.6	1016.1
41	20	88.9	370.3	1012.2	991.6
41	21	154.3	27.1	995.4	1008.9
41	22	282.7	85.7	992.0	1002.0
41	23	212.3	-275.0	1005.4	975.6
41	24	173.8	-389.1	978.4	991.0
41	25	-66.6	-348.5	972.9	987.1
41	26	165.8	-300.4	973.0	957.4
41	27	313.9	310.4	977.3	959.6
41	28	-235.4	417.4	958.6	965.9
41	29	225.4	-178.0	960.4	957.5
41	30	20.0	557.4	975.7	973.2
41	31	-826.6	-517.1	977.9	968.3
41	32	752.4	634.1	973.1	1000.2
41	33	-791.5	-45.1	977.0	985.5
41	34	1506.0	-132.4	992.4	995.3
41	35	-900.3	602.8	982.4	994.8
41	36	1182.9	-617.0	973.8	997.7
41	37	-362.2	1149.9	982.9	965.3
41	38	52.5	-695.9	994.4	970.7
41	39	-787.8	615.3	989.5	991.0
41	40	1252.1	1301.4	969.8	969.3
41	41	1687.0	247.3	908.6	951.5
42	0	-564.3	.0	1044.0	.0
42	1	-212.2	-407.8	1003.3	1056.9
42	2	-212.9	744.2	1003.8	1068.9
42	3	-585.9	-164.5	1052.6	1005.7
42	4	689.6	335.7	1031.5	1038.7
42	5	-311.4	129.3	1035.5	1020.5

42	6	479.0	-415.6	1025.5	1036.0
42	7	-171.4	203.8	1013.3	1033.9
42	8	78.9	-388.1	1029.7	1024.1
42	9	-46.0	282.1	1024.6	1013.4
42	10	-203.5	-339.9	1016.6	1026.7
42	11	74.8	468.4	1012.6	1015.6
42	12	-168.9	-199.3	1023.2	1006.5
42	13	66.0	202.1	1009.3	1003.4
42	14	-411.5	-79.3	998.2	1012.2
42	15	344.3	421.6	996.9	1002.0
42	16	-736.8	36.6	1000.4	992.4
42	17	147.0	-49.5	999.3	985.4
42	18	124.6	339.8	990.7	986.6
42	19	173.8	-349.3	974.5	1000.3
42	20	40.5	1.6	989.7	982.1
42	21	313.0	-271.5	977.2	987.0
42	22	-301.2	70.9	980.7	981.7
42	23	21.2	-481.0	988.5	966.0
42	24	-268.5	-121.0	964.1	975.5
42	25	-381.1	-266.3	958.7	973.1
42	26	-294.8	-43.2	957.2	960.0
42	27	145.0	97.6	946.0	946.5
42	28	-50.8	252.0	958.9	943.6
42	29	375.6	148.6	931.1	956.7
42	30	-678.4	209.5	936.9	950.3
42	31	452.1	81.9	980.0	939.1
42	32	-298.0	620.4	959.5	954.5
42	33	512.4	-909.9	969.9	968.2
42	34	488.9	461.1	968.4	959.1
42	35	-573.7	-766.0	972.3	978.4
42	36	877.5	287.7	960.5	979.3
42	37	-1225.0	282.4	980.5	958.5
42	38	97.0	-674.6	962.8	951.4
42	39	-435.3	882.5	961.5	971.8
42	40	313.4	507.4	967.8	984.0
42	41	630.6	-1217.8	953.4	962.7
42	42	514.0	-1140.6	932.1	912.3
43	0	-383.1	.0	1010.2	.0
43	1	181.4	617.2	981.7	1037.1
43	2	-217.3	598.0	973.8	1032.3
43	3	424.7	-256.7	1029.6	987.5
43	4	109.0	189.3	999.6	1004.1
43	5	-189.2	-511.0	1018.6	996.1
43	6	195.7	5.8	992.6	1004.1
43	7	-262.7	-104.2	994.0	1014.4
43	8	-196.1	209.9	1002.2	986.4
43	9	-117.5	53.0	1010.9	991.9
43	10	198.8	298.0	982.7	997.7
43	11	-374.1	-76.3	992.3	1001.0
43	12	169.8	16.6	992.4	980.5
43	13	-397.3	511.6	990.4	987.7
43	14	164.3	-199.2	978.2	983.7
43	15	308.1	398.0	976.9	983.1
43	16	-346.4	-225.1	973.7	978.7
43	17	165.2	139.1	974.7	969.8
43	18	-130.8	-289.8	974.2	967.9
43	19	334.7	-16.5	958.9	975.3
43	20	-223.0	22.8	979.9	957.0
43	21	-57.2	-223.6	963.5	965.2
43	22	-14.2	380.0	956.8	970.5
43	23	-61.1	-96.6	970.8	949.7
43	24	-325.6	295.2	953.9	962.5
43	25	-209.6	227.5	941.2	957.3
43	26	-51.7	385.0	953.1	941.5
43	27	-85.0	150.8	948.7	927.9
43	28	282.5	-282.4	928.8	929.5
43	29	-42.1	273.8	928.3	941.3
43	30	-438.8	-179.0	930.3	925.6
43	31	601.0	365.1	932.1	926.6
43	32	-397.9	-263.9	927.0	962.2
43	33	832.3	-185.0	935.6	944.1
43	34	-1015.8	-44.4	958.0	943.9
43	35	262.9	-557.9	946.1	943.2
43	36	-357.2	1110.9	957.1	954.9
43	37	-918.5	-104.7	957.8	943.8
43	38	495.3	724.7	964.5	940.3
43	39	-578.8	673.5	928.0	948.8
43	40	769.9	21.0	949.2	949.1
43	41	-235.8	-271.3	957.6	963.5
43	42	-425.3	450.4	944.7	944.1
43	43	-1343.4	384.7	918.5	908.1
44	0	297.4	.0	988.5	.0
44	1	296.2	530.4	954.2	1005.3
44	2	172.9	-140.7	954.9	1009.1
44	3	290.8	-217.5	999.3	957.8
44	4	-345.8	-73.1	979.4	984.0
44	5	-162.9	-235.9	984.0	970.6
44	6	-288.4	103.1	974.2	984.9
44	7	-5.5	26.2	966.5	980.0
44	8	-176.4	401.6	980.0	973.3
44	9	194.8	-131.7	972.7	966.7
44	10	63.4	514.6	968.6	978.1
44	11	96.2	-193.9	964.9	966.7
44	12	184.9	438.4	975.0	963.0
44	13	-130.0	-243.1	962.6	960.4
44	14	648.2	251.4	958.6	967.9
44	15	-200.6	-264.5	952.0	960.8
44	16	467.4	-95.3	959.5	953.5
44	17	-241.6	64.4	959.9	945.3
44	18	-104.1	-306.7	948.3	949.9
44	19	32.0	-14.9	938.0	961.2
44	20	-94.2	-84.8	949.7	941.7
44	21	-169.1	307.5	943.0	953.0
44	22	343.6	-283.7	943.1	942.6
44	23	-197.9	194.7	959.0	929.2
44	24	52.7	103.2	930.9	947.3
44	25	217.8	351.9	930.6	945.7
44	26	308.5	75.3	931.9	924.9
44	27	118.3	207.5	927.6	927.4
44	28	11.1	-216.5	919.2	918.5
44	29	-296.5	-26.0	909.5	914.3
44	30	119.4	-154.3	915.3	921.3
44	31	-168.2	105.0	923.6	898.2
44	32	155.0	-508.9	919.0	910.5
44	33	62.9	320.3	924.7	930.8
44	34	-517.7	-161.1	920.5	925.1
44	35	32.9	483.4	926.0	936.5
44	36	-468.2	562.6	921.2	929.2
44	37	197.4	213.6	937.3	932.5
44	38	-44.5	586.4	939.9	921.0
44	39	100.4	-324.1	917.2	947.2
44	40	707.5	314.5	919.8	915.1
44	41	-646.2	-694.6	926.4	933.6
44	42	473.2	738.8	950.1	930.9
44	43	138.0	282.3	929.7	928.1
44	44	503.2	1539.4	888.1	914.4
45	0	353.2	.0	964.4	.0
45	1	-255.9	-323.1	929.9	975.2
45	2	59.7	-390.2	931.9	982.2
45	3	-291.5	160.3	969.6	934.2
45	4	-82.6	46.1	953.0	957.7
45	5	22.5	177.4	957.9	945.5

45	6	191.2	237.0	949.0	956.6
45	7	155.6	284.3	942.4	954.9
45	8	242.7	-261.1	951.3	947.9
45	9	201.2	119.4	952.7	939.8
45	10	-353.7	-233.3	943.5	947.3
45	11	642.0	-190.4	940.2	947.6
45	12	-209.7	250.5	943.0	937.4
45	13	280.3	-538.1	942.7	940.4
45	14	-19.9	158.1	933.1	936.1
45	15	-305.6	-660.9	936.4	939.0
45	16	462.6	313.3	928.7	930.4
45	17	-490.5	-63.9	935.6	928.8
45	18	299.7	133.5	931.0	923.6
45	19	-676.5	74.5	920.6	931.7
45	20	198.3	-84.6	934.3	919.6
45	21	61.3	292.7	920.6	925.5
45	22	32.0	-359.0	921.1	929.9
45	23	-34.7	277.0	926.6	913.9
45	24	254.8	-131.7	918.1	928.6
45	25	302.9	-81.3	913.6	921.0
45	26	49.2	-218.7	923.2	911.7
45	27	107.0	-258.3	912.5	902.0
45	28	-149.0	154.8	905.8	907.9
45	29	-265.7	27.6	890.9	906.3
45	30	67.2	36.0	894.4	893.8
45	31	-342.8	93.4	908.6	893.0
45	32	217.6	-292.4	880.4	906.0
45	33	-273.8	195.1	895.1	902.2
45	34	335.6	116.5	917.2	899.9
45	35	-203.0	352.6	907.5	898.6
45	36	187.2	19.4	908.3	910.0
45	37	61.8	258.1	903.5	904.3
45	38	-184.3	-203.1	912.4	913.3
45	39	36.4	-313.1	897.0	921.6
45	40	-493.1	461.9	910.6	912.8
45	41	-215.6	-842.4	901.5	893.5
45	42	-69.6	1277.4	916.8	901.8
45	43	-275.7	-919.8	916.6	922.9
45	44	-85.1	273.2	913.7	909.5
45	45	807.3	-887.8	898.6	874.1
46	0	-119.5	.0	933.7	.0
46	1	-84.1	-390.6	910.8	953.5
46	2	83.6	-33.7	905.3	946.6
46	3	-72.7	45.6	949.0	914.8
46	4	-16.0	57.3	924.0	925.7
46	5	155.0	212.1	936.2	925.2
46	6	73.8	49.5	919.7	927.4
46	7	118.8	-96.7	923.4	931.9
46	8	86.7	-43.7	922.9	920.4
46	9	-172.4	-58.8	928.3	920.5
46	10	139.1	-283.6	916.9	922.4
46	11	24.5	113.1	918.8	921.2
46	12	-86.3	-451.2	921.8	913.4
46	13	269.2	101.7	915.8	914.2
46	14	-495.1	-80.9	913.8	917.8
46	15	121.6	-139.2	905.5	912.6
46	16	-72.1	303.9	914.0	910.5
46	17	163.3	-87.7	909.3	899.6
46	18	-21.4	195.6	908.0	909.2
46	19	-16.0	173.3	892.6	912.0
46	20	152.5	162.9	910.0	896.9
46	21	-69.1	-192.7	902.3	904.4
46	22	-49.9	19.9	897.6	902.1
46	23	151.0	99.2	912.0	891.4
46	24	76.0	-105.7	892.8	901.9
46	25	32.2	-173.0	892.6	906.9
46	26	-82.3	-38.5	898.0	889.4
46	27	-216.6	-176.4	895.8	890.9
46	28	-172.2	88.5	881.9	887.0
46	29	33.8	75.5	885.1	883.4
46	30	-47.8	24.2	877.7	876.8
46	31	-61.1	130.0	876.9	871.4
46	32	2.3	-19.7	879.4	881.4
46	33	13.2	-14.8	874.0	871.2
46	34	364.5	97.2	879.7	879.7
46	35	55.4	-160.5	883.8	887.6
46	36	70.9	59.3	879.2	881.3
46	37	-269.6	-251.5	886.0	884.2
46	38	-358.3	-136.4	882.0	879.5
46	39	-159.0	65.9	881.6	896.0
46	40	-716.0	206.3	888.6	885.3
46	41	136.4	-60.5	895.5	880.4
46	42	-941.9	746.9	878.6	871.0
46	43	290.4	-670.8	888.4	885.3
46	44	-1007.5	753.9	896.4	896.3
46	45	42.6	68.8	889.2	894.6
46	46	-1199.2	-137.5	866.3	871.4
47	0	-169.1	.0	910.8	.0
47	1	-175.1	-57.3	882.8	915.6
47	2	1.0	32.4	885.4	923.1
47	3	-62.1	143.9	911.7	885.6
47	4	243.9	72.4	901.4	904.5
47	5	276.0	-8.8	900.4	895.3
47	6	-106.2	-104.3	899.2	904.1
47	7	-68.4	-346.7	894.4	897.2
47	8	50.3	77.6	897.9	899.5
47	9	-357.7	-281.2	896.1	891.7
47	10	282.7	108.4	895.6	894.1
47	11	-465.0	219.9	890.5	892.8
47	12	195.7	-336.0	892.2	889.4
47	13	-192.7	356.3	889.4	888.3
47	14	-54.0	-230.6	885.6	888.1
47	15	30.9	514.9	882.1	889.5
47	16	-160.0	-247.9	882.3	880.0
47	17	475.7	19.8	886.5	879.5
47	18	-314.9	74.0	877.4	876.3
47	19	443.9	-251.5	875.8	886.7
47	20	-84.1	25.3	877.5	872.0
47	21	-51.9	-164.9	875.0	879.5
47	22	-162.7	22.5	875.4	876.9
47	23	113.0	-299.8	879.7	866.6
47	24	-104.0	-31.9	868.7	880.8
47	25	-97.3	-158.5	870.2	872.1
47	26	-12.2	49.1	877.5	868.0
47	27	-54.4	202.8	867.8	865.9
47	28	-46.3	141.1	864.9	868.4
47	29	184.0	-33.3	856.8	861.7
47	30	126.6	-54.6	859.2	857.9
47	31	267.5	-124.8	858.3	848.1
47	32	-151.7	87.1	845.8	857.8
47	33	160.9	85.2	852.4	861.9
47	34	-73.6	-130.3	854.1	845.1
47	35	276.1	-301.0	860.6	852.9
47	36	-433.0	150.7	861.1	859.2
47	37	-141.2	-225.4	854.8	855.2
47	38	-218.8	221.6	860.6	857.5
47	39	-163.9	62.2	851.2	860.0
47	40	-230.3	207.5	868.7	857.7
47	41	219.8	292.2	866.3	859.3
47	42	-421.4	-221.6	866.9	859.3
47	43	689.4	-77.5	852.1	852.1
47	44	-821.4	-132.6	859.2	867.6

47 45	682.0	109.9	870.6	874.2
47 46	-45.7	-281.5	868.7	870.3
47 47	321.5	926.1	846.1	855.1
48 0	-14.9	.0	883.5	.0
48 1	96.3	-161.1	862.4	893.9
48 2	4.2	-27.5	861.6	892.2
48 3	140.0	-34.8	890.0	865.6
48 4	84.6	-154.1	876.4	875.0
48 5	2.8	41.2	879.7	874.0
48 6	-158.9	-132.1	871.3	877.4
48 7	39.3	210.1	872.3	877.2
48 8	-260.6	-66.6	871.3	872.4
48 9	108.0	.4	876.0	869.3
48 10	-108.4	209.5	868.9	868.6
48 11	-132.6	-264.2	866.7	872.1
48 12	217.5	253.6	866.5	864.6
48 13	-433.8	-32.2	866.7	865.3
48 14	222.9	-187.5	862.0	862.6
48 15	-186.2	395.2	860.7	863.6
48 16	70.0	-453.9	859.6	858.1
48 17	1.6	104.5	860.1	853.6
48 18	51.9	-140.6	857.6	856.9
48 19	32.2	15.0	848.7	856.5
48 20	-259.6	-114.0	860.7	851.4
48 21	205.6	76.2	849.6	850.0
48 22	-275.5	227.1	850.1	855.5
48 23	74.0	-149.7	854.4	845.6
48 24	-172.8	82.2	845.6	850.5
48 25	-27.2	-86.0	846.1	851.6
48 26	-20.7	36.3	847.6	844.3
48 27	76.8	71.3	848.2	843.6
48 28	164.1	138.1	838.7	842.5
48 29	11.4	-49.8	839.4	839.8
48 30	-25.1	-178.6	833.7	832.3
48 31	91.6	-137.8	833.2	832.3
48 32	-144.2	45.5	825.7	830.9
48 33	133.1	106.8	830.8	824.9
48 34	-249.1	51.2	834.3	828.4
48 35	9.0	-118.5	821.1	828.1
48 36	-392.6	49.0	829.2	833.4
48 37	86.8	197.5	830.7	833.4
48 38	-146.6	73.0	828.3	827.5
48 39	244.4	230.4	827.0	835.3
48 40	-158.1	-144.1	833.0	824.7
48 41	40.7	126.0	838.5	833.0
48 42	-138.0	-351.8	838.8	835.4
48 43	18.5	117.7	834.4	838.2
48 44	-303.3	-684.3	824.3	831.4
48 45	2.0	509.1	837.1	839.6
48 46	-343.8	-978.1	841.3	851.2
48 47	-114.6	558.7	844.8	844.5
48 48	1052.4	-515.1	836.8	822.1
49 0	-65.5	.0	860.9	.0
49 1	8.9	78.6	840.6	868.3
49 2	-92.7	62.4	840.6	868.8
49 3	-60.1	-187.9	864.6	844.5
49 4	-73.3	77.0	851.8	855.1
49 5	-248.9	-18.6	855.7	851.1
49 6	-18.5	-64.5	851.0	853.9
49 7	-51.2	239.6	850.9	851.7
49 8	-158.8	-78.4	848.5	853.3
49 9	277.0	114.4	848.9	847.5
49 10	-153.7	44.2	850.1	848.0
49 11	115.8	-64.8	844.6	843.9
49 12	-92.4	164.5	847.6	843.9
49 13	58.8	-146.7	841.2	840.9
49 14	27.0	224.4	841.3	843.7
49 15	-.9	-106.2	835.3	840.4
49 16	-89.8	69.1	840.4	836.1
49 17	-199.2	22.4	837.4	831.6
49 18	139.0	-127.1	834.4	834.7
49 19	-14.9	261.6	827.8	838.2
49 20	-7.6	42.8	832.9	827.9
49 21	-47.2	82.8	831.3	832.8
49 22	199.3	129.6	826.0	828.1
49 23	-48.9	77.7	835.5	824.7
49 24	8.5	24.6	822.9	828.7
49 25	-77.9	127.4	822.6	828.1
49 26	37.3	-20.4	828.2	821.7
49 27	-74.4	87.8	823.1	822.1
49 28	182.2	-199.0	819.2	823.5
49 29	-136.4	-54.3	817.1	816.0
49 30	-141.7	-212.1	816.2	814.2
49 31	-287.5	127.3	810.0	809.0
49 32	83.7	62.1	807.0	811.6
49 33	99.8	35.8	804.2	806.6
49 34	107.0	55.0	806.4	804.8
49 35	-186.2	157.3	809.0	805.1
49 36	-58.9	80.5	802.5	799.6
49 37	123.4	238.1	804.8	807.9
49 38	84.4	-204.0	804.6	805.3
49 39	-84.6	162.1	798.6	804.8
49 40	-150.0	-266.1	806.6	801.9
49 41	-147.0	98.6	801.9	802.4
49 42	-38.5	-172.0	806.5	810.9
49 43	-232.5	71.1	811.4	809.7
49 44	174.5	-358.5	806.9	811.9
49 45	-390.6	247.2	802.5	804.9
49 46	301.4	-550.8	810.7	815.2
49 47	-418.7	640.8	821.5	819.0
49 48	236.7	467.4	820.7	820.0
49 49	-378.8	-345.5	808.6	809.9
50 0	144.7	.0	834.6	.0
50 1	-78.7	98.9	814.6	838.3
50 2	-13.6	-59.4	815.7	841.0
50 3	120.4	5.9	835.0	818.2
50 4	-49.0	104.7	828.5	825.5
50 5	1.8	-82.4	827.9	823.6
50 6	259.0	237.0	822.9	829.0
50 7	-203.3	-40.5	823.9	824.7
50 8	434.4	-76.6	822.7	824.6
50 9	-92.4	195.3	824.6	820.8
50 10	30.3	-295.6	822.4	819.4
50 11	134.1	238.9	819.4	821.4
50 12	-311.3	-74.1	817.0	817.1
50 13	311.1	-15.6	817.1	817.1
50 14	-125.3	176.7	813.8	814.1
50 15	223.9	-237.3	811.9	816.0
50 16	-167.1	312.8	812.2	809.1
50 17	-52.2	-202.4	811.5	808.8
50 18	4.7	245.5	807.3	807.5
50 19	-86.0	-194.4	803.8	811.5
50 20	245.0	-1.0	806.5	804.6
50 21	-224.5	75.1	804.5	803.8
50 22	332.2	-238.0	803.5	804.8
50 23	-249.6	40.8	802.5	798.8
50 24	101.8	-90.0	799.8	805.2
50 25	-4.0	105.7	798.1	798.2
50 26	78.3	-92.6	799.2	797.7
50 27	84.8	-71.7	798.0	796.0
50 28	-171.5	-146.7	794.9	795.3
50 29	-124.4	51.2	792.6	792.8

50 30	-1.0	35.2	789.2	789.8
50 31	-171.0	185.8	786.7	787.3
50 32	205.3	-80.3	781.2	784.8
50 33	-7.8	19.2	784.1	781.2
50 34	143.9	-144.0	782.9	776.7
50 35	51.4	67.4	778.8	781.7
50 36	-66.1	-41.3	778.5	781.9
50 37	27.0	-10.2	775.5	775.7
50 38	114.6	-177.0	780.6	778.5
50 39	-227.2	-27.6	776.1	778.2
50 40	-48.7	-111.7	777.5	773.3
50 41	-212.3	79.4	777.5	777.1
50 42	185.9	-54.4	774.6	778.5
50 43	-241.1	-59.9	782.6	782.6
50 44	253.0	-36.4	782.8	787.5
50 45	-364.3	-153.4	784.3	783.6
50 46	438.0	98.1	780.4	779.6
50 47	-479.0	256.3	788.7	786.4
50 48	235.6	275.8	795.5	791.1
50 49	-107.2	-145.3	792.1	795.4
50 50	-449.5	889.5	786.9	786.6

TECHNICAL REPORT STANDARD TITLE PAGE

1. Report No. JPL Pub. 95-5	2. Government Accession No.	3. Recipient's Catalog No.
4. Title and Subtitle The JPL Mars Gravity Field, Mars 50c, Based Upon Viking and Mariner 9 Doppler Tracking Data		5. Report Date February 1995 6. Performing Organization Code
7. Author(s) Alex Konopliv		8. Performing Organization Report No.
9. Performing Organization Name and Address JET PROPULSION LABORATORY California Institute of Technology 4800 Oak Grove Drive Pasadena, California 91109		10. Work Unit No. 11. Contract or Grant No. ~~NASX-XXXX~~ NAS7-1260 13. Type of Report and Period Covered
12. Sponsoring Agency Name and Address NATIONAL AERONAUTICS AND SPACE ADMINISTRATION Washington, D.C. 20546		14. Sponsoring Agency Code RF150 BP88920000000015
15. Supplementary Notes		

16. Abstract

This report summarizes the current JPL efforts of generating a Mars gravity field from Viking 1 and 2 and Mariner 9 Doppler tracking data. The Mars 50c solution is a complete gravity field to degree and order 50 with solutions as well for the gravitational mass of Mars, Phobos, and Deimos. The constants and models used to obtain the solution are given and the method for determining the gravity field is presented. The gravity field is compared to the best current gravity GMM1 of Goddard Space Flight Center.

17. Key Words (Selected by Author(s)) 120. Astrodynamics 221. Geophysics 358. Lunar and Planetary Exploration 359. Celestial Mechanics		18. Distribution Statement	
19. Security Classif. (of this report) unclassified	20. Security Classif. (of this page) unclassified	21. No. of Pages 80	22. Price

JPL 0184 R 9/83